332.8
P567

OCT 3 1958

SPSE

Photographic

SCIENCE AND ENGINEERING

On the Quantum Efficiency of Photographic Negatives · *R. Clark Jones* 57

The Evaluation of Optical Images *George C. Higgins and Fred H. Perrin* 66

The Production of Precision Resolving Power Test Reticles · *P. Hariharan* 77

A Sensitometric Processing Machine Using Small Film Strips and Small Developer Volume · *R. W. Henn and K. R. Hughes* 81

Apparatus and a Laboratory for Processing Thick Nuclear Track Emulsions · *John F. Garfield* 85

A Continuous Rapid-Processing System for Side-Looking Radar Mapping · *Edgar D. Seymour* 91

Photographic Emulsions for Missile Photography *Hutson K. Howell* 95

Technicalia Photographica · *Frank Smith* 105

Notes from the Editor 119

Patent Postscripts · *Robert H. Zappert* 120

AUGUST · 1958

Volume 2 · Number 2

Editorial Policy

Photographic Science and Engineering is dedicated to the advancement of the knowledge and application of photography and other directly related sciences. Its pages are open to all who wish to report on new studies dealing with the theory of photosensitive systems, the design of photographic instruments and apparatus useful in the treatment of photographic materials, photographic optics and illuminants, the use of photography for scientific or engineering measurement or recording, and photographic instrumentation and data recording. Only original papers should be submitted except on special invitation.

Manuscripts should be typed double-spaced on white bond paper with $1^1/_4$-inch margins all around. Literature references should be exact, and should include titles of papers and journals, names of authors, numbers of volumes and pages, and year of publication. Book references should include title of volume, names of authors, publisher, number of edition, year of publication, and chapter and pages cited.

Graphs, charts, and other line illustrations should conform to good usage such as given in the American Standards Association Document Y-15, "A Guide for Preparing Technical Illustrations for Publication and Projection." Continuous-tone photographs should be made on 8- by 10-inch glossy paper and should show pertinent image detail sufficiently clearly to permit reduction to fit a 3-inch column in this journal. All illustrations should be numbered in soft blue pencil on the back to correspond with captions typed on a separate page. Tables should also be submitted on separate pages appropriately identified. An abstract should accompany each manuscript.

All papers submitted for publication will be reviewed by members of the Editorial Review Board and if not accepted will be returned to the author. Published papers become the property of the Society and are protected by appropriate copyrights. Authors receive five copies of issues in which their contributions appear. Additional copies and reprints may be obtained. The Society does not assume responsibility for material in transit, nor guarantee publication of unsolicited material.

Photographic
SCIENCE AND ENGINEERING

official publication of the
Society of Photographic Scientists and Engineers

AUGUST 1958
Volume 2, Number 2

EDITORIAL STAFF

Peter Krause, *Editor*
Jennie H. Allen, *Managing Editor*
Frank Smith, *Feature Editor*
Robert H. Zappert, *Feature Editor*
Willard W. Van Allen, *Associate Editor*
Jean St. Thomas, *Foreign Editor*

EDITORIAL REVIEW BOARD

T. H. James, *Chairman*
R. S. Barrows
R. Davis
H. E. Edgerton
K. G. Leistner
J. A. Maurer
H. F. Nitka
J. H. Waddell

Photographic Science and Engineering is published four times a year by the Society of Photographic Scientists and Engineers. The publication office is at 20th and Northampton Streets, Easton, Pa. Address correspondence to the Society at Box 1609, Main Post Office, Washington, D.C. Subscription to non-members of the Society, $8.00 per year, members $4.00; single copies, $2.00 each. The Society is not responsible for the accuracy of statements made by authors and does not necessarily subscribe to their views. Second-class mail privileges authorized at Easton, Pa.

© Copyright 1958 by the Society of Photographic Scientists and Engineers, Inc. Permission to reprint any part of the contents, except in reviews and abstracts, must be obtained in writing from the Editorial Vice President.

NG

of the

phic

eers

958

er 2

ditor

ditor

ditor

ature
ditor

ciate
ditor

ditor

RD

rman

rows

Davis

erton

stner

aurer

Nitka

ddell

ring is
y the
s and
is at
on, Pa.
ociety
shing-
mbers
mbers
. The
accu-
rs and
their
es au-
pyright
raphic
mission
s, ex-
ust be
al Vice

PHOTOGRAPHIC SCIENCE AND ENGINEERING
Volume 2, Number 2, August 1958

On the Quantum Efficiency of Photographic Negatives

R. CLARK JONES, *Research Laboratory, Polaroid Corporation, Cambridge, Mass.*

The detective quantum efficiency of four Eastman Kodak films (abbreviated names: Royal-X, Tri-X, Plus-X, and Pan-X) is computed from sensitometric and granularity data generously supplied by the manufacturer. The detective quantum efficiency is identical with the concept of quantum efficiency introduced by Rose in 1946, and is defined as the square of the ratio of the measured detectivity (reciprocal of the noise equivalent energy) to the maximum possible detectivity, where the maximum possible detectivity is set by the statistical fluctuations in the number of pre-exposure photons. The detective quantum efficiency Q of a film depends on the wavelength of the radiation, and on the amount of the pre-exposure. For each of the films, a curve of Q versus the pre-exposure (for a radiation wavelength of 430 mμ) is presented in Fig. 4. Q passes through a maximum as the pre-exposure is increased. The maximum values of Q for 430 mμ radiation are 0.90, 0.59, 0.62, and 0.30% for the four films, and these maxima occur for pre-exposures of 0.0011, 0.0040, 0.010, and 0.018 erg/sq cm.

1.0 Introduction

In this paper we compute the detective quantum efficiency of several types of Eastman Kodak black-and-white negative films. The quantum efficiency is computed as a function of the exposure for the four films: Royal-X, Tri-X, Plus-X, and Panatomic-X (*see* Section 4.0). The final results are shown in Figs. 4 and 5.

The term "quantum efficiency" has been used by various authors to designate a number of different concepts. Only one of these concepts, namely, the concept of detective quantum efficiency is considered in detail here.

2.0 The Concept of Quantum Efficiency

Up to 1946, the term quantum efficiency always meant the ratio of the numbers of two kinds of countable events. This type of quantum efficiency we call the *responsive* quantum efficiency. The responsive quantum efficiency of a detector is defined as the ratio of the number of countable output events to the number of photons that act on the device. The phrase "act on" is used advisedly, since the number of photons may be either the number of incident photons or the number of absorbed photons. For example, the quantum efficiency of a vacuum phototube is usually defined as the ratio of the number of photoelectrons to the number of *incident* photons.

The responsive quantum efficiency may be greater than unity. For example, in a multiplier phototube that has many dynodes, the ratio of the number of electrons that reach the anode to the number of incident photons may be a million, in which case the responsive quantum efficiency is quite correctly stated to be one million.

Our chief interest in this paper, however, is with what we call here the *detective* quantum efficiency. This concept was first introduced by Rose[1] in 1946.

The detective quantum efficiency is formulated in terms of the detecting ability of a detector on which steady ambient radiation is incident in addition to the radiation signal that is to be detected. The quantum fluctuation in the steady ambient radiation introduces noise in the output of the detector, and even an ideal detector will have a detecting ability that is limited by these fluctuations.

The importance of the concept of detective quantum efficiency for any given kind of detector depends on whether, in fact, the noise due to the steady ambient radiation is dominant over the other noises in the output of the detector. This condition is almost always satisfied in the practical use of photographic negatives, multiplier phototubes, and image orthicons, is sometimes satisfied in the use of photoconductive cells, and is never satisfied in the use of thermocouple radiation detectors.

The detective quantum efficiency Q of a detector is now defined quite simply as the square of the ratio of the measured signal-to-noise ratio to the maximum possible signal-to-noise ratio on the same signal in the presence of the same ambient radiation.

The key part of this definition is the concept of "the maximum possible signal-to-noise ratio," given the signal and the ambient radiation. We now proceed to develop this concept.

We consider the radiation that is incident on the area A of a detector during a period of length T, and we consider first the ambient radiation. The strength

Received 26 February 1958.

of the steady ambient radiation is defined by the number of photons M_a that are incident on the area A in the time T. The fact that these photons occur randomly in time leads to the conclusion that the distribution of the number of photons in successive periods of length T will be a Poisson distribution,[2] which fact in turn permits us to conclude that the root-mean-square fluctuation N in the number of photons in successive periods is equal[3] to the square root of M_a

$$N = \text{rms fluctuation} = M_a^{1/2} \tag{2.1}$$

Second, consider the signal. The average number of signal photons incident on the area A in the period T is denoted by both M_s and S:

$$S = \text{signal} = M_s \tag{2.2}$$

It is supposed that M_s is small compared with M_a, so that the noise N is not changed appreciably by the presence of the signal. From these two equations we conclude directly that the signal-to-noise ratio S/N in the radiation incident on the detector is given by

$$S/N = M_s/M_a^{1/2} \tag{2.3}$$

This is the signal-to-noise ratio in the radiation incident on the detector. If we can imagine an ideal detector in which every incident photon contributes equally to the output of the detector, and in which furthermore there is no other kind of noise present in the output, then the signal-to-noise ratio in the output of this ideal detector will be as given by Eq. (2.3). Clearly, no detector can deliver a higher signal-to-noise ratio, and thus we have found in Eq. (2.3) an expression for the maximum possible signal-to-noise ratio on a given signal in the presence of a given ambient radiation. Thus the last equation is rewritten

$$(S/N)_{max} = M_s/M_a^{1/2} \tag{2.4}$$

We are now ready to make use of the definition given above for the detective quantum efficiency. If the measured signal-to-noise ratio of a detector is denoted by $(S/N)_m$[2] then the definition of the detective quantum efficiency is

$$Q = \frac{(S/N)_m^2}{(S/N)_{max}^2} \tag{2.5}$$

By combining the last two equations, we obtain:

$$Q = \left(\frac{S}{N}\right)_m^2 \frac{M_a}{M_s^2} \tag{2.6}$$

This is the fundamental expression for the detective quantum efficiency Q.

The remainder of this section we shall discuss a number of aspects of this definition, and the last expression will be changed to a form that is more directly applicable to actual detectors.

The first question to be discussed is the reason for defining the detective quantum efficiency in terms of the *square* of the ratio of signal-to-noise ratios. The second power is essential if the detective quantum efficiency is to be in accord with the responsive quantum efficiency in those cases where both concepts are simultaneously applicable.

The type of detector to which both concepts are clearly applicable is best represented by the simple vacuum photoemissive tube. We shall imagine a slightly idealized vacuum phototube and amplifier in which the noise of the amplifier is negligible in comparison with the noise produced by the quantum fluctuations of the background. It is supposed that a randomly-chosen fraction F of the incident photons each contribute one electron to the current in the external circuit, and that the other photons (the fraction $1-F$) produce no effect. Then the number of contributing photons in the steady ambient radiation is not M_a, but is rather FM_a, so that the fluctuation in the number of contributing photons is

$$N' = (FM_a)^{1/2} \tag{2.7}$$

Similarly, the number of contributing signal photons is not M_s, but is rather FM_s, so that we have

$$S' = FM_s \tag{2.8}$$

From the last two relations, the signal-to-noise ratio in the output of our slightly idealized vacuum phototube is given by

$$(S'/N')_m = F^{1/2}M_s/M_a^{1/2} \tag{2.9}$$

which relation, when solved for F, becomes

$$F = \left(\frac{S'}{N'}\right)_m^2 \frac{M_a}{M_s^2} \tag{2.10}$$

We now point out that F is the *responsive* quantum efficiency of the idealized phototube. On comparing Eq. (2.6) with Eq. (2.10) we see that the detective quantum efficiency Q is equal to the responsive quantum efficiency F for this particularly simple and slightly idealized detector. If the detective quantum efficiency had been defined as any power but the second of the ratio of the signal-to-noise ratios, we would have failed to make the two kinds of quantum efficiency as similar as possible.

In the simple phototube we have just discussed, the detective quantum efficiency is the same for a large range of intensity of the ambient radiation. For more complex detectors, however, this is not the case and we may expect that the detective quantum efficiency will depend on the amount of the ambient radiation. With respect to photographic negatives, this is the fact.

Photographic negatives have another characteristic that sets them off from other detectors—namely, their ability to integrate the radiation that falls on the detector over a long period of time. With most detectors, the only ambient radiation that is relevant is the ambient radiation that falls on the detector simultaneously with the signal. But with photographic negatives, the "ambient" radiation may precede or follow the signal radiation. For this reason, it is convenient with photographic negatives to refer to the ambient radiation as the "pre-exposure."

For small pre-exposures, the detective quantum efficiency of any given type of photographic negative

will be zero. As the pre-exposure rises the detective quantum efficiency will rise and pass through a maximum, as illustrated by the curves in Fig. 4. A partial explanation of this behavior is offered in Section 9.0.

It is a simple matter to transform Eq. (2.6) into a form better suited for practical use. We note that the ambient energy E_a, and the noise equivalent value E_N of the signal energy are given by

$$E_a = M_a\mathcal{E} \tag{2.11}$$

$$E_N = M_s\mathcal{E}/(S/N)_m \tag{2.12}$$

where $\mathcal{E}$ is the energy of the individual photon. By combining the last two equations with Eq. (2.6), we find

$$Q = \mathcal{E}E_a/E_N^2 \tag{2.13}$$

Q may also be expressed in terms of U, the energy per unit area

$$Q = \frac{\mathcal{E}U_a}{AU_N^2} \tag{2.14}$$

where $U = E/A$. Either of the last two equations is suitable for computing the detective quantum efficiency of an actual detector.

For detectors with an electrical output, the integration time T is related to the frequency bandwidth of the detector by $2T\Delta f = 1$. But for photographic negatives the integration time T is of course equal to the duration of the exposure.

The equations derived above involve several unstated simplifications. The quantum efficiency has been assumed to be the same for the ambient radiation as for the signal. This assumption will be justified in the next section by requiring that the ambient radiation and the signal be of the same wavelength distribution. Another simplification is the assumption that the photons are statistically independent; this would be rigorously true if photons obeyed Maxwell-Boltzmann statistics. But photons are "spin zero" particles, and therefore obey Bose-Einstein statistics. Accordingly the simplification mentioned, though well justified for visible light of the luminance ordinarily incident on a photographic negative, is decidedly not justified in the microwave and radio regions of the spectrum.

3.0 Transformation to Photographic Quantities

The detective quantum efficiency Q of a given photographic negative may be expected to depend on the following:

1. The amount of ambient exposure
2. The spectral distribution of the radiation signal
3. The method of development

In this paper, the dependence of Q on the first two items will be discussed. Standard developing conditions are assumed.

In application to photography, the concepts formulated in Section 2.0 may be interpreted as follows. The "noise" in the photographic negative is the density fluctuation from place to place on the surface: if one measures the density with an aperture of area A at a large number of different places on the developed negative, the measured densities will not all be the same. The set of measured densities may be characterized by a mean density that will be denoted simply by D, and by a root-mean-square deviation from D that is denoted by σ. Suppose, then, that the entire surface of a negative is uniformly pre-exposed by the "ambient" radiation, and that on one small region of area A, a small additional radiation "signal" is incident. The noise equivalent value of this signal is the value that produces a density increment equal to the root-mean-square density fluctuation σ measured with apertures of the same area A.

The value of σ will depend, of course on the area A of the aperture, and indeed there is now good evidence[4] that σ varies as $A^{-1/2}$ for apertures substantially larger than the size of the grains in the emulsion. The numerical values given in this paper are for an arbitrarily-chosen aperture 10 μ in diameter.

As indicated in Section 2.0, the symbol U is used to indicate the exposure of the film in ergs per square centimeter. The pre-exposure is denoted by U_a. The amount of additional exposure that produces a density increment equal to the root-mean-square fluctuation σ may be called the noise equivalent exposure U_N, and is given by

$$U_N = \sigma dU/dD \tag{3.1}$$

where dU/dD is the slope of the U vs D curve at the point where the exposure U is equal to U_a. In practice, the slope dD/dU is determined by taking the ratio of small finite increments ΔD and ΔU. Thus U_N may be written

$$U_N = \sigma\Delta U/\Delta D \tag{3.2}$$

The detective quantum efficiency given by Eq. (2.14) now may be written

$$Q = \frac{\mathcal{E}U_a}{A}\left(\frac{\Delta D}{\sigma\Delta U}\right)^2 \tag{3.3}$$

where U_a is the exposure at the middle of the range ΔU.

The results derived in this paper are for 430 mμ radiation. At this wavelength, the energy of a photon is

$$\mathcal{E} = 4.6180 \times 10^{-12} \text{ erg} \tag{3.4}$$

based on $h = 6.6238 \times 10^{-27}$ erg-sec and $c = 2.9979 \times 10^{10}$ cm/sec. The area of the 10-μ circular aperture is

$$A = 78.54 \times 10^{-8} \text{ sq cm} \tag{3.5}$$

The last three relations then yield

$$Q = 0.5880 \times 10^{-5}U_a(\Delta D/\sigma_{10}\Delta U)^2 \tag{3.6}$$

This is the "working" expression for the detective quantum efficiency of photographic negatives. U_a and ΔU must be expressed in ergs per square centimeter.

4.0 The Films

The Eastman Kodak Company has very generously provided sufficient data for the calculation of the detective quantum efficiency of four of its current films. The four films are:

I. Kodak Royal-X Pan Film, Code 6128
II. Eastman Tri-X Panchromatic Negative Film, Type 5233
III. Eastman Plus-X Panchromatic Negative Film, Type 4231
IV. Kodak Panatomic-X Film, Code 5240

The data supplied by Eastman Kodak for these films are representative of the films at the time of manufacture, but it should be recognized that their characteristics can be expected to vary with manufacturing tolerances and may change as improvements are made. The first is sheet film, and the last three are 35mm roll films. The films were manufactured in February 1957.

Table A shows the abbreviations used in this paper for these films, the developing conditions, and the gamma to which the films were developed.

TABLE A
Film Data

Material	Abbreviation	Time	Developer	Gamma
I	Royal-X	5 min	DK-50	0.65
II	Tri-X	6.5 min	SD-28	0.54
III	Plus-X	6.5 min	SD-28	0.79
IV	Pan-X	6 min	D-76	0.67

5.0 Sensitometric Data

Eastman Kodak has supplied density versus log exposure curves for each of the materials. The exposures were made to radiation that had passed through a narrow-band Wratten filter, whose effective wavelength was 430 mμ. The exposures through the filter were calibrated against exposures made with a prism monochromator.

The duration of the sensitometric exposures was 15 sec. There was a significant reciprocity failure at this duration, and the exposures were corrected at a density of 0.38 above base to the exposure that would be required for a 0.1-sec exposure. The reciprocity correction amounted to 0.45, 0.34, 0.29, and 0.29 log exposure units for Materials I through IV respectively.

The density of the film base was 0.22 for all of the materials, and all of the densities in this paper are densities above base (except in Section 7.0 and Fig. 3).

The density D was read off the curves at points separated by 0.1 in $\log_{10}U$. As indicated by Table B, the values of log U at which the densities were read contained 5 in the second decimal place, in order that the mid-points of the intervals between successive values of log U would have zero in the second decimal place. In the Tables I through IV, the value of log U_a in the first column is the logarithm of the value of U_a at the mid-points of the intervals. One hundred times U_a is given in the second column, and the third column shows one hundred times ΔU, where ΔU is defined as the difference between the two adjacent values of U_a in Table B. (For example, for $\log_{10}U_a = -2.00$, the value of 100 U_a is 1.00, and the value of 100 ΔU in the third column is obtained from the values of U_a corresponding to log $U_a = -1.95$ and log $U_a = -2.05$.)

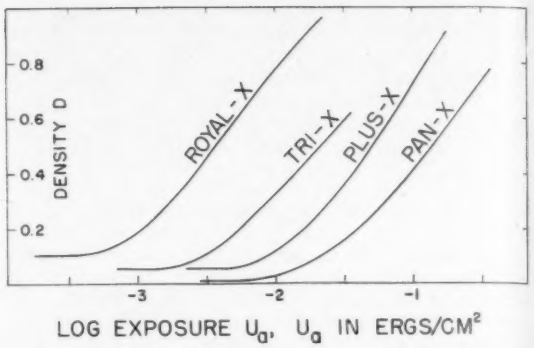

Fig. 1. Optical density of the developed films as a function of the 430 mμ exposure expressed in ergs per square centimeter. The curves are plotted from the data in Table B.

The densities were read off the curves with an estimated reading accuracy of 0.001 density unit. The densities so read were differenced, the differences ΔD were smoothed, and re-summed. The resulting smoothed densities D are shown in Table B, and in the fourth columns of Tables I through IV. Then the differences ΔD were themselves differenced, smoothed, and re-summed. The resulting smoothed ΔD values are shown in the fifth columns of Tables I through IV. This two-step smoothing operation was found necessary to yield values of ΔD that would plot smoothly against log U. The value of ΔD shown in the tables, when multiplied by ten, is the finite difference approximation to the derivative dD/d log U of the D versus log U curve.

The characteristic curves of the four materials are plotted in Fig. 1.

6.0 Granularity

With the aid of the automatic scanning microdensitometer described by Altman and Stultz,[5] the density fluctuation of each type of film was measured—on specimens of four different densities with apertures 10, 20 and 40 μ in diameter. The individual density readings were recorded on punched cards, and the calculation of σ was made on an IBM 705.

The 40 values of σ supplied to the writer by Eastman Kodak are shown in Table C. Each of the 40 values involves 2000 individual density measurements. Actually, the entries in the table are σ_{10}, $2\sigma_{20}$, and $4\sigma_{40}$. If there were no sampling error in the results, and no effects of diffraction, one would expect these three values for the same film to be identical. With two exceptions, this expectation is fairly well

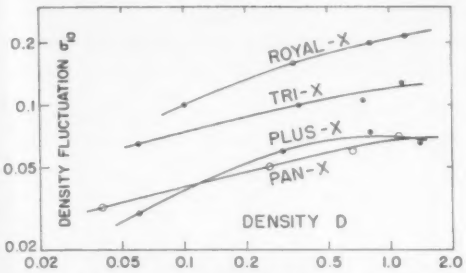

Fig. 2. Root-mean-square density fluctuation as a function of the mean optical density for the four films. The films were uniformly exposed to 430 mμ radiation. The ordinate is the root-mean-square density fluctuation measured with a circular aperture 10 μ in diameter. The points represent the data in the last column of Table C.

confirmed by the numbers in the table. There is a noticeable tendency for the σ_{10} to be perhaps 10% lower than $2\sigma_{20}$ and $4\sigma_{40}$. This would be expected on the basis of the inevitable blurring of the edges of the circular spot by diffraction and the finite thickness of the developed layer. The three values are averaged with equal weight in the last column of Table C, except that the entry 0.260 was given zero weight, and the entry 0.172 was given weight $^1/_3$ relative to unit weight for the other two entries.

The 16 values of σ_{10} in the last column are plotted in Fig. 2 versus the density, and the indicated smooth curve was drawn through the points for each of the four materials. These curves were used to find the values of σ_{10} for intermediate densities. The value of σ_{10} was read from the curve for each of the densities shown in the fourth column of Tables I through IV. The values so read were differenced, smoothed, and re-summed to obtain the values of σ_{10} shown in the sixth column of the tables.

7.0 Wavelength Dependence

The Eastman Kodak Company has also supplied data on the absolute sensitivity versus wavelength characteristics of these four films. The data supplied, however, are not for the same emulsion numbers as those for the other data in this report.

The data were supplied in the form of curves showing the sensitivity (reciprocal of the energy per unit area in ergs per sq cm required to produce a density of 1.0 above the gross fog density) versus the wavelength. This density is of course much higher than the densities at which the detective quantum efficiency is a maximum. Since there is some change in the shape of the H and D curve as the wavelength is varied, the curves should be used with caution.

As the wavelength is varied, one would expect the detective quantum efficiency to vary in proportion to the sensitivity divided by the wavelength. If we denote the sensitivity as defined above by $S(\lambda)$, then the function

$$W(\lambda) = S(\lambda)/\lambda$$

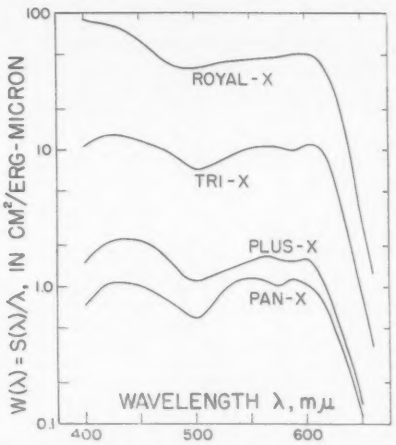

Fig. 3. Sensitivity divided by the wavelength as a function of the wavelength. The sensitivity is the reciprocal of the number of ergs per square centimeter required to produce a density of 1.0 above gross fog. The sensitivity divided by the wavelength is in the units: square centimeters per erg-micron.

will vary with wavelength in the same way as the detective quantum efficiency. That is to say, the detective quantum efficiency at the wavelength λ is given by

$$Q(\lambda) = Q(430)W(\lambda)/W(430)$$

We might have chosen to plot $Q(\lambda)$,$W(\lambda)$ or $W(\lambda)/W(430)$. We chose to plot $W(\lambda)$ in Fig. 3 because this choice not only preserves all of the information in the original data, but also provides a separation among the four curves.

The values of $W(430)$ for Materials I through IV are 78.8, 12.67, 2.196, and 1.078 sq cm/erg per micron. Thus if one wishes to find the values of $Q(\lambda)$ that correspond to the values of $Q(430)$ shown in Table D, the values of $W(\lambda)$ shown in Fig. 3 must be multiplied by the factors 0.01137, 0.0464, 0.281, or 0.274 respectively.

8.0 Numerical Results

The second, third, fifth, and sixth columns of Tables I through IV contain the information required for the calculation of the detective quantum efficiency by Eq. (3.6).

The result of the calculation is shown in the seventh column of the tables; the value of Q is tabulated in percent. The detective quantum efficiency Q is plotted in Fig. 4 versus the exposure U, and in Fig. 5 against the gradient $g = dD/d \log_{10}U$, approximated by ten times ΔD.

Both of the figures indicate clearly that the detective quantum efficiency has a maximum value within the range of exposures included in the calculations. Table D lists a number of properties associated with

TABLE B

Film Density versus Exposure

$\log_{10}U_a$ ergs/sq cm	Density D			
	Royal-X	Tri-X	Plus-X	Pan-X
−3.55	0.105			
−3.45	0.105			
−3.35	0.110			
−3.25	0.121			
−3.15	0.141			
−3.05	0.170			
−2.95	0.207	0.055		
−2.85	0.251	0.055		
−2.75	0.302	0.050		
−2.65	0.360	0.073		
−2.55	0.422	0.095	0.051	
−2.45	0.487	0.124	0.051	0.009
−2.35	0.552	0.161	0.054	0.009
−2.25	0.617	0.204	0.063	0.010
−2.15	0.681	0.251	0.079	0.014
−2.05	0.742	0.300	0.103	0.022
−1.95	0.801	0.350	0.134	0.035
−1.85	0.859	0.401	0.173	0.054
−1.75	0.913	0.453	0.218	0.078
−1.65	0.964	0.506	0.269	0.107
−1.55		0.560	0.326	0.141
−1.45		0.614	0.388	0.180
−1.35			0.455	0.223
−1.25			0.526	0.270
−1.15			0.601	0.322
−1.05			0.679	0.378
−0.95			0.758	0.438
−0.85			0.837	0.500
−0.75			0.916	0.565
−0.65				0.631
−0.55				0.698
−0.45				0.765

TABLE C

Granularity Data

D	σ_{10}	$2\sigma_{20}$	$4\sigma_{40}$	$(\sigma_{10})_{Av}$
		Royal-X		
0.10	0.097	0.102	0.100	0.100
0.34	0.147	0.168	0.164	0.160
0.80	0.260	0.206	0.192	0.199
1.18	0.186	0.230	0.232	0.216
		Tri-X		
0.06	0.056	0.074	0.064	0.065
0.36	0.085	0.104	0.128	0.106
0.74	0.090	0.112	0.116	0.106
1.14	0.122	0.122	0.172	0.129
		Plus-X		
0.06	0.030	0.030		0.030
0.30	0.061	0.058		0.060
0.80	0.074	0.074		0.074
1.40	0.069	0.062		0.066
		Pan-X		
0.04	0.029	0.034		0.032
0.26	0.048	0.054		0.051
0.66	0.057	0.062		0.060
1.10	0.076	0.066		0.071

TABLE D

Parameters Corresponding to the Maximum Value of Q

Film	Q_{max} (per cent)	g	g/γ	$\log_{10}U_a$	D
Royal-X	0.895	0.416	0.640	−2.94	0.211
Tri-X	0.588	0.370	0.685	−2.40	0.142
Plus-X	0.618	0.310	0.392	−2.00	0.118
Pan-X	0.295	0.260	0.388	−1.75	0.078

TABLE E

Film Data for Figure 6

Film	Abbreviation	Developer	Time (min)
Kodak Aerographic Tri-X Panchromatic	Tri-X	D-19	8
Kodak Aeromap Super-XX	Super-XX	D-19	8
Kodak Panatomic-X Panchromatic	Pan-X	D-76	12
Eastman Fine Grain Panchromatic Duplicating Negative	FG Neg.	D-76	6

TABLE I

Calculation of Q for Royal-X Film

$\log_{10}U_a$ (Exposure U is in ergs/sq cm)	100 U_a	100 ΔU	D	10 ΔD	σ_{10}	Q (per cent)
−3.4	0.03981	0.009191	0.1075	0.045	0.1040	0.0519
−3.3	0.05012	0.01156	0.1155	0.115	0.1070	0.255
−3.2	0.06311	0.01456	0.1310	0.197	0.1120	0.541
−3.1	0.07944	0.01834	0.1555	0.282	0.1200	0.767
−3.0	0.1000	0.02307	0.1885	0.365	0.1294	0.879
−2.9	0.1259	0.02910	0.2290	0.444	0.1392	0.889
−2.8	0.1585	0.03650	0.2765	0.514	0.1487	0.836
−2.7	0.1995	0.04610	0.3310	0.573	0.1575	0.730
−2.6	0.2512	0.05791	0.3910	0.618	0.1654	0.615
−2.5	0.3162	0.07301	0.4545	0.643	0.1726	0.484
−2.4	0.3981	0.09191	0.5195	0.650	0.1790	0.365
−2.3	0.5012	0.1156	0.5845	0.644	0.1848	0.268
−2.2	0.6311	0.1456	0.6490	0.625	0.1900	0.189

TABLE II

Calculation of Q for Tri-X Film

$\log_{10}U_a$ (Exposure U is in ergs/sq cm)	100 U_a	100 ΔU	D	10 ΔD	σ_{10}	Q (per cent)
−2.8	0.1585	0.03650	0.0575	0.050	0.0645	0.042
−2.7	0.1995	0.04610	0.0665	0.125	0.0667	0.194
−2.6	0.2512	0.05791	0.0840	0.210	0.0706	0.390
−2.5	0.3162	0.07301	0.1095	0.295	0.0754	0.534
−2.4	0.3981	0.09191	0.1425	0.370	0.0804	0.587
−2.3	0.5012	0.1156	0.1825	0.430	0.0854	0.559
−2.2	0.6311	0.1456	0.2275	0.470	0.0902	0.475
−2.1	0.7944	0.1834	0.2755	0.490	0.0946	0.372
−2.0	1.000	0.2307	0.3250	0.504	0.0986	0.289
−1.9	1.259	0.2910	0.3755	0.515	0.1021	0.222
−1.8	1.585	0.3650	0.4270	0.525	0.1051	0.174
−1.7	1.995	0.4610	0.4795	0.534	0.1076	0.136
−1.6	2.512	0.5791	0.5330	0.540	0.1096	0.107

TABLE III
Calculation of Q for Plus-X Film

$\log_{10}U_a$ (Exposure U is in ergs/sq cm)	$100\,U_a$	$100\,\Delta U$	D	$10\,\Delta D$	σ_{10}	Q (per cent)
−2.3	0.5012	0.1156	0.0585	0.090	0.0295	0.205
−2.2	0.6311	0.1456	0.0710	0.162	0.0327	0.430
−2.1	0.7944	0.1834	0.0910	0.237	0.0369	0.573
−2.0	1.000	0.2307	0.1185	0.312	0.0417	0.618
−1.9	1.259	0.2910	0.1535	0.383	0.0467	0.588
−1.8	1.585	0.3650	0.1955	0.450	0.0516	0.532
−1.7	1.995	0.4610	0.2435	0.512	0.0561	0.460
−1.6	2.512	0.5791	0.2975	0.570	0.0600	0.398
−1.5	3.162	0.7301	0.3570	0.624	0.0632	0.340
−1.4	3.981	0.9191	0.4215	0.673	0.0657	0.291
−1.3	5.012	1.156	0.4905	0.716	0.0675	0.248
−1.2	6.311	1.456	0.5635	0.752	0.0688	0.209
−1.1	7.944	1.834	0.6400	0.776	0.0697	0.172
−1.0	10.00	2.307	0.7185	0.790	0.0703	0.140
−0.9	12.59	2.910	0.7975	0.790	0.0706	0.109
−0.8	15.85	3.650	0.8765	0.790	0.0706	0.088

TABLE IV
Calculation of Q for Pan-X Film

$\log_{10}U_a$ (Exposure U is in ergs/sq cm)	$100\,U$)	$100\,\Delta U$	D	$10\,\Delta D$	σ_{10}	Q (per cent)
−2.2	0.6311	0.1456	0.0120	0.040	0.0237	0.050
−2.1	0.7944	0.1834	0.0180	0.080	0.0262	0.129
−2.0	1.000	0.2307	0.0285	0.126	0.0291	0.207
−1.9	1.259	0.2910	0.0445	0.177	0.0323	0.262
−1.8	1.585	0.3650	0.0660	0.230	0.0356	0.292
−1.7	1.995	0.4610	0.0925	0.283	0.0388	0.294
−1.6	2.512	0.5791	0.1240	0.336	0.0419	0.283
−1.5	3.162	0.7301	0.1605	0.388	0.0448	0.262
−1.4	3.981	0.9191	0.2015	0.437	0.0475	0.235
−1.3	5.012	1.156	0.2465	0.483	0.0500	0.206
−1.2	6.311	1.456	0.2960	0.524	0.0523	0.176
−1.1	7.944	1.834	0.3500	0.562	0.0544	0.148
−1.0	10.00	2.307	0.4080	0.595	0.0564	0.123
−0.9	12.59	2.910	0.4690	0.623	0.0582	0.100
−0.8	15.85	3.650	0.5325	0.645	0.0599	0.0811
−0.7	19.95	4.610	0.5980	0.661	0.0614	0.0640
−0.6	25.12	5.791	0.6645	0.670	0.0628	0.0501
−0.5	31.62	7.301	0.7315	0.670	0.0640	0.0382

the maximum value of Q; the table includes the maximum value of Q, the gradient g at the maximum, the ratio g/γ of this gradient to gamma, the exposure U, and the density D. The numerical values of all of these quantities, except Q itself, are not too well determined by the data, since a slight change in the smoothing operations could conceivably shift the position of the maximum by an appreciable amount.

In a prior publication[6] the writer has determined the noise equivalent energy E_N for a set of four different Kodak films that were described in the literature in 1945 and 1946.[7] The films are described in Table E; for further information about these films, the reader is referred to the cited 1955 publication. The detective quantum efficiency has also been calculated for these films, with the data and methods of reduction described in Ref. 6. The results are shown in Fig. 6. As described in the next section, the results in Fig. 6 are much less reliable than those in Figs. 4 and 5.

9.0 Discussion

All of the detective quantum efficiency curves in Figs. 4, 5, and 6 show a maximum for an intermediate value of the pre-exposure U_a. The qualitative reasons for the existence of this maximum are easy to understand. It is well known that in order for a grain to become developable, the grain must be acted on by a number of photons, of the order of magnitude 10. At exposures much less than that for Q_{max}, the large majority of the incident photons are wasted on grains that receive less than the necessary number to become developable. On the other hand, for exposures much greater than that of the maximum, a large majority of the incident photons are wasted on grains that have already received a number sufficient to make them developable. At some intermediate exposure, corresponding to the maximum, there is a situation in which these two tendencies are balanced. It must be understood that this argument is qualitative, and cannot be made the basis of a detailed analysis.

The detective quantum efficiency is one of the best single measures of the detecting ability of a photographic negative. More precisely, as one changes

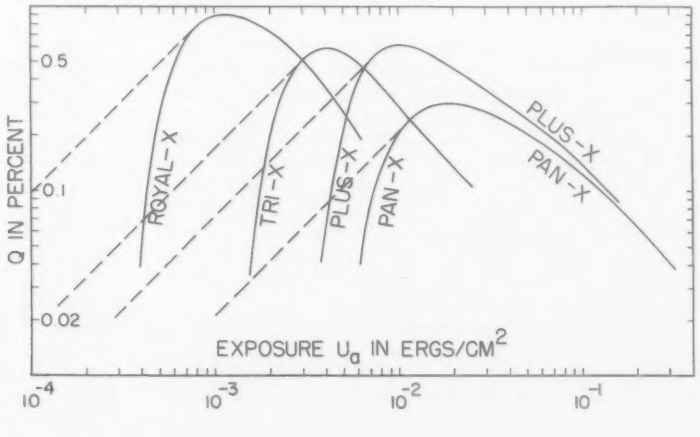

Fig. 4. Detective quantum efficiency as a function of the exposure in ergs per square centimeter for 430 mμ radiation. The results are for the standard developing conditions shown in Table A. The data are from the last columns of Tables I through IV.

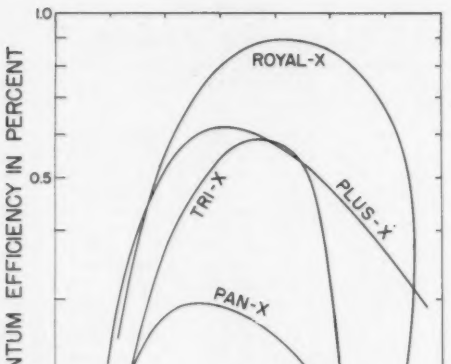

Fig. 5. Detective quantum efficiency as a function of the gradient of the D versus $\log_{10}U$ curve (H and D curve) for 430 mμ radiation. The quantity 10 times the value of ΔD (that corresponds to an increment of 0.1 in $\log_{10}D$) is the finite increment approximation to the gradient $dD/d\log_{10}U$ of the H and D curve. All of the curves are multi-valued as a function of the gradient, but only the curve for Royal-X is shown explicitly as a multi-valued function. The data plotted are the same as those shown in Fig. 4; however, a different abscissa is used here.

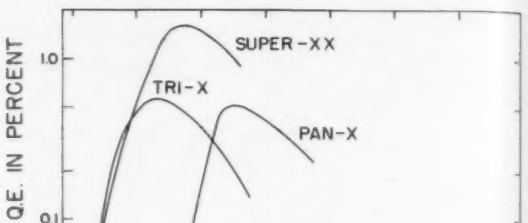

Fig. 6. Detective quantum efficiency as a function of the 420 mμ exposure in ergs per square centimeters for a different set of four films. As indicated in the text, the results are of much lower reliability than those shown in Figs. 4 and 5. The films and the developing conditions are described in Table E.

the size of the grains in an emulsion, a constant value of Q would indicate an optimum swapping of freedom-from-granularity for detectivity. In the light of this comment, it is interesting to observe that the maximum value of Q for the Royal-X, Tri-X, and Plus-X films is within plus or minus 17% of the value 0.75%. The maximum value of Q for the Pan-X film is definitely lower. Indeed, the inferior performance of the Pan-X film is also noticeable in the energy detectivity and contrast detectivity of this same group of films.

To be sure, the scattering of light in the undeveloped film is an important limitation on the ability of these films to resolve detail, and the detective quantum efficiency fails to take this aspect of image structure into account. And indeed, examination of the resolving power values for Plus-X and Pan-X (95 and 130 lines per millimeter respectively), indicates that the particular usefulness of Pan-X film lies in its smaller light-scattering power relative to Plus-X. This smaller light-scattering power is not evident in the granularity data, and indicates a basic difference in the structure of the emulsion.

For each of the films shown in Fig. 4, one notes that the detective quantum efficiency Q drops off quite rapidly as the exposure U is decreased below the value at the maximum of the curve. It can be shown, however, that by pre-exposing the film we may ensure that at low exposures Q will never decrease faster than the exposure itself. The dashed lines in Fig. 4 show the way that Q decreases if the optimum pre-exposure is used. The optimum amount of pre-exposure is the amount which, when it is added to the ambient exposure, produces a total exposure equal to the exposure at the point where the dashed line is tangent to the curve.

As an example consider the detective quantum efficiency of Royal-X film at the exposure 4×10^{-4} erg/sq cm. Figure 4 indicates the value $Q = 0.052\%$. But by pre-exposing with another 4×10^{-4} erg/sq cm to produce a total of 8×10^{-4} erg/sq cm, the detective quantum efficiency is raised to 0.38% as indicated by the dashed line. This is a gain by a factor of more than 7.

It can be shown that the point where the curves in Fig. 4 have a slope of +1 corresponds to the exposure at which the energy detectivity has its maximum value. Thus the point where the dashed lines are tangent to their respective curve is the point corresponding to the maximum energy detectivity. Similarly, the point where the curves in Fig. 4 have a slope of −1 corresponds to the exposure at which the contrast detectivity has its maximum value. These facts will be established in a later paper.

As indicated in detail in Ref. 6, the sensitometric data for the films of Table E and Fig. 6 apply to films manufactured about 5 years later than the film for which the granularity data were obtained. For this reason, the reliability of the data in Fig. 6 is far inferior to that in Figs. 4 and 5. No significance may be ascribed to the fact that the Super-XX film of Fig. 6 has a higher detective quantum efficiency (1.6%) than any of the more recent films, and little significance to the fact that the Q of the Super-XX film is higher than that of the 1946 Tri-X and Pan-X films. It is significant, however, that the detective quantum

efficiency of the Fine Grain Duplicating Film is much lower than that of the other three films in Fig. 6. It is clear that in this film the swapping of freedom-from-granularity for detectivity has been far from optimum.

The value of the detective quantum efficiency Q for a given film depends on the ambient exposure U_a, the wavelength λ of the radiation and on the method of development. The dependence on U_a is shown explicitly in the tables and in Figs. 4, 5, and 6. The dependence on the wavelength is shown in Fig. 3. The value of Q is independent of the area A. In this paper, only the standard method of development specified in Table I is considered.

The writer believes that the detective quantum efficiency is a sufficiently fundamental property of a film that it will be found to be relatively insensitive to the method of development, but at present this is only a hypothesis.

We conclude this section with a discussion of the data illustrated in Figs. 1 and 2, relating to the sensitometric curve, and to the granularity.

The sensitometric curves of the four films are all different. The Royal-X curve has a gradient that falls off rapidly after reaching its maximum gradient, but the other three curves, particularly the Tri-X and Plus-X, have a long straight line portion after the maximum gradient is reached. In the toe region, the Tri-X curve is different from the others in that the gradient increases rapidly at first, and then increases at a much slower rate; at $\log U = -2.1$, the gradient is already 0.49, but it does not reach its maximum value of 0.54 until $\log U = -1.6$.

In the granularity curves (σ versus D) in Fig. 2, there is a clear tendency for the Tri-X and Pan-X data to have lower slopes than the other two films. On the other hand the data for the Plus-X film is unique in indicating a maximum in σ near the density $D = 1.0$. All of the curves show a lower average slope than the slope 0.4 indicated by the granularity data published in 1946 by L. A. Jones and G. C. Higgins,[6,7] although the beginning portions of the Royal-X and Plus-X curves do have a slope of about 0.4. (The slope here considered is the derivative $d \log \sigma / d \log D$.)

Acknowledgment

The writer wishes to thank the Research Laboratories of the Eastman Kodak Company for supplying data not previously released. He is indebted to many people at the Eastman Kodak Company for discussions about the subject matter of this paper and related problems. He wishes to thank particularly Hans Zweig, Robert Wolfe, Joseph Altman, Frederick Kottler, George C. Higgins, John Tupper, Otto Sandvik, and J. A. Leermakers.

References

1. Rose, Albert, "A Unified Approach to the Performance of Photographic Film, Television Pickup Tubes, and the Human Eye," *J. SMPE*, *47:* 273–94 (1946). [A more detailed discussion is given by Rose in *Advances in Electronics*, L. Marton, ed., *1:* 131–66, Academic Press, Inc., New York, 1948.]
2. Fry, Thornton C., *Probability and its Engineering Uses*, Van Nostrand, New York, 1928, pp. 216–27.
3. Levy, H., and Roth, L., *Elements of Probability*, Oxford University Press, London, 1936, pp. 142–45.
4. Zweig, Hans J., "Autocorrelation and Granularity," *J. Opt. Soc. Am.*, *46:* 805–20 (1956).
5. Altman, J. H., and Stultz, K. F., "Microdensitometer for Photographic Research," *Rev. Sci. Inst.*, *27:* 1033–36 (1956).
6. Jones, R. Clark, "On the Minimum Energy Detectable by Photographic Negatives," *Phot. Sci. Tech.*, *2:* 56–65 (1955).
7. Jones, L. A., and Higgins, G. C., "Photographic Granularity and Graininess," Part I, *J. Opt. Soc. Am.*, *35:* 435–75 (1945); Part II, *ibid.*, *36:* 203–27 (1946).

PHOTOGRAPHIC SCIENCE AND ENGINEERING
Volume 2, Number 2, August 1958

The Evaluation of Optical Images

GEORGE C. HIGGINS AND FRED H. PERRIN, *Research Laboratories, Eastman Kodak Company, Rochester, N.Y.*

It is shown that the quality of a photograph cannot be indicated adequately by any single number. The point and the line spread-functions are defined and the relation of the latter to resolving power, acutance, and the sine-wave response is outlined. Resolving power and acutance are shown to be independent of each other and are explained on the basis of the character of the spread function. The significance of the power spectrum and the manner in which it can be used to design a photographic system, even in the presence of granularity, are shown. A practical example of the application of some of these procedures to predicting the appearance of photographs is presented.

We shall attempt to evaluate the aspect of an image that is associated with the clarity by which detail is reproduced. This aspect of the image is referred to as *definition*.[1]

It should be emphasized at once that no single number can be attached to any system to describe completely its capability of reproducing detail clearly. The three pictures in Fig. 1 were devised to demonstrate this point.*

In the large picture, the definition is good in the flowers and in the hands of the two women. On the other hand, the faces of the women are somewhat lacking in definition and the faces of the men are definitely out of focus. The over-all definition in this picture is poor, even though the definition in the flowers and the women's hands is good.

This picture was made to have good definition along a central horizontal strip and progressively poorer definition towards the top and bottom edges. How, then, can a single number adequately indicate the definition of this picture as a whole? One method of deriving an index might be to weight the different areas, as has been done in photogrammetry. The procedure is to divide the picture into elementary areas, attach a definition index to each area, and average the individual indices. This is rather difficult, and furthermore it is questionable in many cases whether the single index thus laboriously derived would have any meaning.

In the medium-sized picture, the definition in the women's faces is good but the definition of the men's faces, although improved, is still not satisfactory. The third picture is unpleasantly small, but its definition is good throughout. The men as well as the women and the flowers all appear to be quite sharp. If we were to attach a single index of definition to the pictures, we would say that the smallest picture has good definition, the medium-sized picture fair definition, but the men are still poorly defined, while the largest picture has poor definition although certain regions are sharp.

These three pictures were all made from a single negative that was prepared by R. N. Wolfe, of these Laboratories. The only thing that is different is the size of the picture and consequently the angle under which it is viewed. The same effect could be obtained by viewing the largest picture from varying distances. In other words, to evaluate an image, we have to know not only the physical characteristics of the image throughout the whole picture area but also the conditions under which the image is to be viewed.

We shall now discuss methods of following the image through the photographic system without considering the manner in which a single number might be attached to the results. If the object space is assumed to consist of a large number of luminous points, each of which is imaged as a point by a lens and film combination, the image can be studied by considering the manner in which these points are individually imaged. The total image is obtained by simply summing the contributions from each of the points. As is well known, even for a perfect lens the image is not a point, but is a "mound" of light spreading over a significant area. This spreading of light is caused by diffraction and is a consequence of the undulatory nature of radiation. The spreading caused by the aberrations of individual lenses is added to this basic diffraction pattern.

The three images at the bottom of Fig. 2 are photomicrographs of the image of a point formed by a certain lens at three different positions.[2] The axial image is at A. Although this is a fairly small symmetrical spot, it is definitely not a point. The other images are at increasing distances from the axis, and they are increasingly asymmetrical. Image C, at the outer part of the field, bears little resemblance to a point.

Based on a paper of the same title presented at the Annual Conference, Asbury Park, N.J., 11 September 1957. Received 11 December 1957.

* At the lecture, sheets bearing these pictures were distributed to the audience.

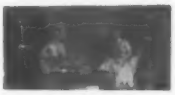

Fig 1. Especially prepared photograph at three different scales (1:3:6.5) to show how judgment of definition is affected by the angle subtended by details at the eye. The picture decreases in acutance from the center to the top and to the bottom.

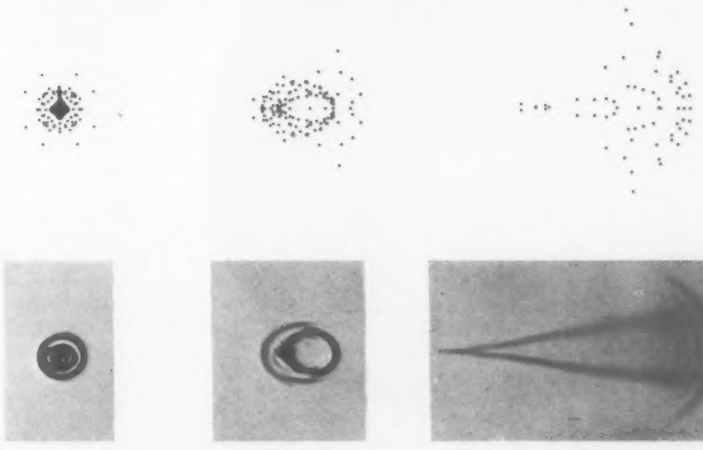

Fig. 2. Comparison between photomicrographs of images of a point object at selected places in the field of a certain lens and the corresponding spot diagrams computed from the design data. Image A is on the axis.

The spot diagrams above the three images in Fig. 2 represent the distribution of light in the images, as calculated from the lens specifications by a formula that M. Herzberger, of these Laboratories, has developed.[3] The correspondence between the calculated spot diagrams and the photomicrographs of the actual images is obviously very close.

We shall now consider in more detail how the image of an object point is carried through a photographic system. If the lens is so free from aberrations that it is essentially limited by diffraction alone, the image consists of a minute disk surrounded by weak rings. A photomicrograph of such an image (Fig. 3), made by R. L. Lamberts, of these Laboratories, was made so as to emphasize the ring pattern surrounding the central disk. The arrangement with which this image was made is shown diagrammatically in Fig. 4. If this image is scanned with a microphotometer having a pinhole aperture and if the path of the aperture passes directly through the center of the image, the resulting trace is a curve of illuminance as a function of distance having a shape somewhat like that shown at the bottom of the figure. This distribution of illuminance in the image of the point measured by scanning with a small spot is known as the *point spread-function*.

This point spread-function is a valuable tool but is almost impossible to measure. In the first place, it is necessary to scan precisely through the center of the image pattern, and in the second place, a pinhole aperture that is small enough to produce a significant scan is so small that little energy is available for operating the microphotometer. In addition, when the image is asymmetrical, the shape of the point spread-function as measured depends upon the direction in which the scan is made.

Let us consider again a diffraction-limited lens whose image of a point is a disk surrounded by a series of concentric circles. However, as shown in Fig. 5, this time let us assume the aperture of the microphotometer to be a long slit instead of a pinhole. In this case, it is easily seen that the illuminance as measured by the microphotometer will never fall to zero and so the resulting trace will have the shape shown at the bottom of the figure. This distribution of illuminance in the image of the point as evaluated with a slit (which integrates in one direction) is known as the *line spread-function*. While the point spread-function is two-dimensional in that it shows how illuminance varies in both the x- and the y-directions, the line spread-function shows the variation in only one direction, the energy being integrated in the perpendicular direction according to the formula

$$A(x) = \int_{-\infty}^{\infty} a\,(x, y)\,dy, \tag{1}$$

where $A(x)$ is the line spread-function and $a(x, y)$ is the point spread-function. These functions are expressed in terms of illuminance.

It is much easier to measure the line spread-function than the point spread-function, since the long slit allows more energy to enter the microphotometer than does the pinhole. In addition, since the integration takes place in only one direction, the original source may be a narrow, bright line instead of a point, and its image can be scanned with a slit oriented parallel to the line source.

Now let us assume that a parallel beam of light falls on a knife-edge and that this knife-edge source is imaged with a lens, as sketched in Fig. 6. The problem is to determine the type of image that is obtained from this knife-edge source. Imagine that the region beyond the knife-edge is divided into infinitely narrow, bright strips, of which four are sketched in the figure. Each of these strips serves as a line source, and its image is by definition the line spread-function $A(x)$ of the lens. The resultant illuminance is simply the sum of these spread functions. For example, the illuminance at the point x_0 is the sum of the ordinates of the line spread-functions at that point, and as the elementary strips become narrower and correspondingly more numerous, at the limit the sum will be I_{x_0}, the actual illuminance at x_0. If this figure is studied carefully, it will be seen that the illuminance at x_0 can be represented by the integral

$$I_{x_0} = \int_{-\infty}^{x_0} A(x)\,dx, \tag{2}$$

where $A(x)$ is the line spread-function of the lens. If the line spread-function is known, therefore, the distribution of energy in the image of the knife-edge can be calculated by this simple integral equation.

And the process can be reversed. If the edge function is the integral of the line spread-function, then the line spread-function must be the derivative of the edge function, or

$$A(x) = dI/dx. \tag{3}$$

This means that the line spread-function of a lens can

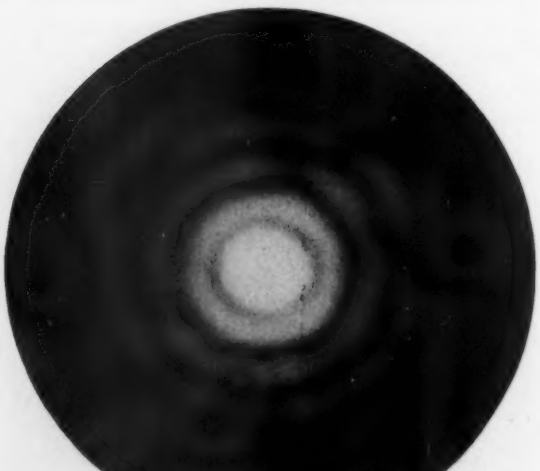

Fig. 3. Photomicrograph of image of point object formed by diffraction-limited lens, showing Airy pattern.

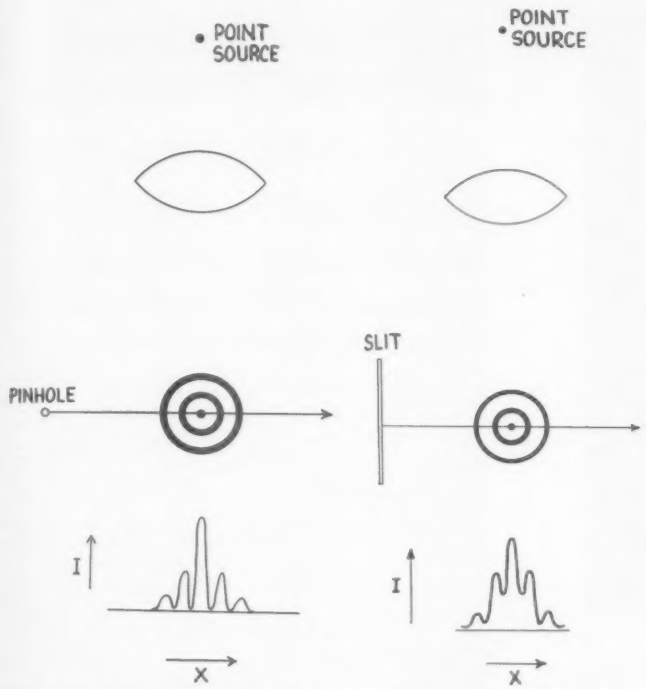

Fig. 4. Method of forming and scanning a point spread-function and graph of the function.

Fig. 5. Method of integrating a point spread-function with a slit to form a line spread-function, and graph of the latter.

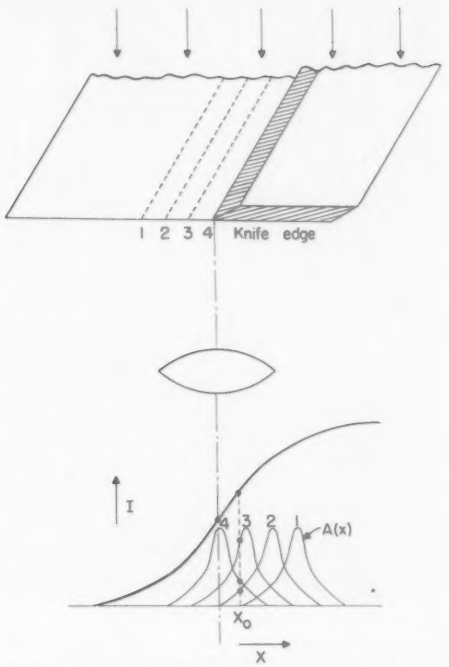

Fig. 6. Geometrical illustration of the convolution of a semi-infinite plane with the line spread-function of a lens. Each linear element of the illuminated area (of which four are shown) forms its own spread function $A(x)$, and the sum of these is the image of the entire edge. The summation is indicated for x_0.

be calculated by using the lens to form the image of a knife-edge, tracing this image, and then plotting the slope dI/dx as a function of the distance x across the image.

This technique can be used to construct the image of the resolving-power test object. The type of test object that has been used in the Kodak Research Laboratories[4] for many years to measure resolving power is shown in Fig. 7. It is imaged on the film on a microscopic scale so that the sets of bars or lines have the indicated spatial frequencies in lines per millimeter. After the film is processed, the images are examined in a microscope. The coarse bars are distinguishable individually or *resolved*, but the fine ones merge into one another. The greatest spatial frequency (narrowest bars and spaces) for which the bars can be resolved is said to be the resolving-power limit.

The distribution of illuminance in such a test object is shown at the top of Fig. 8. If each of the bright bars is considered to be made up of a large number of elementary narrow, bright lines, the image can be completely reconstructed. Consider just one of the elementary lines in each of two adjacent bars, B_1 and B_2, as shown by the dotted lines. The distribution of illuminance in the image of line B_1 is the line spread-function, shown as B'_1 in the middle of the figure. The same relation exists between B_2 and B'_2. To reconstruct the entire test object, it would be necessary to add the spread functions corresponding to all the elementary lines that constitute each of the two bars. For the purpose of illustration, however, the bars in this test object can be considered as consisting of merely the two elementary lines shown. The addition of these spread functions gives the distribution of energy in the complete image, as shown by the broken curve $B'_1 + B'_2$ in this figure.

While the illuminance in the image of the dark interspace should be zero, it is clear that it is actually not zero but that there is a contribution from both of the bars on each side. This illumination comes from the light that is spread out of the image of the two bars and is obtained at the expense of the illumination within the geometrical images of the bars themselves. Thus the amplitude A' in the image is less than the amplitude A of the luminance distribution in the original test object.

This same construction can be carried out for a range of spatial frequencies, and the resulting values of amplitude A', when plotted against frequency, would give a curve somewhat like the one at the bottom of the figure. This method of plotting amplitude as a function of line frequency is very useful for representing the fidelity with which a target of this type is reproduced. For the curve shown in this figure, the amplitude drops to practically zero at about 100 lines

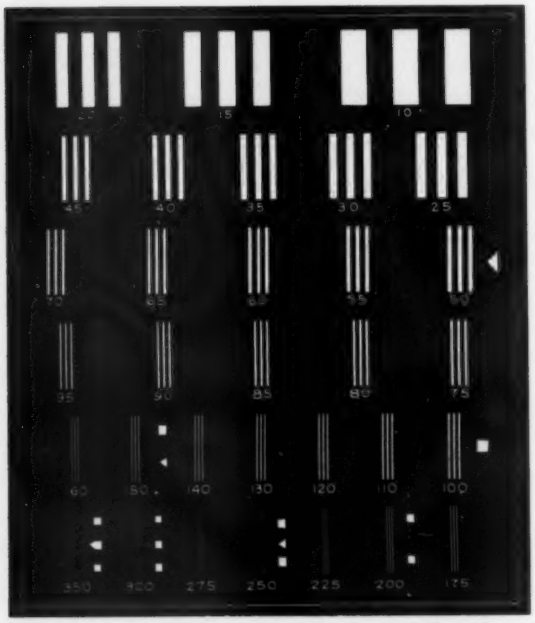

Fig. 7. Typical test object for measuring the resolving power of photographic materials. The numbers (which are not on the test object itself) indicate spatial frequency in lines per millimeter when the test object is used in the camera for which it was designed.

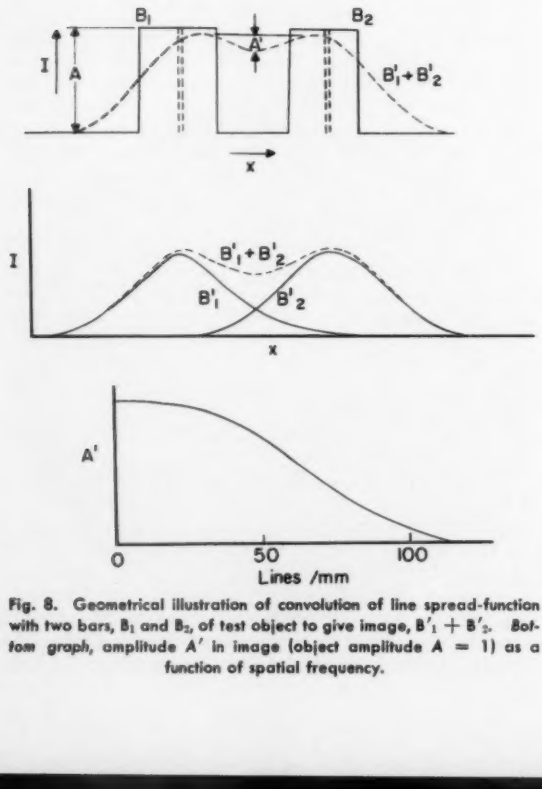

Fig. 8. Geometrical illustration of convolution of line spread-function with two bars, B_1 and B_2, of test object to give image, $B'_1 + B'_2$. *Bottom graph*, amplitude A' in image (object amplitude $A = 1$) as a function of spatial frequency.

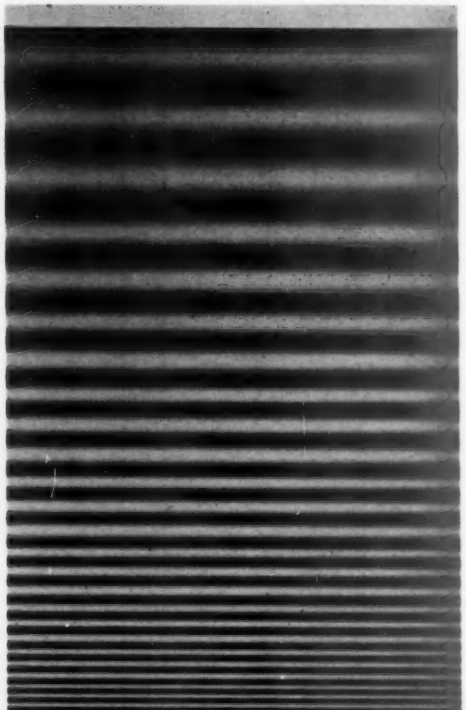

Fig. 9. Sinusoidal resolving-power test object of graded spatial frequency.

per millimeter, and this value might be taken as the resolving power of the system.

Although test objects in which the luminance changes abruptly at the edges of the bars have been used extensively in the past, another type has come into use in recent years. It is known as the sinusoidal type because, as can be seen in Fig. 9, the variation in luminance follows a sine law. The sinusoidol variation is not clearly apparent in the figure, partly because of the inevitable loss of fidelity in reproduction and partly because the variation is sinusoidal in transmittance whereas the visual response is more nearly logarithmic.

The sinusoidal pattern can be treated exactly like the bar pattern of Fig. 8. Let the sine curve S in Fig. 10 having an amplitude A represent the luminance of the test object. Imagine as before that the pattern is divided into elementary bright lines, each of which forms its own spread function, as shown in the graph in the middle of the figure. In contrast to the preceding case, the heights of the spread functions now are not constant but are related to the luminance in the pattern. Thus the spread function representing the elementary line at *c* is lower than the spread function representing the line at *b*, although its shape is the

same. When all the elementary, bright lines comprising the test-object pattern are summed up, the result is a sinusoidal curve S′ with amplitude A' as shown. This operation can be expressed mathematically by the integral

$$A = \int_{-\infty}^{\infty} A(x) \cos 2\pi n x \, dx, \qquad (4)$$

where $A(x)$ is the spread function and n is the spatial frequency. If the separation of the peaks or "wavelength" is λ, then $n = 1/\lambda$. As in the case of the bar pattern, if the amplitude A' is evaluated for a series of spatial frequencies and then plotted against frequency or $1/\lambda$, the solid curve shown in the bottom graph of the figure is obtained. This is commonly called the *sine-wave response curve*.

Attempts have been made to use the sine-wave response for indicating image quality by a single number. One such attempt involves drawing the rectangular broken curve that includes the same area as the sine-wave response and has the same height as this curve at zero frequency. The index of quality would then be a single number n_e on the frequency axis. The difficulty with this procedure is that this number n_e does not specify uniquely the shape of the response curve. Thus the dotted curve would lead to the same value of n_e as the solid curve but it would represent a higher response below n_e and a lower response beyond.

So far only objective criteria have been discussed. The methods of predicting resolving power and of computing the sine-wave response from the line spread-function have been described, but nothing has been said about the importance of resolving power or the sine-wave response from a practical standpoint. Wolfe and his associates[1,5] studied the relation between resolving power and definition a few years ago and found that resolving power correlated very poorly with definition, which is the ability to reproduce detail clearly. In some instances, as will be shown later, resolving power was found to be completely misleading. That is, pictures having a high resolving power may have poor definition while other pictures having a low resolving power may have good definition. It is because of these results that experiments were performed to find a new property of the image which could be associated significantly with definition. This property was termed *acutance*.

Although there are times when the ability to distinguish repetitive detail, which is measured by resolving power, is important, the manner in which well-resolved details are reproduced is usually of still greater importance. That is, the significant feature of a photograph from the standpoint of definition is the manner in which edges are reproduced. When an image of a knife-edge is formed, the distribution of illuminance in the image is somewhat as shown in Fig. 11. In this figure, the ordinates represent the logarithm of illuminance because the eye responds more nearly logarithmically than it does linearly. To determine acutance,[6] the curve is divided into short segments, with Δx along the axis of abscissas, and

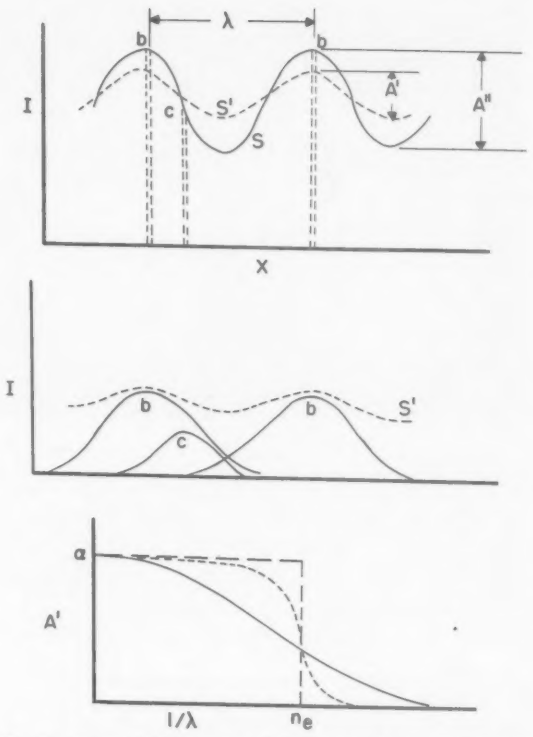

Fig. 10. Geometrical illustration of convolution of line spread-function with two cycles of sinusoidal test object S to give image S′. *Bottom graph*, solid curve, sine-wave response (image amplitude A' for object amplitude $A'' = 1$ as a function of spatial frequency $1/\lambda$); broken curve, rectangular graph having same value of α for $1/\lambda = 0$ as solid curve and containing the same area; dotted curve, illustrative intermediate curve.

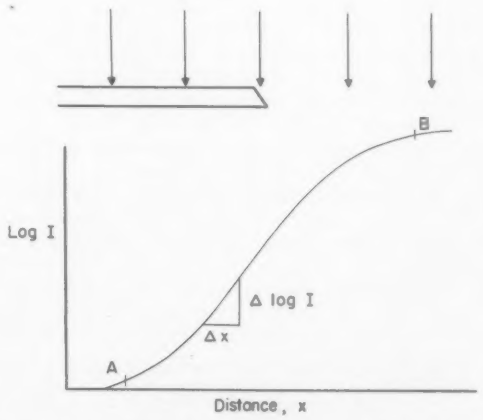

Fig. 11. Edge trace of image of a knife-edge, showing analysis for computing acutance.

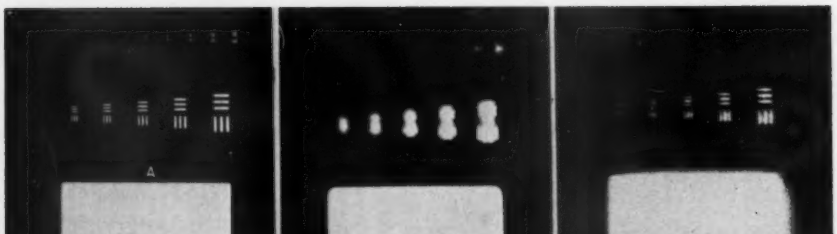

Fig. 12. *Left*, test object containing patterns for measuring resolving power and acutance. *Center*, enlarged reproduction of image of test object formed by lens at a place in the field where acutance is high but resolving power is low. *Right*, reproduction of image where acutance is low but resolving power is high.

the slope $\Delta \log I/\Delta x$ of each of these segments is measured. The individual values of these slopes are then squared and added together and then this sum is divided by the number of elements to give the mean-square gradient, which is designated

$$\overline{G_x^2} = \Sigma\,(\Delta \log I/\Delta x)^2/N. \qquad (5)$$

Inasmuch as the toe and the shoulder of the curve may be very sweeping, it is necessary to start and end the summation at certain arbitrary points A and B, and these initial and terminal points must be determined experimentally. Acutance is then defined as the mean-square gradient divided by the density difference $D_B - D_A$ between these points, or

$$\text{Acutance} = \overline{G_x^2}/(D_B - D_A).^* \qquad (6)$$

The slope $\Delta \log I/\Delta x$ can be obtained from the line spread-function, as indicated by Eq. (3), which means that acutance can be computed when the line spread-function is known.

It is sometimes difficult to believe that a meticulous distinction must be made between resolving power and acutance, but the necessity for such a distinction can be readily demonstrated. Figure 12 shows at the left a test object that was used in an investigation into photographic definition previously cited.[1] This test object was photographed in various parts of the field of a certain lens, and two such images are reproduced in the figure. The image at the center of the figure, made where the acutance was high, reproduces the square with very sharp boundaries but reproduces the resolving-power pattern so poorly that even the coarsest pattern is not resolved in this reproduction. But the resolving power of this lens varies widely from one part of the field to another, and the right-hand image was made where resolving power was a maximum. Here, however, the edges of the square are markedly blurred, which means that the acutance is low.

This figure points up the difficulty of evaluating image quality by means of a single number. Which of the two images in this figure should be accorded a higher over-all rating? A scene (two-dimensional to obviate complications arising from depth of field) was photographed under the same conditions as these images and the definition at various parts of the field was then evaluated by a group of observers. Although the definition was not considered to be really good at the parts of the field represented by either of these images, the consensus was that the definition was about equal in the two places. This would seem to indicate that any "index of quality" would be substantially the same for both images, but if a generally sharp picture was desired, the middle image in Fig. 12 would surely be considered superior, while for distinguishing extremely fine detail, the right-hand image would be preferred. Distinctions of this sort would be totally obliterated by any over-all index of quality.

The question has often been asked, "What causes these differences in image characteristics?" The answer of course is the shape of the line spread-function. In Fig. 13 the luminance distribution at a knife-edge is shown by the dotted curve in the upper left-hand corner and the distribution in a bar test-object is similarly shown in the right-hand corner. Suppose now that these test objects are imaged by two lenses, one having the spread function shown at A and the other having the spread function shown at B. The image of the edge, as has been shown, is the integral of the line spread-function. For spread function A this would be the curve A′, which must span a distance x that equals the width of the base of the spread function. Such a curve obviously has a low value of acutance and hence would produce an unsharp picture. The spread function B, on the other hand, leads to the much sharper image B′.

The resolving-power image can be synthesized by

* Although in the original paper[6] the suggestion was made that acutance be expressed by $\overline{G_x^2}\cdot(D_B - D_A)$, there are theoretical reasons[7] for preferring the form expressed by Eq. (6). Some results obtained by P. G. Powell in the Research Laboratories of Kodak, Limited, as well as others obtained in our Laboratories, are in accordance with Eq. (6).

the procedure shown in Fig. 8. To get an accurate representation, it would be necessary to sum up the spread functions of all the elementary line sources into which each bar of the test object is considered to be made up, but the general characteristics can be seen by considering only the spread functions arising from the element at the center of each of the bars. This is done in the right-hand side of Fig. 13, and the results are shown by curves A″ and B″ at the top. This construction makes it evident that a spread function of type A, having a sharp peak, although it leads to a low value of acutance, also leads to a comparatively high value of resolving power, while the opposite is true for a spread function of type B with a broad, flat peak. This result may be generalized in the rule that resolving power is sensitive to the shape of the neck of the spread function while acutance is sensitive to the width of the base or skirt. The spread function thus tells the story in both cases.

When an observer views a photograph, he is dissatisfied unless he can see all the details that he expects to see and can also see these details sharply. The relative importance of these factors in the appraisal of definition is not immediately apparent, so Higgins and Wolfe[1] studied this problem. They worked on the assumption that when, as is usually the case, resolving power is adequate, one's appraisal of definition is based primarily on acutance but that this appraisal is increasingly weighted by a resolving-power term as resolving power becomes visibly deficient. The results of their particular experiment were well represented by the formula

$$\text{Definition} = \text{acutance} \times [1 - e^{-k(RP)^2}]. \quad (7)$$

The function of resolving power shown in the brackets becomes unity when resolving power reaches a predetermined limiting value and approaches zero as resolving power approaches zero. For a viewing distance of 14 in. with the unaided eye, resolving power need be only 10 or 15 lines per millimeter, and this condition is taken into account by setting the constant $k = 0.007$. It has not been determined whether or not a function having the form of Eq. (7) will hold universally.

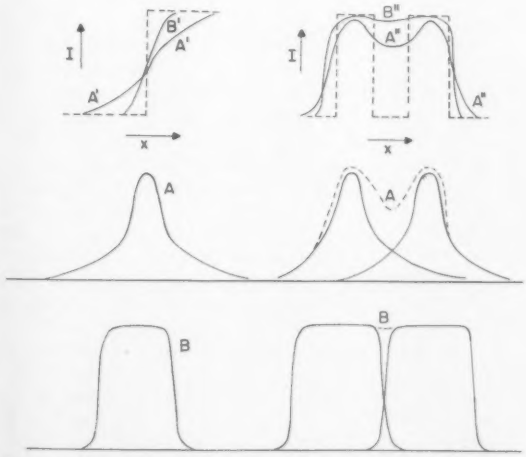

Fig. 13. Diagrams showing how a spread function with a narrow neck and wide skirt (A) leads to low acutance but good resolving power while a steep, flat-topped function (B) leads to low resolving power but good acutance.

So far it has been tacitly assumed that the spread function arises from the lens alone, but, because of the diffusion of light within a photographic emulsion, it is evident that an emulsion must also be characterized by a spread function. However, the spread function of an emulsion, unlike that of a lens, is always symmetrical. This circumstance may contribute to simplicity, but the performance of an emulsion is complicated by a factor that does not characterize the lens, namely, granularity.

It has been found possible to discuss granularity—the distribution of density in a uniformly exposed and processed emulsion as measured with a small aperture—by methods that have been developed in communication theory.[8] Communication theory involves a sequence of events—for example, voltage—related in time. Photographic imagery involves a configuration of elements—for example, density—varying in space. Thus space in photographic theory takes the place of time in communication theory, and density or transmittance takes the place of voltage, but the treatment and the formulae are substantially identical.

When a uniformly exposed and processed photographic emulsion is scanned with a slit, as shown at ① in Fig. 14, the familiar granularity trace representing transmittance T as a function of distance x is obtained. If a bright bar is sharply imaged on this emulsion, as shown at ②, the image should have sharp, straight boundaries. However, because the line spread-function of the emulsion and the lens do not have perfectly sharp boundaries, the image will have diffuse boundaries after development as shown at ③. Since this curve represents transmittance and not density, it is lower in the region of the image than in the surrounding background region.

The communication engineer would call the height by which this phenomenon is represented a signal, which, in this case, is in terms of a transmittance difference ΔT_s. In other words, the information about the illuminance difference in the object has been translated in terms of transmittance difference in the photographic image. This is the signal. But when this image is scanned with a microphotometer, the resulting trace appears as shown at ④. The microphotometer not only records the transmittance difference that represents the original object but also, superposed upon this, random transmittance differences introduced by granularity. The variation of this signal ΔT_n due to granularity represents what the communication engineers call noise.*

* Strenuous objections have been raised to the extension of the term "noise" from the field of acoustics to the fields of photography and optics, but the use of the term in communication theory to mean an unwanted signal of any description seems to be firmly established. Any extension of the term "noise" to the photographic or visual aspects of granularity is still objectionable.

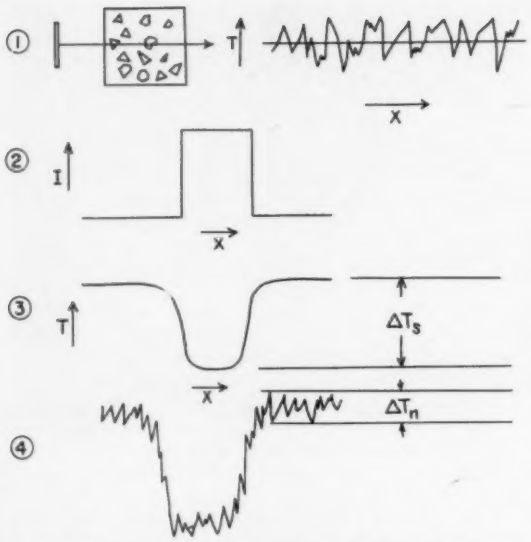

Fig. 14. Diagrams showing how granularity interferes with the reproduction of details; in the language of communication engineering, how noise ΔT_n interferes with the signal ΔT_s.

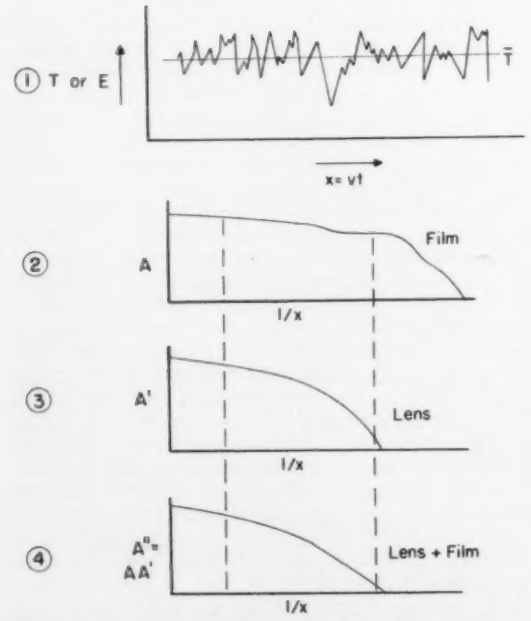

Fig. 15. ①, granularity trace of photographic emulsion, transmittance versus distance or voltage (in microphotometer) versus time. ②, power spectrum of trace (amplitude of Fourier components versus frequency, 1/x). ③, sine-wave response of a certain lens. ④, power spectrum of granularity image as formed by the lens (product of Curves ② and ③).

The signal, in terms of a transmittance difference ΔT_s on which is superposed a random difference ΔT_n introduced by granularity, would have a signal-to-noise ratio equal to $\Delta T_s/\Delta T_n$. If the presence of the bar is to be detected, this signal-to-noise ratio must exceed some critical threshold value. It is generally expected that the signal-to-noise ratio under these conditions should lie somewhere between 3:1 and 5:1 if the information is to be extracted.

The granularity trace shown at ① in Fig. 14 represents transmittance plotted as a function of distance. It is replotted at ① in Fig. 15. Actually, of course, it represents the output of the microphotometer in terms of a voltage E as a function of time t. Since the voltage is proportional to transmittance and the sample moves at a constant velocity v so that the time t equals the distance along the sample x divided by v, the trace can be interpreted as a representation of transmittance T as a function of the distance x along the sample.

Suppose now that this curve was given to a communication engineer as a curve of voltage against time (which, strictly speaking, it is) with no comment as to its origin. He would analyze it by breaking it up into its Fourier components—that is, a summation of sine and cosine terms that would give the original curve when added together. These terms would represent the harmonics that constitute the original curve, and the coefficients of the successive terms would represent the amplitudes of these harmonics. These amplitudes could then be plotted to give a spectrum analogous to the sine-wave response that was derived in Fig. 10 for a lens. Exactly the same thing can be done when the trace is considered as a curve of transmittance against distance along the sample, and the result is the curve of amplitude A against frequency $1/x$ shown at ② in Fig. 15.

When the granularity pattern of the negative that has just been discussed is printed, the characteristics of the image formed by the enlarger lens on the printing stock are determined by the characteristics of the granularity trace as modified by the spread function of the lens. Since the spectrum of the granularity in the negative is available, it is simpler to use, not the spread function itself of the lens, but the sine-wave response derived as shown in Fig. 10. The mathematician calls this the *Fourier transform* of the spread function. Let us assume that it has the shape shown at ③ in Fig. 15. By definition it is simply the relative amplitude by which different frequencies are transmitted through the lens. Analogously, curve ② is the Fourier transform representing granularity. Consequently the combined effects of the lens characteristics and the film granularity can be determined by multiplying the curves ② and ③ together, ordinate by ordinate. The result is a curve of the type shown at ④, which is the spectrum of the granularity as imaged by the lens.

In the absence of these statistical methods, it would be possible to derive the combined spread-function for every point in the granularity trace and then to analyze the resulting combined spread-function, but such a procedure would be prohibitively laborious.

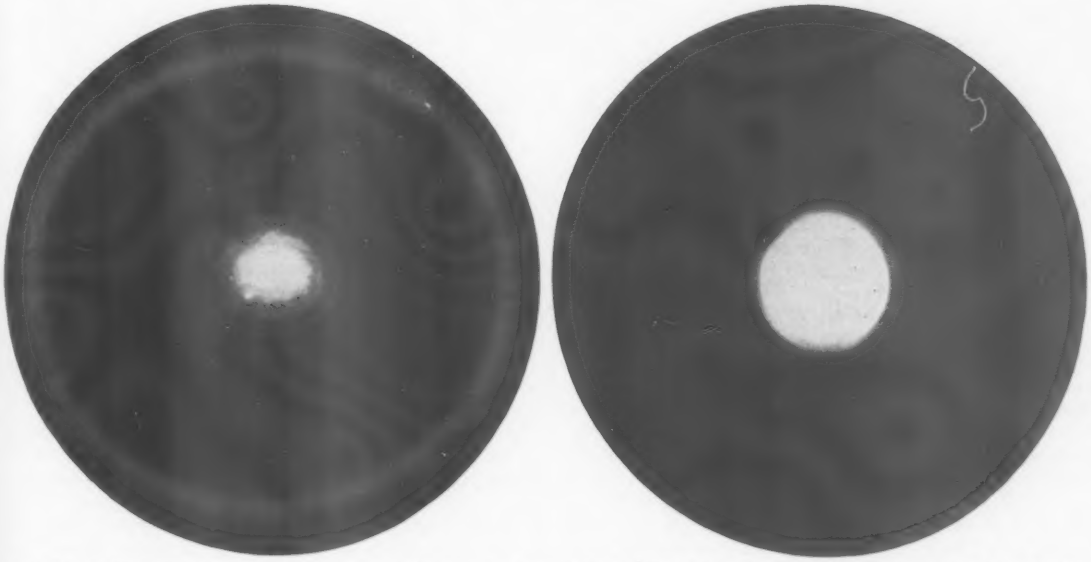

Fig. 16. Photomicrographs of the images of a point object as formed by a certain lens. The positions of the film were such as to give (A) maximum resolving power and (B) maximum acutance.

Fig. 17. Photographic reproductions of a scene for which the negatives were made at the positions of (A) maximum resolving power and (B) maximum acutance. These correspond to the respective point images in Fig. 16.

Furthermore, its significance would be uncertain because the shape of the trace would vary with the portion of the sample that was scanned. On the other hand, statistical methods are sufficiently simple so that a large enough portion of the sample to be representative can be treated.

These concepts and procedures are not merely mathematical exercises but are tools for treating situations that actually arise in practical photography. Figure 16 shows two actual images of an object point made by a certain lens at different points along the axis. At position A the light forms a small, solid core surrounded by dim rings. One ring is unusually strong because of spherical aberration, but all the rings are so weak that they do not contribute to the formation of the image unless, as in the case of this particular picture, special means are taken to make them visible. If this image were scanned with a slit, the spread function would rise very slowly at first, with slight undulations as the slit traversed the rings. Then it would rise rapidly to a sharp peak, fall rapidly, and finally trail out slowly to give a spread function of the type shown at A in Fig. 13. It was shown previously that this type of spread function leads to low acutance but high resolving power. At position B, the image would have a spread function of the shape shown at B in Fig. 13, with a flat, uniform peak and steep sides. As was shown before, this spread function should lead to high acutance but low resolving power.

The point object was replaced by a photographic transparency, and photographs were made at each of the two positions A and B. These photographs are shown in Fig. 17, where the photographs correspond to the similarly lettered images in Fig. 16. When these images were discussed in the preceding paragraph, it was predicted that the acutance at position B would be higher than at position A, and it is clear that photograph B in Fig. 17 is notably sharper than photograph A. On the other hand, it was also predicted that the resolving power for photograph A should be higher than for B, and a close examination of the tiles on the roof of the dormer in the upper left-hand corners of the respective pictures will show that these tiles are resolved fully as well in A as in B, if not better, despite the generally unsharp appearance of photograph A as a whole. Here again, as in the case of Fig. 12, no single number will indicate the quality of the image in all its aspects.

Conclusions

By following the procedures outlined in this paper, a photographic system can be designed and detail can be followed through the system to determine in what form and at what contrast the detail will be reproduced. The analysis involves only a few elements: the spread function of the lens, the spread function of the emulsion, the granularity of the material, and the sensitometric properties of the material. Although the performance of the system cannot be evaluated usefully in terms of a single number, such characteristics as acutance and resolving power can be computed. Progress in this field has been rapid, and there is hope that, before long, it will be possible to appraise a system in terms of its approach to a given set of requirements.

References

1. Higgins, G. C., and Wolfe, R. N., *J. Opt. Soc. Am.*, *45:* 121 (1955).
2. Herzberger, M., *J .Opt. Soc. Am.*, *37:* 485 (1947).
3. ———, *J. Opt. Soc. Am.*, *47:* 584 and 736 (1957).
4. Perrin, F. H., and Altman, J. H., *J. Opt. Soc. Am.*, *41:* 265 (1951).
5. Higgins, G. C., Wolfe, R. N., and Lamberts, R. L., *J. Opt. Soc. Am.*, *46:* 752 (1956).
6. Higgins, G. C., and Jones, L. A., *J. SMPTE*, *58:* 277 (1952); *PSA Jour.*, *19B:* 55 (1953).
7. Higgins, G. C., and Wolfe, R. N., *J. SMPTE*, *65:* 26 (1956).
8. Zweig, H. J., *J. Opt. Soc. Am.*, *46:* 805 and 812 (1956); Marriage, A., and Pitts, E., *J. Opt. Soc. Am.*, *46:* 1019 (1956); Pitts E., and Marriage, A., *J. Opt. Soc. Am.*, *47:* 321 (1957). [These are only some of the many recent papers on the subject.]

PHOTOGRAPHIC SCIENCE AND ENGINEERING
Volume 2, Number 2, August 1958

The Production of Precision Resolving Power Test Reticles

P. HARIHARAN, *Division of Applied Physics, National Research Council, Ottawa, Canada**

Procedures used in the preparation of precision resolving power test reticles are described with particular reference to a method of photographic compensation which permits very precise correction of changes in line width in the copying process. These procedures are illustrated with data obtained during the production of a set of three-line targets for a resolving power camera.

Transparent reticles containing several geometrically similar test patterns of successively decreasing size are normally used for measurements of photographic resolving power in the laboratory. Since the values of resolving power obtained depend quite critically on the ratio of the width of the lines and spaces in the test pattern,[1] as well as on the density difference between the clear areas and the background,[2] these reticles have to be made to very exacting specifications. It is desirable that the width of the lines and spaces should not differ by more than 1%, while the density difference in the case of low-contrast reticles should be within 0.01 density unit of the nominal value. In practice, this usually means that the dimensions of the smallest test patterns have to be held to a tolerance of $\pm 1\ \mu$.

Outline of Procedure

The normal procedure for making such reticles is to photograph a large master chart on a fine grain material of high resolving power. Unfortunately, various effects result in changes in the widths of the lines in such a copy.[3]

In the first instance, the lens does not produce an image with a truly rectilinear intensity distribution but one with slightly sloping edges. The result, with a high-contrast emulsion, is that the width of the lines depends on the exposure. This difficulty can be reduced by using microscope objectives, but these cover only a very small field, necessitating a number of separate exposures to cover the whole target. Again, because of the contraction of the emulsion in the exposed areas, due to the tanning action of the oxidation products of development (Ross effect), there is a tendency for the dark lines to decrease in width. This tendency is augmented by accumulation of developer byproducts between the lines (Kostinsky effect). The change in width actually observed is the sum of these changes and, as it can amount to several microns, it is quite serious with the finer lines.

The usual method of counteracting these effects is to adjust the width of the lines in the original drawing to compensate for the errors in the copying process. Alternatively, the exposure can be adjusted so that the spreading of the image compensates for the shrinkage. It is difficult, however, to achieve perfect correction by these methods, particularly when there are several test patterns of varying sizes on the same reticle, or when the reticle has to have a specified contrast. A better procedure is to employ a method of photographic compensation[4] based on the introduction of an extra step of photographic printing

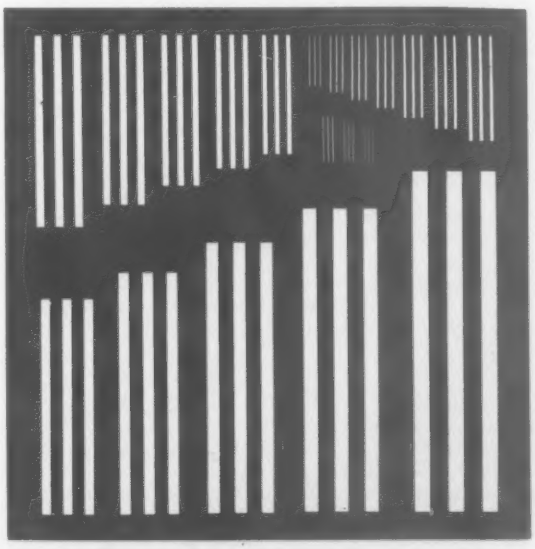

Fig. 1. The three-line resolving power reticle.

Received 28 December 1957.

* Mr. Hariharan is now with the Optics Division, National Physical Laboratory of India, Hillside Road, New Delhi 12, India.

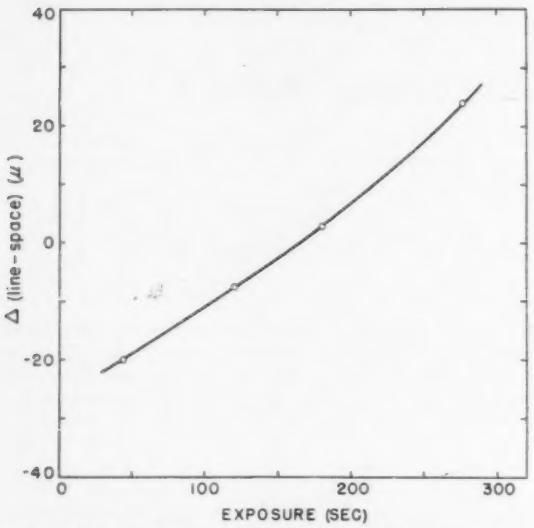

Fig. 2. Variation of $\Delta(l - s)$, the difference in width between the lines and the spaces in the three-line master negative, with the exposure.

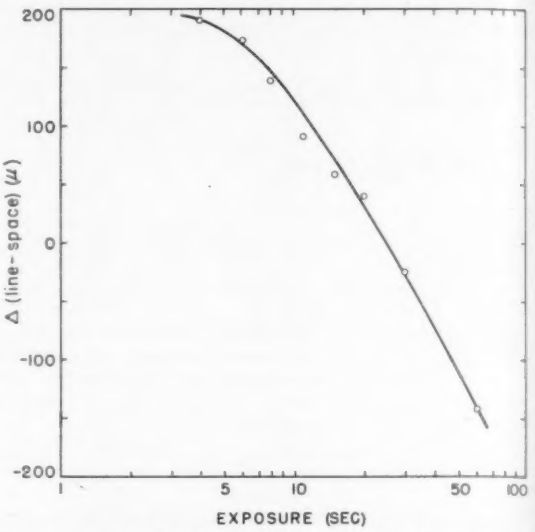

Fig. 3. Change in the values of $\Delta(l - s)$ in a $\times 10$ enlargement of a three-line master negative, shown as a function of the exposure given to the enlargement.

in which the same effects act in the opposite direction. This procedure immediately reduces the errors by nearly an order of magnitude so that, by adjusting the exposure and development in the two steps, it is possible to ensure practically perfect compensation at any given contrast.

Another problem which merits consideration is the preparation of the master chart. While hand-drawn masters are frequently used, it is difficult to achieve the required degree of accuracy unless they are made very large, particularly when they contain a number of test patterns. For this reason some experimenters have resorted to such elaborate techniques as printing the master chart from engraved zinc plates,[5] or assembling accurately cut strips of aluminum foil to make up the master.[6] A simpler method is to use a photographic copying technique for making the individual test patterns.

A procedure which has been found satisfactory consists of the following six steps:

1. A large drawing of a single test pattern is made.
2. This master drawing is photographed on a reduced scale.
3. The negative resulting from Step 2 is used to prepare a series of enlargements with dimensions corresponding to those of the patterns on the master chart.
4. These enlargements are mounted in the required configuration to make up the master chart.
5. The master chart is photographed at a suitable reduction, to give a negative of the same size as the actual reticle.
6. The final reticle is contact printed from the negative obtained in Step 5.

These steps are described below in more detail with particular reference to the actual procedure followed in the preparation of two reticles—one of high contrast and another of low contrast—for a resolving power camera. These two reticles contained twenty patterns of three lines each, arranged in the manner shown in Fig. 1, the size ratio between successive patterns being equal to the sixth root of 2. The actual reticles were approximately 40 mm square and the test patterns covered the range from 0.5 to 4.5 lines/mm.

Preparation of Master Chart

The drawing of the master pattern should be made on as large a scale as conveniently possible to ensure accuracy. The three-line target shown here was 64 cm long, with lines and spaces 32 mm wide. The master drawing was outlined with black India ink on smooth surfaced white Bristol board, after which the dark areas were filled in with matte black paint (drawing ink can give rise to specular reflections). All critical dimensions were checked to see that they were within a tolerance of 0.5%.

This drawing was then set up on an angle-iron frame illuminated with four lamps opposite the four corners (so that the illumination over the whole area was uniform to within ±3%) and photographed on Kodak 649-GH plates. The lens used was a 63mm Kodak Micro-File Ektar working at $f/8$. The camera was equipped with a micrometer focussing adjustment, and focussing was done with the help of an auxiliary microscope. The coated side of the plate was forced against an accurately machined locating surface in the camera, to ensure that it was always held in the same plane. Particular care was taken to see that the camera was squared on to the easel. The plates were brush-developed in Kodak D-8 for 2 min at 20 C. After fixing and washing they were rinsed in methanol

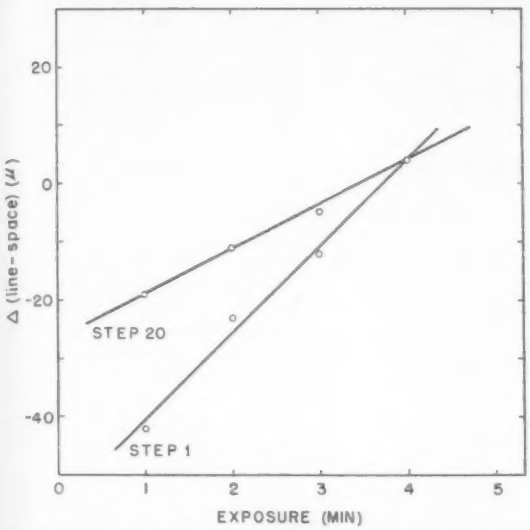

Fig. 4. Variation of $\Delta(l - s)$, the difference in width between the lines and the spaces in the largest and the smallest patterns (Step 1 and Step 20) in the negative of the master chart, with the exposure given to the negative.

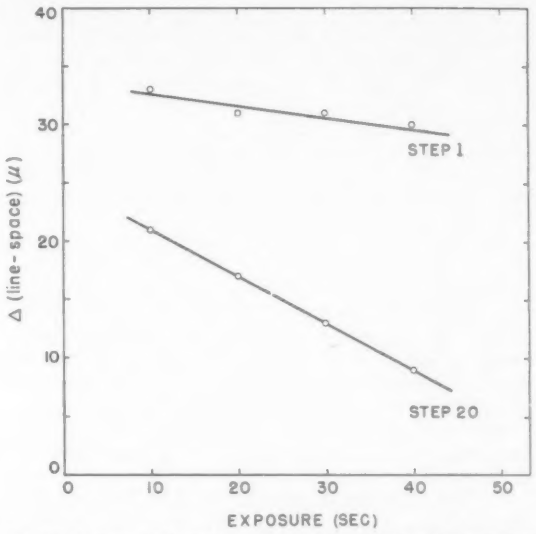

Fig. 5. Change in the value of $\Delta(l - s)$ during the printing process for the largest and the smallest patterns (Step 1 and Step 20) on the target, shown as a function of the exposure given to the final reticle.

for 30 sec, allowed to drain, and set aside to dry in a vertical position. This procedure ensured uniform and rapid drying and eliminated risks of local shifts in the emulsion.

Measurements on negatives made with exposures ranging from 45 to 270 sec showed that the width of the lines consistently increased with the exposure as shown in Fig. 2, the widths of the lines and spaces being equal for an exposure of 170 sec.

The next step was to make a series of enlargements from one of these negatives in order to determine the dimensional changes occurring in this process. The enlarger used was a Leitz Focomat with a 50mm Elmar lens, stopped down to an aperture of $f/8$. The enlargements were made on Kodak Bromide paper. A contrasty grade with a glossy surface was found most suitable (F.4). Exposures ranged from 4 to 60 sec at an approximate magnification of $\times 10$. The prints were carefully dried between sheets of photographic blotting paper and then measured. They were not ferrotyped, as preliminary tests showed that ferrotyping or forced drying could result in dimensional changes and distortions as great as 2%.

The deviations of the widths of the lines and spaces from their nominal values are plotted as a function of the logarithm of the exposure in Fig. 3, from which it is seen that practically complete compensation is attained with an exposure of 25 sec.

However, since this exposure was more than twice that required to give a dense black background in the prints, a negative was chosen in which the spaces were slightly wider than the lines. Compensation could then be obtained with shorter exposures.

Before making the actual enlargements for the master chart, a calibration curve was prepared for the enlarger. Five enlargements were made of a scale ruled on glass at different magnifications, the lower edge of the lens mount in each case being set with a vernier height gauge at a definite height above the enlarger easel. From measurements on the enlargement, a graph was then plotted of the magnification, m, against x, the height of the lens in centimeters above the baseboard. This was found to be a straight line given by the equation

$$x = 5.195\,(m + 0.558)$$

This graph was then used to read off the height of the lens for any required magnification. The automatic focussing feature of the enlarger was found to be a great convenience for this work.

The sizes of the patterns on the master chart having been calculated, enlargements were made from the three-line negative at the required magnifications. The exposure in each case was estimated, on the basis of the magnification, from the data in Fig. 3. Measurements showed that most of the enlargements were within the permissible dimensional tolerance of 0.5% but in a few cases fresh prints had to be made with slightly more or less exposure to get equality of the lines and spaces.

These enlargements were then dry mounted on matte surfaced black Bristol board in the arrangement previously decided upon. Measurements on a sample print before and after dry mounting showed a uniform shrinkage of the order of 0.2%, for which it did not seem necessary to make any special allowance.

Preparation of Final Reticles

The completed master chart was set up on the copying board of the precision camera and photographed.

The reduction ratio of the camera was carefully adjusted, by trial, so that the negative was of the same size as the final reticle. After this, a series of negatives was made with exposures ranging from 1 to 4 min.

The largest and smallest patterns on these negatives (Steps 1 and 20) were then carefully measured. The variation of $\Delta (l - s)$, the difference in width between the lines and spaces, with the exposure time (for these two patterns), is shown in Fig. 4.

The next step was to print one of these negatives with different exposures and determine the corresponding changes in the line-space value for the printing process. These prints were also made on 649-GH plates in a contact printer using parallel light. The exposure was given by a roller blind shutter controlled by an electric timer. In order to avoid difficulties with interference fringes and multiple reflections between the surfaces,[8] a thin layer of a liquid having the same refractive index as gelatin was spread between the negative and unexposed plate surfaces. Glycerine and immersion oil were both found suitable for this purpose.

The change in $\Delta (l - s)$ during the printing process, for the largest and smallest patterns on the target, is shown as a function of the print exposure in Fig. 5. From Figs. 4 and 5 it can be seen that an exposure for the negative of about 2 min and an exposure for the print of approximately 30 sec should give a high-contrast reticle with practically perfect compensation on Step 20 and a net error, $\Delta (l - s)$, on Step 1 of about 7 μ (which is only 0.35% of the line width on this step).

Actual measurements on prints made from such a negative showed that an exposure of about 40 sec gave the best overall results in printing. The difference between the width of the lines and the spaces on all the patterns in the finished reticles was less than $\pm 1\%$ of the line width, and the density of the dark areas was over 2.5.

Low-Contrast Reticles

In the case of low-contrast reticles, it is also necessary to keep the density difference between the clear lines and the dark background at a specified value (0.20 in this instance). Preliminary tests showed that a density of approximately 0.20 could be obtained with a printing exposure of 12 sec. Since the change in the values of $\Delta (l - s)$ during the printing process is greater for shorter exposures, it was found necessary to use a negative which had also been given a shorter exposure. A negative which had been exposed for 1 min was actually used, and practically perfect compensation was obtained on all the patterns.

Considerable difficulty was experienced, however, in holding the density of the prints within the permissible tolerance of ± 0.01, because of the extremely high contrast of the emulsion. The procedure finally adopted was to make a series of prints with slightly different development times and select those which came nearest to the required density. After some trials it was found possible to secure two or three acceptable reticles from every batch of six prints

Acknowledgment

The author wishes to thank P. D. Carman for his interest and valuable advice.

References

1. Sandvik, O., *J. Opt. Soc. Am.*, *14:* 169 (1927).
2. ———, *J. Opt. Soc. Am.*, *16:* 244 (1928).
3. Mees, C. E. K., *The Theory of the Photographic Process*, The Macmillan Co., New York, 1954, p. 1029.
4. Baird, K. M., and Turner, T. E., (unpublished work), National Research Council of Canada.
5. Coleman, H. S., and Clark, D. G., *J. Opt. Soc. Am.*, *37:* 272 (1947).
6. Dew, G. D., *J. Sci. Instr.*, *32:* 24 (1955).
7. Hariharan, P., *J. Opt. Soc. Am.*, *46:* 315 (1956).
8. Stevens, G. W. W., *Phot. J.*, *87B:* 34 (1947).

PHOTOGRAPHIC SCIENCE AND ENGINEERING
Volume 2, Number 2, August 1958

A Sensitometric Processing Machine Using Small Film Strips and Small Developer Volume

R. W. Henn and K. R. Hughes, *Research Laboratories, Eastman Kodak Company, Rochester, N.Y.*

The processor described comprises a series of tubes containing the film strips and the developer, fastened radially to a water-driven wheel. The force required to drive the wheel and invert the tubes is supplied by the tempering water, which is circulated through a pump, its temperature being controlled by an appropriate heater, a cold-water supply, and a thermoregulator.

The tubes most commonly employed hold 10 ml of developer and a 1 by 10-cm film strip. Advantages obtained for the system include rapidity and ease of working, high uniformity and reproducibility, and economy of materials. It has proved particularly valuable in developer comparisons where only small quantities of chemicals were available.

In the routine testing of a large number of film–developer combinations, it became necessary to devise a sensitometric processing machine that would not only provide good temperature control but also varying degrees of agitation that could be reproduced from time to time. In addition, it had to utilize as small a film strip and as small a volume of developer as possible, for research where only small quantities of an experimental coating or an experimental developing agent were available.

A device was made, the essential feature of which was a water-driven wheel having metal clips to hold test tubes in a radial arrangement. The test tubes contained the developer and the film strips so that, while the wheel revolved in a constant-temperature bath, the film was agitated by continuous inversion. Original models consisted of cypress or Plexiglas plastic tanks, both the temperature control and the water power to turn the wheel being derived from the output of a Powers thermoregulator valve. The model to be described is made of stronger construction materials and is designed to be independent of the water supply of the laboratory.

Present Model

The present machine employs a stainless-steel (16-gauge, AISI, Type 316) tank with folded edges, rounded corners, and welded seams. Angle stock has been fastened to the base to provide greater stability, and stainless-steel pipe fittings have been welded into the side at the appropriate places for the temperature-regulating and pump-system attachments (Figs. 1 and 2). V-brackets are spot-welded on the inside and lined with nylon strips to act as bearings for the wheel axle (Fig. 3, bottom). A lighttight lid is provided. This is flanged and has a gasket of very soft sponge rubber to make the seal (Fig. 3, top).

The wheel itself (Fig. 4) is made of Plexiglas plastic with small vanes of the same material and a stainless-steel axle held in place by two rubber stoppers bored to fit tightly. These stoppers also act as bumpers for the test tubes as they are fitted into place on the wheel. Notches on the rim of the wheel identify the different tube positions. The tubes are held in heavy copper (30 amp) fuse clips, fastened onto the wheel with stainless-steel machine screws. The clips are bent to fit 15- × 125-mm test tubes, the bottom one quite firmly and the upper one less tightly.

The dimensions are not given here, since none of them are critical. With slight modification, similar devices could be made which would incorporate either more tubes or tubes containing larger film sizes.

The temperature control is achieved through the use of a Fenwal Thermo-switch (Type 17100-5/11), used with a Potter-Brumfield KRP11A relay. The thermoswitch opens and closes near the desired temperature, causing the relay to turn on a Chromalox 450 W, Type C-622 heater at lower temperatures or, at higher temperatures, to open a Detroit Control 5625, No. 685, Type 3, solenoid-operated valve on the chilled water line (40 F). The thermoswitch is shunted by an 0.005-microfarad capacitor and a 22-ohm resistor in series, as recommended by its manufacturer, to prevent chatter (see Fig. 5). The heater is located in a well, built into the side of the tank, and all the wiring is enclosed in watertight, stainless-steel boxes and conduit. Wires enter through conduit CGB connectors.

The temperature-regulator system, as described here, is adequate for ±0.3 F control. A control needle valve in the chilled-water line is opened only

Communication No. 1930 from the Kodak Research Laboratories, presented at the Annual Conference, Asbury Park, N. J., 10 September 1957. Received 19 November 1957.

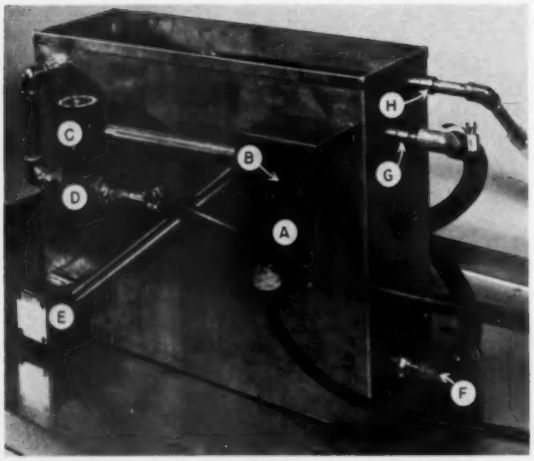

Fig. 1. External view of tank. "A" houses thermostat control and relay, which are adjusted through the rubber stopper "B." The solenoid "C" operates the valve "D" which controls the flow of cold water. The wiring to the heater is housed in "E." The water enters from the pump at "F" and leaves at "G." The outlet "H" is for overflow.

Fig. 2. External view showing the pump, tank cover, and a test tube being inserted in the wheel.

far enough to allow a low rate of flow when the solenoid valve is open. This prevents the temperature from getting too low before the thermoswitch closes, and keeps the cycling time less than one minute. Ordinary cold water could be used, except that the input would have to be increased as the temperature of the water approached 68 F. A thermistor and accessory electronic equipment have been used to give more precise temperature regulation, but the thermoswitch proved adequate for this application. Instead of a heater, the relay could be used to control another solenoid valve on the hot-water line, where this supply is convenient and dependable.

The water is circulated with an Eastern D-11 centrifugal pump. The flow is controlled with a needle valve at the output of the pump, and this can be adjusted to give various wheel rotation rates, resulting in different agitation levels. Rates of about 10–30

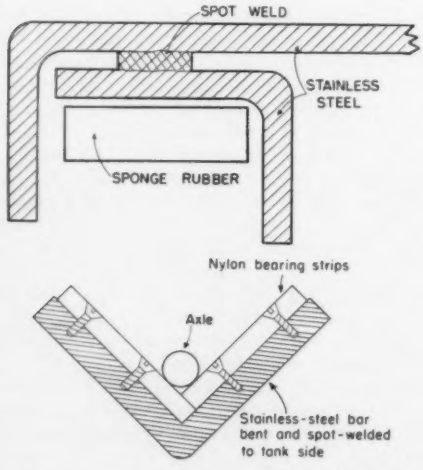

Fig. 3. The upper diagram shows a detail of the flanged lid, the lower a detail of the nylon-lined bearings. The wheel may be lifted out from the bearings at will.

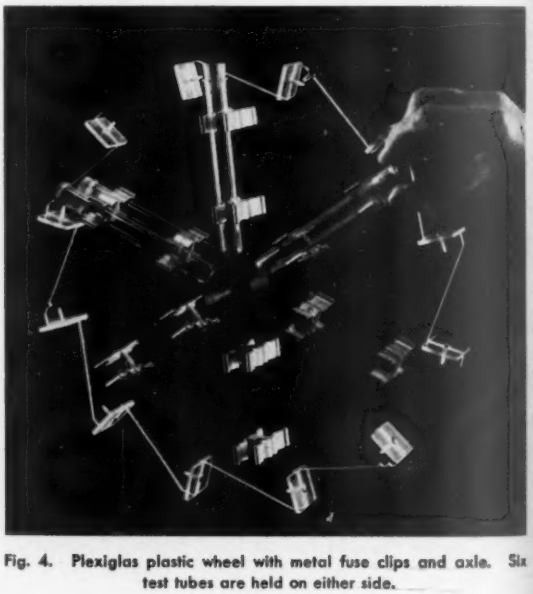

Fig. 4. Plexiglas plastic wheel with metal fuse clips and axle. Six test tubes are held on either side.

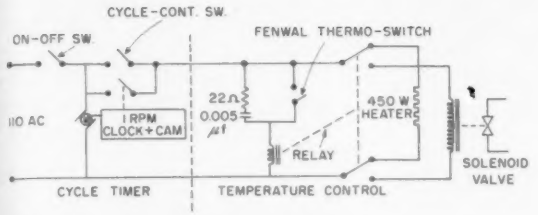

Fig. 5. The electrical circuit described in the text. The cycle timer is used only when intermittent agitation is employed.

rpm are possible. Where still lower or intermittent agitation is required, a cycle timer can be used in series with the pump motor (see Fig. 5).

This apparatus lends itself to other applications beside those incorporating the water-driven wheel. The tempered water can be routed from the pump through any type of jacketed device, such as a developer tray or tank, and then back to the tank input. In addition, with the wheel removed, the tank can be used as a constant-temperature bath for development in cylinders.

Use

In general use, where, for example, a series of developers are to be tested, as little as 50 ml of developer is sufficient for a time–gamma series consisting of five developments, 10 ml being required in each tube. The tubes are stoppered with No. 4 extra select corks (discarded after each use), placed in the clips on the wheel and allowed to come to temperature. Film strips are previously exposed on a sensitometer or other test device, generally as 4- × 5-in. sheets or 35mm strips. These are cut into strips $^1/_4$ to $^3/_8$ in. × 4 in. (about 1 × 10 cm) and arranged on a special rack. From this rack, the strips can be transferred to the tubes in the machine at regular intervals in the following manner. First, the wheel is stopped with the hand, then allowed to rotate slowly until the desired tube is found. This is removed, unstoppered, and the film strip inserted. The tube is again stoppered, shaken, and reinserted into its position on the wheel. With a little practice, this operation can be done at 15-sec intervals.

To remove film, the tube desired is again located and removed from the clips. The stopper is removed and the film strip is lifted out of the test tube with stainless-steel forceps. This is quite simple to do, even in total darkness, since the film strip occupies most of the entire width of the tube and orients itself against the direction of rotation. The film is then transferred to a stop bath or directly into the fixer. The developer is discarded after each use.

The wheel is most commonly employed at a high, easily reproducible level of agitation. The 10 ml of developer employed fills about 70% of the volume of the test tube, leaving a relatively large air space which creates considerable turbulence and a high level of agitation when the tube is inverted at about 24 rpm. This gives uniform development, end to end and side

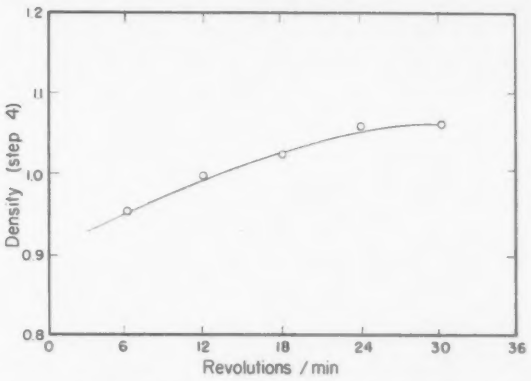

Fig. 6. The effect of the rate of rotation on development. At the normal operating rate of 24 rpm a variation of as much as 6 rpm makes only a 2 to 3% difference in density.

to side, while moderate variations in volume or rate of revolution make only small differences in the degree of development obtained (Figs. 6 and 7).

An idea of the reproducibility of the system is given in Fig. 8. These data are from a developer test repeated a number of times over a period of several weeks in connection with a study of developing agents. In addition to any errors due to agitation differences and timing, variables include mixing errors and exposure errors. The total spread of these cumulative errors is not great, the largest density variation being obtained in the short times, where the time required to insert and remove the strip becomes important.

The rate of agitation described above slightly exceeds that obtained in the conventional vane-type of sensitometric processing machine[1] and approaches that of spray processing.[2,3] Alternately, the lower

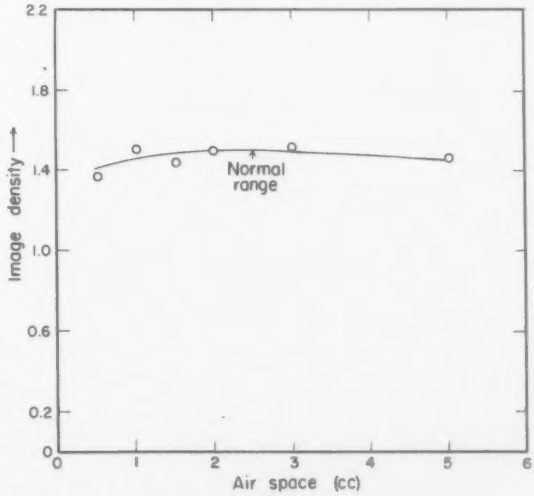

Fig. 7. The effect of air space. This is not critical.

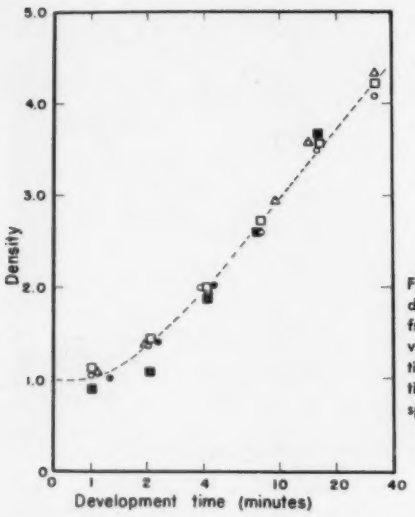

Fig. 8. Reproducibility. Data from an Elon developer and positive film, run five times at widely spaced intervals.

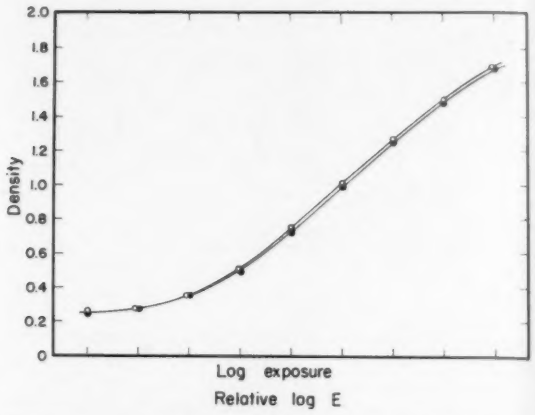

Fig. 9. Intermittent agitation. The open circles represent densities of a strip processed on the wheel; the dots, of a strip processed in a roll-film tank. In both cases the developer was agitated twice a minute.

levels of agitation obtained in hand-processing and in photofinishing may be obtained by working at lower rotation rates, or intermittent agitation may be employed using the cycle timer mentioned.

This can be set to give various on-and-off times during the period of a minute. In order to simulate the agitation level of roll-film tank development, the cycle timer is set to go on 5 sec out of every 30 sec, while the valve at the pump output is adjusted to give about $1^1/_2$ revolutions every time the pump comes on. With this intermittent agitation, roughly 13 ml of developer per tube are used, in order to keep the strips covered during the still portion of the cycle (Fig. 9). When using the machine with intermittent agitation, e.g., every $^1/_2$ min, care must be taken not to upset the cycle in any way. Strips are inserted at $^1/_2$-min intervals, and the wheel is allowed to rotate so that the desired tube is uppermost without any additional handling.

Conclusion

This equipment was designed for the economical employment of small quantities of developer chemicals. Its advantages, however, have led to its extension to other areas in which larger quantities of films and chemicals are available. These advantages include the rapidity and the ease of working on a small scale and the uniformity and reproducilibity of the results obtained.

The ease of working is a material aid in the reduction of the time required to compare a number of developers. For example, when working with ten variants of a developer, it is easy to prepare a liter, divide it, and make appropriate addends. The handling of the small volumes in the darkroom is another convenience. Time is also saved in making the exposure, since it is convenient to expose a larger area and cut it into the small strips before development. A 4- × 5-in. sheet will yield twelve of the small strips, and a 35-mm by 8-in. strip will yield six. A wedge of 5-mm step width is employed, which is standard to the Eastman Processing Control Sensitometer and may be fitted into other equipment. The strips can be read on automatically advancing densitometers designed for 10-mm wedges by reading every other step, repeating to fill in if desired.

The construction and design of the equipment is simple and adaptable to other sizes. Much of this simplicity is due to the use of a water drive. This type of drive shows advantages over a mechanical transmission in the ease of construction of a watertight and lighttight enclosure. The water drive makes it possible to stop the wheel at any position, to remove it from the tank with ease, and to operate it safely in the dark.

Few maintenance problems have been encountered other than the occasional adjustment of the thermostat or the replacement of worn axles and bearings. Some manipulative skill must be acquired in the loading and unloading of the strips, but this has been readily acquired by the ten or twelve workers who have had occasion to use this type of machine.

Acknowledgment

We wish to acknowledge the considerable contribution of Howard A. Miller and Arthur A. Rasch, of these Laboratories, toward the design and construction of experimental models.

References

1. Jones, L. A., Russell, M. E., and Beacham, H. R., "A Developing Machine for Sensitometric Work," *J. SMPE, 28:* 73–94 (Jan. 1937).
2. Ives, C. E., and Kunz, C. J., "Simplification of Processing Methods," *J. SMPTE, 55:* 3–26 (July 1950).
3. Ives, C. E., "The Application of Treating Liquids and Drying Air in Photographic Processing," *Phot. Eng., 2:* 116–126 (1951).

PHOTOGRAPHIC SCIENCE AND ENGINEERING
Volume 2, Number 2, August 1958

Apparatus and a Laboratory for Processing Thick Nuclear Track Emulsions

JOHN F. GARFIELD, *Brookhaven National Laboratory, Upton, N.Y.*

Photographic studies in high-energy physics frequently utilize stacks of special emulsions 400 to 600 μ thick. These emulsions require specialized processing techniques, often involving temperatures as low as 5 C and development for as long as 96 hr. Details of these procedures are given, including handling of the emulsion pellicles, temperature control, and description of the equipment.

In high energy nuclear physics research, visual techniques involving photographic emulsions, cloud chambers, and bubble chambers have proven quite successful. They allow microscopic nuclear phenomena to be studied on an individual basis and in considerable detail within the sensitive volume of the detector. For charged particles photographic emulsions yield the most accurate information.

The Problem

Emulsions of sufficient sensitivity and thickness to record tracks of individual charged particles are produced by Ilford, Ltd., and others. The composition of nuclear emulsions in comparison with a conventional photographic film emulsion, as given by Webb,[1] is shown in Table I. It will be noted that the silver bromide content of nuclear emulsions is much higher, and the grain diameter much lower, than that of conventional emulsions.

TABLE I

Property	High-Speed Optical Type	Nuclear Type
AgBr: Gelatin (Wt)	47:53	80:20
AgBr: Gelatin (Vol)	15:85	45:55
Grain diameter	0.5 to 3 μ	0.1 to 0.4 μ
Emulsion thickness	10 μ	25–600 μ
Sensitivity to light	Very high	Low
Response to α-particle	High	Individual tracks
Response to β-particle	Moderate	Individual tracks

As it is desired to examine the tracks of charged particles over a long distance, a nearly solid block of emulsion, composed of multiple layers of unsupported emulsion, or pellicles, is assembled and pressed into stacks for exposure. Since the particles may take paths up or down through the stack, it is important that each layer be as thick as convenient to lessen the problem of following the tracks from layer to layer after processing. This is done under the microscope at about 300× magnification by highly refined but rather tedious scanning techniques. The usual compromise for reducing the difficulties of scanning and processing is to use layers 400 or 600 μ thick.

As the stacks are subject to handling before and after the exposure (which may be of several hours duration) the layers must be held to prevent lateral shifting. This is accomplished primarily by mechanical pressure applied to the stack. In some cases two $^{5}/_{32}$-in. nylon rods are inserted through holes punched in each layer. These holes also serve as register indices for numbered grids which are exposed onto the lower surface of each pellicle and which aid in following particles through the stack. The relative position of one emulsion with respect to the rest is further established with fiduciary marks obtained by exposing the stack to several collimated x-ray beams. Each pellicle must also be coded to show its vertical position in the stack. The size of a stack is governed by the experiment, but ordinarily the stacks vary from 5 × 7.5 × 1 cm thick, to 20 × 25 × 6 cm thick. A stack, ready for exposure, is shown in Fig. 1. Figure 2 reproduces a photomicrograph of a nuclear emulsion showing pi-meson tracks.

The processing of such emulsion stacks presents problems not encountered in normal photographic practice. A conventional development and processing technique, for example, would not produce uniform development in depth. Moreover, the long periods required for solution penetration of the thick layers would cause, at normal temperatures, intolerable distortions due to shifts within the emulsion. In the effort to solve these problems the temperature cycling method, first suggested by Dilworth, Ochialini, and Payne,[2] is most commonly employed. This procedure, slightly modified, is used at the Brookhaven National Laboratory to process 400 and 600 μ Ilford G5 emulsions. It consists of the following steps:

Presented at the Annual Meeting, Asbury Park, N.J., 10 September 1957. Received 19 September 1957. This work was carried out under the auspices of the United States Atomic Energy Commission.

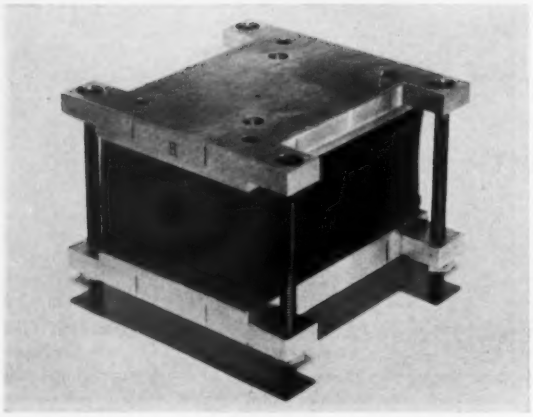

Fig. 1. An emulsion stack prepared for exposure.

1. The exposed pellicles are first mounted on glass plates that are pre-subbed and somewhat larger in area than the pellicles. This is accomplished by allowing the emulsion to adhere to the glass under water at 12 C, and then passing the assembly between rollers under slight pressure.
2. The emulsions are air dried in air of 22 C and 55–60% RH for approximately 48 hr.
3. The dried assemblies, or plates, are soaked in distilled water. The initial temperature is 22 C, but in a $2^1/_2$-hr period the water temperature is gradually lowered to 5 C.
4. The water is drained and replaced by an Amidol developer previously chilled to 5 C. A $2^1/_2$-hr period is allowed for the developer to thoroughly penetrate the emulsion layers.
5. The developer is removed, the emulsion surface lightly blotted, and the temperature raised to 22 C. The emulsions are maintained at this temperature for a period of 1 hr during a so-called "hot-dry" developing stage.
6. Development is arrested by lowering the temperature again to 5 C and introducing 0.5% acetic acid solution.
7. The plates are now transferred to a 30% hypo solution at 5 C. The clearing time, plus 50% additional time, is of the order of 40 hr. Throughout this period the hypo is continuously replenished at a rate such as to hold the silver concentration of the solution between 2 and 8 grams/liter.
8. Washing is started by a very gradual dilution of the hypo solution over a period of 18 hr with water at 5 C. This is followed by 30 hr of continued washing with clean water at 5 C.
9. Excess water is removed by soaking the plates in a series of graded alcohol-glycerine-water solutions, held at 5 C, ending with a bath containing 80% alcohol and 4% glycerine.
10. The plates are finally air dried at 22 C, 55–60% RH. This requires approximately 15 hr.

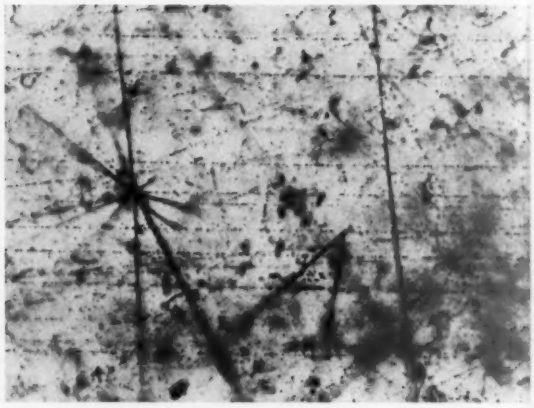

Fig. 2. Photomicrograph (300×) of a nuclear emulsion showing parallel tracks of high energy pi-mesons. One of them produces a nuclear disintegration which appears in the emulsion as a "star" with about 11 prongs.

As is apparent, 7 days are required for this 10-step procedure. Since the process is lengthy and the results are short of ideal, it is not surprising that interesting variations on this procedure have been developed. Some workers process the pellicles unsupported, or supported only by a mesh, with the obvious advantage of solution penetration from both sides to reduce the total processing period. This requires the mounting of the pellicle as it returns to nearly its original dimensions in the alcohol stage. Yagoda[3] employs a series of solutions varying in pH and reducing power, all at low temperature, in place of the temperature cycle, and has processed emulsions up to 3 mm thick. In some procedures the hypo is introduced gradually, and a salt has been used in the wash water to lessen swelling at that stage.

As stated by Waller,[4] the technique of temperature cycling is effective in overcoming the problem of obtaining uniform development in depth, because the rate of penetration of the developer has a much lower temperature coefficient than the rate of development. It has also been stated that the use of Amidol in the developer is effective because its pH is close to that of the emulsion and hence it is able to penetrate the layer more rapidly.[5]

Criteria of Adequate Processing

It is considered that successful processing of nuclear emulsions should:

1. Provide uniformity of development in depth;
2. Yield a favorable track-to-background ratio;
3. Give reproducible results from batch to batch;
4. Cause minimal physical distortion of the emulsion layer.

These criteria are easy to enumerate but they cannot be ascertained by the empirical test routines and cus-

tomary methods of measurement employed in ordinary photographic sensitometry. Extent of development, for example, is measured by counting silver grains per 100 μ in tracks formed by particles with ionization near the minimum value. Since this procedure must be repeated many times to obtain a statistically reliable value, the method is obviously very time consuming. Grain counts must be carried out in depth to determine the gradient in order to evaluate development uniformity. Gradient values for two different development procedures are given in Fig. 3.

Distortion due to processing is determined by measuring the deviation of tracks from their known paths. The emulsions are subject to gross changes in vertical dimension during the process, swelling to four times their original size and drying down to approximately one half their original thickness. In the case of unmounted emulsions the pellicles increase their lateral dimensions by some 25% and are mounted as they shrink to approximately their original size in the alcohol baths. In working with mounted pellicles, this lateral dimensional change is avoided, at least in respect to the layers nearest the glass. The upper layers, however, apparently shift during the processing and their failure to return entirely to their original position produces distortion of the tracks. For steep tracks this displacement may vary from 0 to 50 μ, making the tracks difficult to identify and sometimes to follow.

Factors which are thought to contribute to distortion, in addition to possible strains resulting from manufacture of the pellicles, are:

1. The vertical shrinkage of the emulsion to half its original thickness due to the removal of silver halide during fixing;
2. Physical shock or damage;
3. Rapid or uneven swelling and contraction caused by too sudden shifts in temperature, pH, or pressure;
4. The appearance of bubbles at the emulsion-glass interface, possibly due to excessive osmotic pressure.

The swelling rates of nuclear emulsions have been measured at each step, and typical values are shown in Fig. 4. Swelling is apparently dependent on a number of factors, such as temperature, the pH, and the concentration of solutions, but it has been reported that in distilled water between 4 C and 20 C the swelling is linear with temperature.[6] It was noted at Brookhaven that the rate of temperature drop in the initial bath governed the degree of swelling in the developer, which in turn appeared to relate to grain count, indicating the need for equipment capable of reproducing the temperature cycle. In fact, many of our results in past years indicated that previously unsuspected variables were the cause of inconsistencies in our results. However, the large volume of processing, that is large for a research facility, precluded the carrying through of the number of experiments apparently necessary to isolate all the sources of variation. It was therefore considered necessary to install a laboratory and design equipment that could handle the work load on a regular basis and under more controlled conditions than had previously existed.

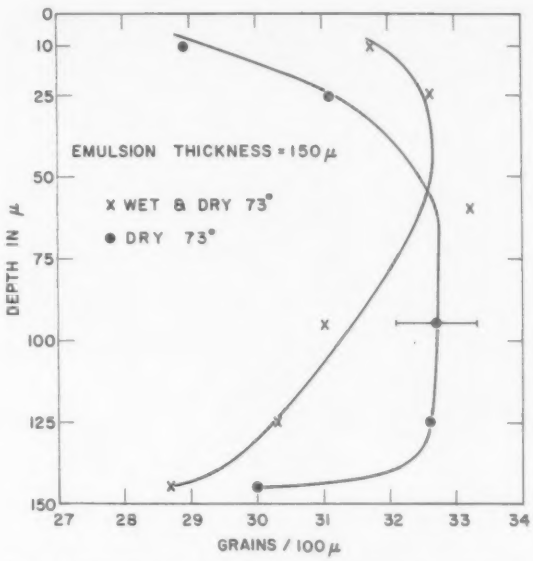

Fig. 3. Grains per hundred microns plotted against depth in the emulsion for two variations of the process.

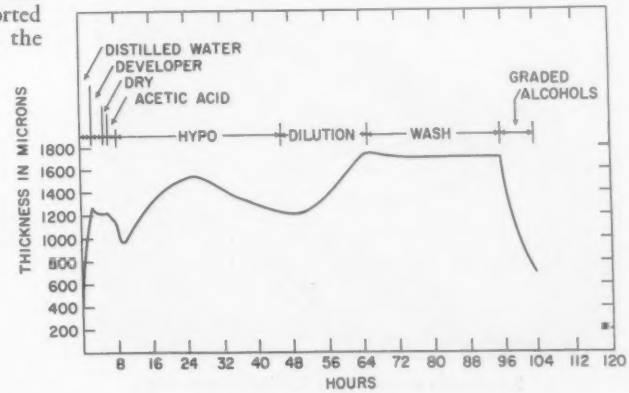

Fig. 4. Typical values for emulsion thickness throughout the process.

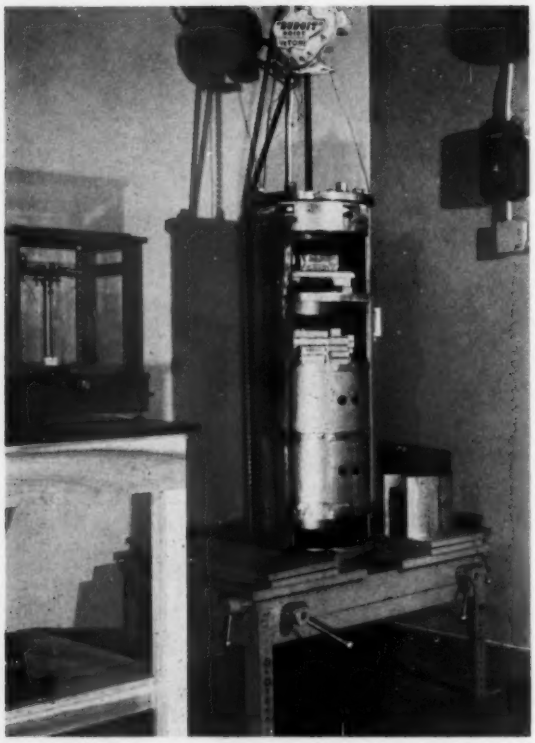

Fig. 5. Canister and dry well for storage of nuclear emulsions.

The target was a laboratory capable of processing 120 sq ft of emulsion per 3-wk period, because 120 sq ft of emulsion was the expected maximum load and 3 wk is considered a safe period before the fading of tracks becomes significant. It should be noted also that at Brookhaven, the Cosmotron, a particle accelerator, provides a continuous work load which we wanted to handle with a minimum staff, in contrast with many academic institutions where occasional work can be handled on a crash basis by a large team working continuously.

The laboratory for processing nuclear emulsions at B.N.L. comprises 4500 sq ft, providing rooms for packing, mounting, and processing, as well as storage space, a chemical mixing room, a utilities area, and shop space.

In addition to conventional services, including temperature and humidity control, it was necessary to provide for the distribution of distilled water and hypo solution, the circulation of chilled water at 2 C, and the circulation of developer and acetic acid solutions at 5 C. This cooling load was divided between a main water chiller with a capacity of 6 gpm, which operates continuously, and two smaller auxiliary units for cooling and circulating the solutions.

Ventilated, light-tight shelves were provided for conditioning and drying the emulsions. A 20-in. × 45-ft drywell, with hoist and storage canister, was included in the stockroom (Fig. 5). The emulsions are stored at the bottom of this well, normally to the shaft, to reduce background exposure by cosmic radiation.

Design of Processing Apparatus

The process, as described, establishes the requirements for the actual apparatus for developing nuclear emulsions. The emulsions must be maintained horizontal, their temperature must be smoothly and uniformly controllable in a range from 3 C to 30 C, and they must be protected against physical shock or damage, yet be accessible during the processing stages. The problem of temperature variation was approached by constructing shallow tanks to hold the mounted emulsions, surmounting chambers in which temperature-conditioning water is circulated (Fig. 6). The common member of the two tanks is a $^1/_8$-in. stainless steel plate, prestressed in assembly to be quite flat when under pressure by the conditioning water. This, together with a water seal which forms under the glass plate, provides a uniform thermal contact between the conditioning water and the emulsion.

The lower chamber is partially divided by fins into

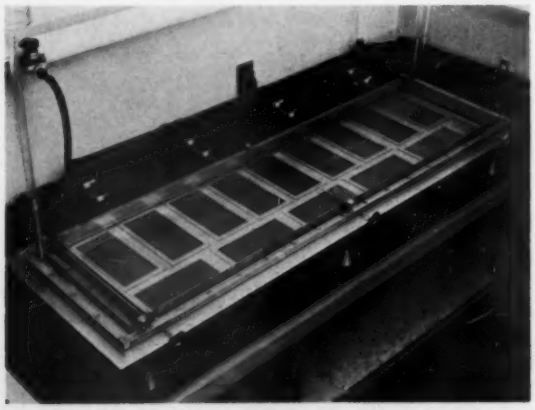

Fig. 6. Temperature controlled tray for development stage.

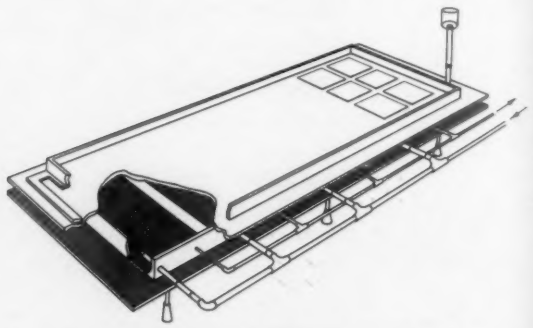

Fig. 7. Detail of development tray shown in Fig. 6.

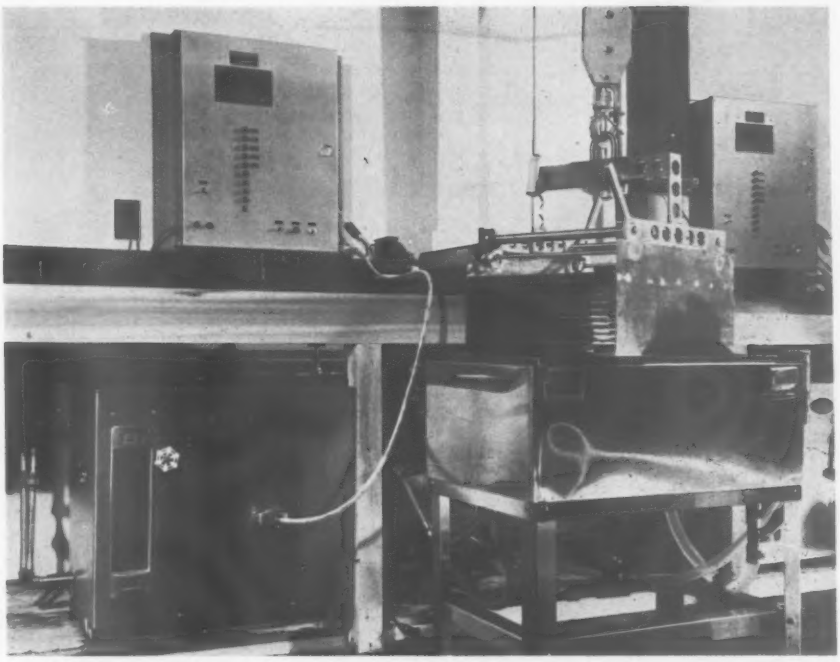

Fig. 8. Hypo-wash unit with rack withdrawn. The control unit is on the left and the programming timer is on the wall above.

four sections, each with individual connections to the input and outlet manifolds, as shown in Fig. 7. By observation of the flow through a temporary transparent plate it was apparent that large air bubbles might accumulate and seriously affect the heat transfer. To allow the bubbles to escape, standpipes were added at each end of the chamber. Construction problems limited the surface of these units to approximately 5 sq ft, so four units were built. These are controllable in pairs to permit the simultaneous operation of two different development routines.

Attempts to improve the reproducibility of runs by the use of alternate hot and cold preset blending valves have not been successful due to the need for manually over-controlling at the time of temperature change. In order to achieve a rise time of 20 min it is necessary to empty the lower chamber of chilled water before introducing the warm water.

Although there are obvious attractions in the thought of a one-position device for all processing steps, this had to be abandoned because of the large

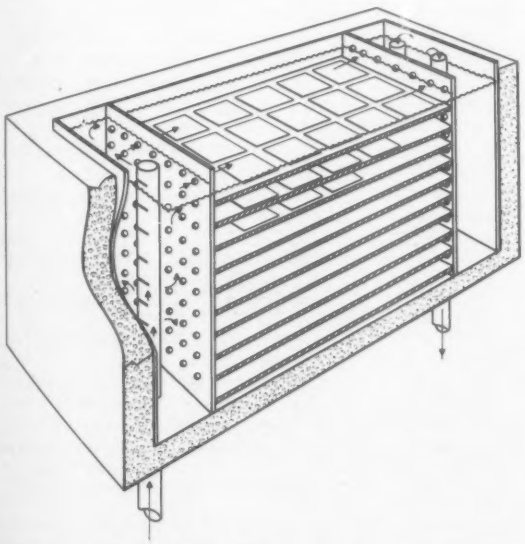

Fig. 9. Cutaway drawing of the hypo-wash unit shown in Fig. 8.

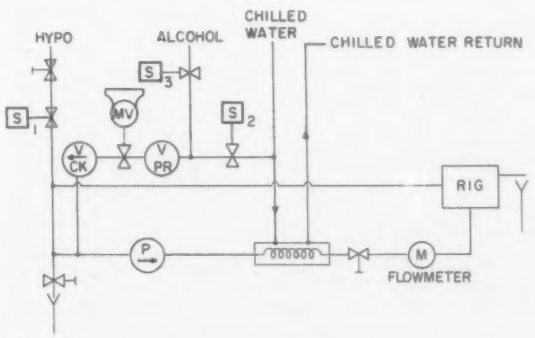

Fig. 10. Schematic of the control system.

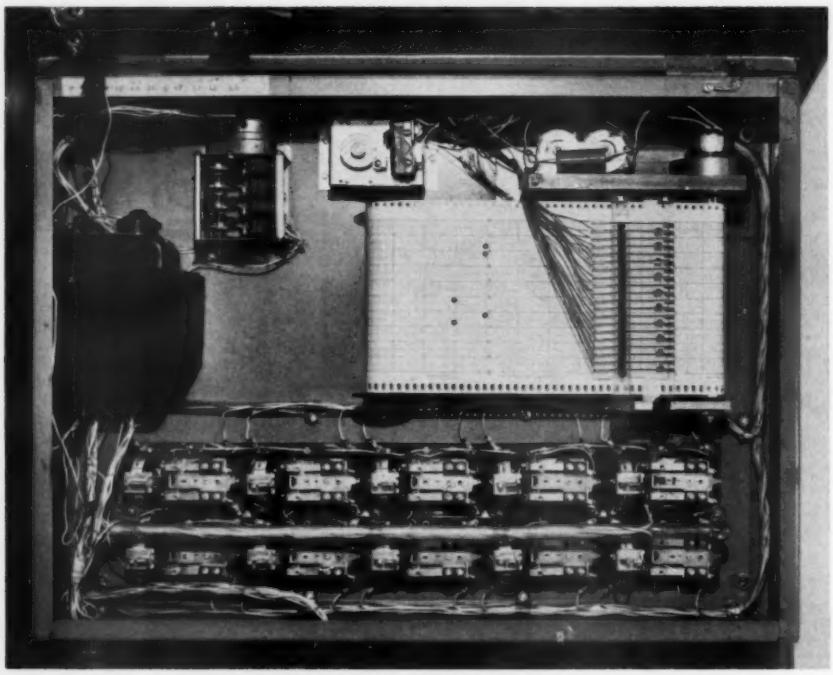

Fig. 11. Arrangement of the programming timer.

size and excessive cost of such a piece of equipment. Since the only position requirement in fixing and washing is that the plates remain horizontal, and since temperature of the plates can be controlled by that of the solutions, it is possible to arrange the plates on shelves, permitting the design of geometrically smaller containers (Fig. 8). Thus we have two hypo-wash units each equal in capacity to the four developing tanks. This arrangement permits two processings a week, and yields the desired capacity of 120 sq ft per 3-wk period. The hypo-wash units are insulated tanks with plenum chambers at each end, the inner faces of which are pierced in a manner designed to produce an even laminar flow of solution across the shelves which are held in a removable rack (Fig. 9). As turbulence from raising or lowering the rack would disarrange the plates, they are held on the shelves in slotted tracks which are adjustable to hold the various sizes. Temperature is controlled by circulating the solutions through a heat exchanger supplied by the main water chiller.

These units are supplied with hypo, water, and alcohol through solenoid-operated valves. The hypo is replenished by adding fresh solution to the intake side of the circulating pump. Dilution is accomplished by the gradual opening of a motorized valve of linear characteristic, which can be operated at three successive speeds to produce a smooth pH change (Fig. 10). All steps in these units are controlled by programming timers in which a paper scroll is advanced hourly by a timing motor (Fig. 11). Circuits are completed by spring contacts to latching relays through holes in the paper. Variations in the schedule are effected by punching a new scroll.

Acknowledgments

The author wishes to acknowledge the contributions of G. T. Zorn of the Brookhaven National Laboratory in many aspects of the apparatus design, and to thank Lloyd E. Varden for his help on preparation of the manuscript and for many interesting discussions of the process generally.

References

1. Mees, C. E. K., *The Theory of the Photographic Process*, 2nd ed., 1954, Chap. 8, p. 303.
2. Dilworth, C. C., Ochialini, G. P. S., and Payne, "Processing Thick Emulsions for Nuclear Research," *Nature*, *162:* 102-03 (July 1948).
3. Yagoda, H., "Isothermal Processing of Thick Nuclear Emulsions," *Rev. Sci. Instr.*, *26:* 263-66 (March 1955).
4. Waller, C., "Nuclear Emulsion Technique," *Jour. Phot. Sci., Sect. B of Phot. J.*, *1:* 41-54 (1953).
5. Bogdanov and Poliakova, "The Rate at Which Developing Agents Penetrate the Emulsion Layer on Thickly Coated Film," *J. Sci. and Applied Phot. and Cinemat.*, *1:* 425-28 (Nov.-Dec. 1956).
6. Meulemans et Mignone, "Sur le Gonflement et la Contraction des Emulsions Nucleaires," *Colloque sur la Sensibilité des Cristaux et des Emulsions Photographique*, Paris, Memoires et Documents, 1951, pp. 309-15.

PHOTOGRAPHIC SCIENCE AND ENGINEERING
Volume 2, Number 2 August 1958

A Continuous Rapid-Processing System for Side-Looking Radar Mapping

EDGAR D. SEYMOUR, *Apparatus and Optical Division, Eastman Kodak Company, Rochester, N.Y.*

A radar map may be made aboard aircraft from side-looking radar-signal returns and presented to an observer within a few seconds. Photographic materials and rapid-processing techniques are employed. Characteristics of the signals to be recorded are explained briefly. A blue cathode-ray tube phosphor was selected to operate with blue-sensitive photographic materials in order that the viewer may be illuminated with minus-blue light (yellow) of high intensity.

A density range of 2.0 from a log exposure range of 2.0 in the processed film has been achieved. Several processing methods were considered and monobath processing was selected. A rapid processor-viewer utilizing this system was developed.

Several years ago the Eastman Kodak Company was asked by the U. S. Air Force to investigate the possibility of continuous-strip recording of signals on airborne radar. The system described here is the result of this investigation.

The radar signals that were to be recorded are presented as brightness differences within a single line on the face of a cathode-ray tube (CRT) and are recorded in a way similar to that of conventional strip photography. This was expected to result in a more usable radar-strip map.

Since radar is virtually independent of cloud cover and visibility conditions, and will operate day or night, an immediate viewing of the radar map in the air is highly desirable.

The design, construction, and installation of the antenna and the electronics are very important, but these details belong to the radar manufacturers. This paper will be confined to a description of a system for presenting the radar map to an observer within a few seconds, by using photographic materials and rapid-processing techniques.

Basic System

Basically, the system incorporates a blue-sensitive film that operates with a blue P11 or P16 phosphor. The film is hardened, allowing it to be rapidly processed in a monobath solution at elevated temperatures and with development and fixation within 18 sec. The film is moved from the exposure station through the processing station and into the viewing station at film-transport speeds of the order of 1 in. per min. In the viewing station, the film passes between two minus-blue filters (yellow) that prevent the actinic blue light from reaching unprocessed film.

The film is dry by the time it leaves the viewing area and is wound onto a take-up reel.

Signals to Be Recorded

In order to design a system of this nature properly, some knowledge of the possible signals that are to be recorded is necessary.

The signals from an airborne radar are similar to the video signals of television. To place the target signals correctly in the image space, the image of the modulated light source must sweep at velocities up to 50,000 in. per sec. In addition, the light source must be capable of modulation to give good tone reproduction. The most common device for displaying these signals is the cathode-ray tube. The characteristics of cathode-ray tubes determine the types of photosensitive materials which can be considered for use in this system.

Two phosphors are of interest, the P11 which peaks at 460 mμ, and the P16 which peaks at 390 mμ. Both of these phosphors have short persistence, although the persistence in the P11 is a function of the beam current, while that of the P16 is not.

Commercial CRT's can be obtained with spot sizes 0.001 to 0.003 in. in diameter that will expose photographic materials properly at these sweep speeds and repetition rates. The spot size is important for it limits the detail that can be recorded.

Radar-signal returns may have a dynamic range of 50 db. The CRT can handle a brightness range of about 100 to 1, or about 20 db. The radar-signal returns must, therefore, be compressed to this order of magnitude and most radar manufacturers do this in

Received 31 January 1958.

This work was supported in part by the Aerial Reconnaissance Laboratory, Wright Air Development Center, Wright-Patterson Air Force Base, Dayton, Ohio.

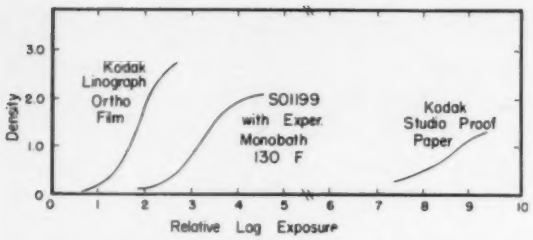

Fig. 1. Characteristic curves of three photographic materials.

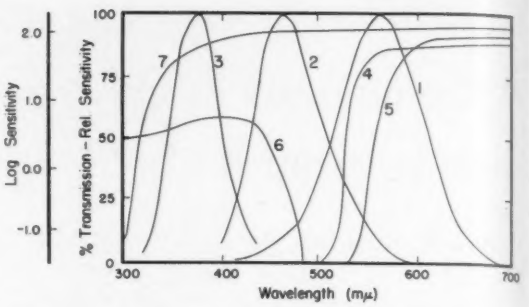

Fig. 2. Spectral relationships of the components of the system: (1) Visibility of the human eye. (2) Relative brightness of P11 phosphor. (3) Relative brightness of P16 phosphor. Note that the relative brightness between Curve 2 and Curve 3 is not indicated. There is reason to believe that the total brightness of P11 is greater than that of P16. (4) Transmission of yellow glass filter. (5) Transmission of orange plastic filter. (6) Log sensitivity of experimental material SO-1199. (7) Transmission of crown glass.

their equipment. A brightness range of 100 to 1 corresponds to a log exposure range of 2.0.

The image on the film is formed by the accumulation of many short exposures, since the spot is finite, the repetition rate is high, and the film-transport rate is low. With noise random and a small signal accumulative, there is probably an increase in the signal-to-noise ratio in this type of integration.

The Sensitized Material

An ideal material for this project would be a blue-sensitive, fine-grain, print-out material (Fig. 1) requiring no processing, similar to Kodak Studio Proof Paper. Unfortunately, such materials require about a million times the exposure that is available.

At the other extreme, a very high speed material, such as Kodak Linagraph Ortho Film could be used. Very high sensitivity was not required in this application, however, and a film having a thin, highly hardened emulsion is preferable for use with rapid-processing methods.

It is desired to have a density difference in the final material of at least 2.0. Since it is difficult to meet this density-difference requirement with photographic paper, transparent film was selected as the sensitized material. Furthermore, in the beginning of the study, it was decided that light-weight airborne equipment for fighter-type aircraft would require an optical projection system. This dictated a specular light source in the illuminator and a clear, fixed film.

An experimental sensitive material (SO-1199) which had been previously developed by the Kodak Research Laboratories appeared to fulfill these requirements and has proved to be most successful in this application.

The characteristic curves for these three materials are shown in Fig. 1. Kodak Linagraph Ortho Film and experimental material (SO-1199) were exposed with a Kodatron Flashtube FT-403, filtered by a Kodak Wratten Filter No. 47B. The Linagraph Ortho was processed in D19 for 7 min at 68 F. The SO-1199 was processed in the experimental monobath at 130 F, giving a density difference greater than 2.0 for a log exposure range of 2.0, but retaining a low fog level of about 0.15 or less.

The characteristic curve for the Kodak Studio Proof Paper was obtained by placing the paper in a densitometer and reading the instrument repeatedly over a period of time. No development was employed with this printing-out paper. Data presented in these curves describe the sensitometric characteristics of the average current product and experimental material. Particular samples of current materials may exhibit variations from these curves, and similarly identified materials manufactured in the future may not have characteristics described in these curves. When quantitative work is planned, therefore, precise data should be obtained under the actual conditions that prevail.

Processing

Many types of processing were considered. Negative processes were preferred because of their simplicity. Stabilizing development and monobath processing systems were regarded as most flexible and easily adapted to the present problems. In view of the desire for a small specular light source and a projection system, it was decided to use a monobath with complete fixation.

Monobath processing in general, is a mixture of developer and fixer, with the developing rate very high and the fixing rate slow enough to allow the density to build up to the required value. It offers several advantages: a simple method of application should suffice, and once the process has gone to completion, high illumination levels will not injure the record. In the past, one of the disadvantages has been the silver-plating problem where silver has been plated on any surface in contact with this solution, including applicator rollers made from stainless steel, glass, Teflon, nylon, and epoxy resins, as well as on the film. An experimental monobath which had been developed at the Kodak Research Laboratories was free from this objection. It has been found to operate successfully in this application; however, it is not regarded at present as being suitable for other uses.

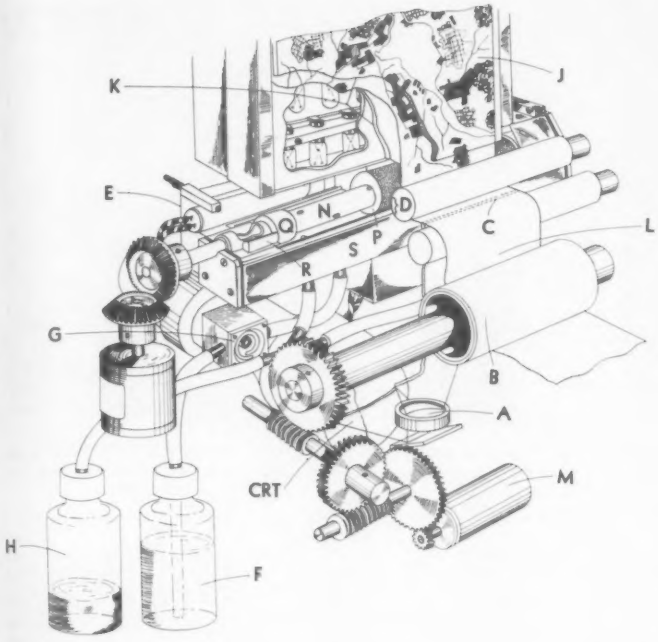

Fig. 3. Equipment configuration: A. Lens. B. Rubber-covered drive roll. C. Exposure station. D. Processing station. E. Thermostat. F. Monobath solution container. G. Solution pump. H. Expended monobath container. J. Viewing station. K. Yellow glass filters. L. Unprocessed film. M. Servo drive motor. N. Stainless-steel tube. P. Dacron felt washers. Q. Collar. R. Nylon bearings. S. Metal block.

Figure 2 shows the spectral relationships of the components of the system. Curve 1 shows the visibility curve of the human eye; Curve 2 is the published curve of the relative brightness of P11 phosphor; Curve 3 is the published curve of the relative brightness of P16 phosphor. No attempt has been made to indicate the absolute values of these two phosphors nor the magnitude of the relationship to each other. The transmission of a yellow glass filter is shown as Curve 4, and the transmission of an orange plastic filter is shown as Curve 5. The log sensitivity of the experimental sensitive material SO-1199 is shown as Curve 6. Curve 7 shows the transmission of crown glass which indicates that ordinary optical glass lenses can be used in the system.

Equipment Configuration

A schematic drawing of the elements of the system and their relationship to each other is shown in Fig. 3. The lens, A, has a focal length of 75mm with an aperture of $f/4.5$. It is designed to work at finite conjugates and is adjusted for maximum resolution in blue light. In this application, it was stopped down to marked $f/5.6$ which gave it an actual aperture of $f/7.0$.

The uniform drive consists of a rubber-covered drive roll, B, driven by a servomotor, M, through a pair of spur gears and a double worm-gear reduction. The gears are of high precision and are mounted very carefully on preloaded class 7 ball bearings. High-quality workmanship was required and has been achieved.

The exposure station, C, is located very close to the processing station in order not to delay the viewing time.

The processing station, D, consists of an applicator roller nearly surrounded by a metal block that serves to hold the bearings for the applicator roller, and provide a housing for the heaters and thermostats, E, used to maintain the 130 F temperature.

The applicator roller is a hollow stainless-steel tube, N, plugged at both ends with small holes drilled radially through the 0.049-in. wall and with die-cut dacron felt washers, P, slipped on the tube and retained by axial pressure of a collar, Q. The outside diameter of the roller is turned concentric with the bearing diameters and mounted in nylon bearings, R. The roller assembly is adjusted so that there is 0.003 to 0.005-in. clearance from the film emulsion surface. Fresh monobath solution enters the metal block, S, where it is brought to temperature and forced under pressure into the applicator tube through small holes in the nylon bearing that coincide with similar holes in the applicator tube. From there it flows out through the dacron felt washers to contact the emulsion. Excess monobath which acts as a flushing and cleaning operation is collected in the block and drained to an expended monobath container, H. The applicator roller is motor-driven independently of the film drive. A solution supply, F, and pump, G, complete the processing station.

The image is developed to substantially its maximum density within 5 sec and is completely fixed in about 18 sec after the solution is applied. The processing of 50 ft of 5-in. film requires about 1 pt of

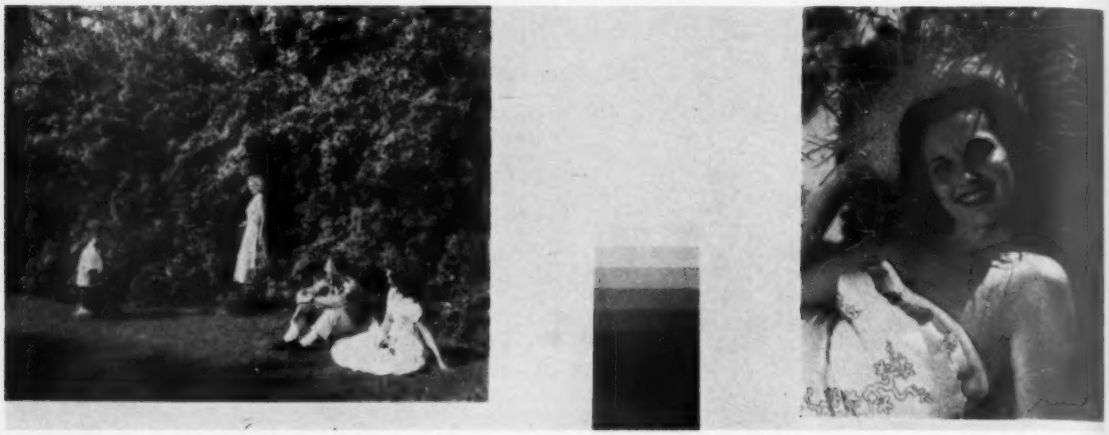

Fig. 4. Photographic quality attainable with the system. Pictures were made by exposing the experimental material (SO-1199) to a negative in a contact printer, and then processing in laboratory equipment, using the experimental monobath at a temperature of 130 F and a transport rate of 1 in./min.

monobath solution, F. This is equivalent to about 600 min, or 10 hr, of radar mapping.

The processed film moves from the processing station into the viewing station, J, and between two yellow glass filters, K, with transmission characteristics as shown in Fig. 2. These filters prevent the actinic blue light from reaching the unprocessed film, L. The illuminator has a controlled surface brightness which can reach more than 2500 ft-L. The illustration shows a diffuse light source which has been found satisfactory if the radar map is viewed directly.

The film emerges from the viewing station dry and is taken up on the take-up reel. It has been found that the take-up motor torque must be quite uniform, since any non-uniformity will show as transverse streaks in the final product.

Ground Processing Follow-Up

Tests have shown that the dried, processed film will keep for several months with no detectable change. It has been found desirable, however, to wash and fix the film within a reasonable time after airborne processing. This will remove the chemicals which have dried on the surface and clear the edges which have not been processed. The final film will look and keep as well as any other well-washed photographic material.

Altitude Tests

Tests with the system in an altitude chamber indicate satisfactory densities up to 35,000 ft pressure-altitude. When the pressure falls below this pressure altitude, the solution boils away very rapidly. With an increased use of monobath, however, images have been recorded up to 50,000 ft. Fixing is not complete above 35,000 ft, but it is possible to complete the fixing later if the film remains dry.

Airborne Equipment

An airborne camera–rapid processor–viewer, capable of processing 50 ft of 5-in. film, can be built weighing less than 20 lb, including the optics, servo amplifiers, servo drives, solution pumps, blowers, etc. This equipment would occupy less than 1000 cu in. and require about 250 w of power. More than half of this power would be consumed in the heaters, which would operate intermittently and would be controlled by the thermostat.

Photographic Quality

Figure 4 is a photograph made on the experimental material, SO-1199, and processed with the experimental monobath at a transport rate of 1 in. per min in laboratory breadboard equipment. This picture is included to illustrate the photographic quality achieved with the system.

Acknowledgment

This radar mapping system has been made possible by the combined efforts of a group of people. The author therefore wishes to express his appreciation to all who have assisted on this project.

PHOTOGRAPHIC SCIENCE AND ENGINEERING
Volume 2, Number 2, August 1958

Photographic Emulsions for Missile Photography

HUTSON K. HOWELL, *Boston University Physical Research Laboratories,* Boston, Mass.*

The suitability of ten black-and-white and three color films for long range missile photography was studied. The materials were judged on the basis of their yellow-red sensitivity, contrast, latitude, and image quality by usual sensitometric techniques as well as by field tests. Daylight exposure indices are poor indicators of the exposure for distant objects against a blue sky. A table of relative speeds and filter factors for this special case is presented. Nearly all the emulsions tested have adequate resolving power to handle the relatively poor image quality resulting from atmospheric turbulence, although the finer-grained materials become more important if image quality gets above a 10-lines/mm level. This seldom occurred in operational tests with long focal-length cameras at Patrick AFB. Color films, although quite useful for ranges up to 20 miles, rapidly lose their effectiveness as atmospheric haze reduces color saturation.

The Boston University Physical Research Laboratories have completed for the U.S. Air Force an investigation of the optical, photographic, and meteorological factors which affect the quality of long range photographs of airborne objects taken from the ground. In this paper only the photographic factors are discussed.

Concurrent with the field program at Patrick Air Force Base, Florida, an investigation was conducted at the Boston Laboratories to determine the suitability of ten black-and-white and three color films for this type of photography. This study included measurement of the sensitometric characteristics of the films, including speed, contrast, red sensitivity, and effect of high and medium energy developers. High and low contrast resolving power was measured also as a function of exposure, and simulated missile photographs were taken on all the films.

Sensitometric Characteristics

Sensitometry in one of its phases is concerned with the measurement of the response of photographic materials to radiation. In the case of missile photography we are concerned with the response of the emulsion to the visible spectrum and the near infrared. Particular emphasis is placed on the wavelength region above approximately 500 mμ since it has been well established that a loss in image contrast occurs when the short wavelengths of the visible spectrum are utilized.[1]

All sensitometric data were obtained using an Eastman Sensitometer, Type Ib. This instrument contains a laboratory daylight source consisting of a 2850-K tungsten lamp, the light of which is modulated by a Kodak Wratten Filter No. 78A to a color temperature of 5500 K. Sensitometric data were obtained also for the daylight source modified with a Kodak Wratten Filter No. 25.

Two developers were used throughout this study. The first, Kodak Developer D-19, is a high-contrast developer that has moderately high activity, excellent keeping properties, and long life in use. The second, Kodak Developer D-76, is less energetic and gives lower contrast and lower maximum density. Its capacity is also less than that of the D-19.

The development times were varied to obtain a normal degree of development for each film. In other words, no attempt was made to develop all films to the same gamma value since widely different emulsion types were included in the test. For example, the maximum gamma obtainable with Kodak Tri-X Film (135)* is approximately 1.2, whereas a high contrast emulsion such as Kodak Linagraph Shellburst Film (gray base) or even Kodak Plus-X Aerecon Film† can be kept to a gamma of 1.2 only by drastic manipulation of developer types and development times.

In the image quality investigation to be described later, the same processing method was used as in the senstometric study. All strips were processed in reel-type 35mm tanks with continuous agitation at 68 F. A conventional acid rinse and a hardening-fixing bath were used.

Presented at the Annual Meeting, Asbury Park, N.J., 12 September 1957. Received 20 December 1957. This is a report of work sponsored by the Ballistic Missile Division, Air Research and Development Command, USAF, under contract No. AF 04(645)-60.

*On 1 January 1958 the Boston University Physical Research Laboratories were separated from Boston University and became a division of the ITEK Corporation, Boston, Mass.

* Kodak Tri-X Film (135) was the material included in this study; since then a new aerial film product, Kodak Tri-X Aerecon, has become available. This film has high contrast, high red sensitivity, is hardened for elevated temperature processing, and is capable of better image quality than the Tri-X (135).

† At the time this investigation was conducted, Kodak Plus-X Aerecon was offered as a Kodak Special Order Product, SO-1166.

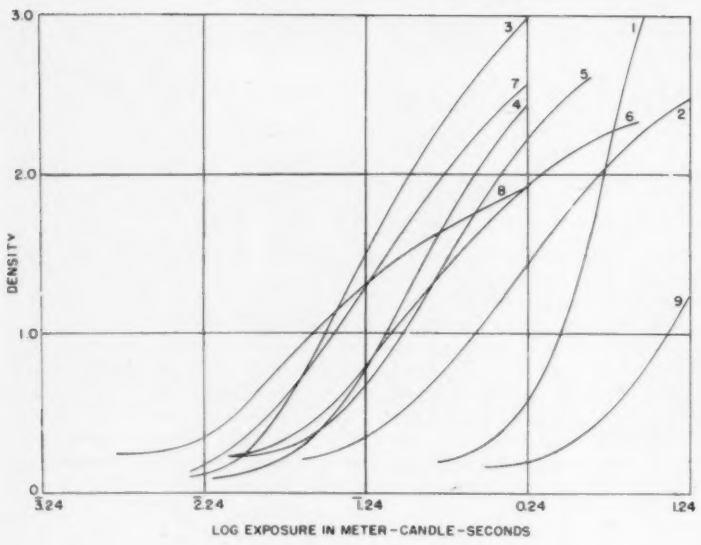

Fig. 1. Characteristic curves for black-and-white emulsions. Curve 1 — Kodak Micro-File Film (35mm), processed in Kodak Developer D-19 for 4 min. Exposure made to laboratory daylight source modified by Kodak Wratten Filter No. 12 (yellow). Curves 2–9 — processed in Kodak Developer D-19. Exposures made to laboratory daylight source modified by Kodak Wratten Filter No. 25 (red). Film names and times for Curves 2–9 are as follows:

2.	Kodak Panatomic-X Film (135)	6 min
3.	Kodak Plus-X Aerecon Film	6 min
4.	Kodak Special Order Product SO-1121	6 min
5.	Kodak Linagraph Shellburst Film	6 min
6.	Kodak Plus-X (135) Film	5½ min
7.	Kodak Super-XX, Aerial Recon R.P.	6 min
8.	Kodak Tri-X (135)	8 min
9.	Eastman Panchromatic Separation Film, Type 5235 (35mm)	6 min

Fig. 2. Characteristic curves for black-and-white emulsions. Curve 1 — Kodak Micro-File Film (35mm), processed in Kodak Developer D-19 for 4 min. Exposure made to laboratory daylight source modified by Kodak Wratten Filter No. 12 (yellow). Curves 2–9 — processed in Kodak Developer D-19. Exposures made to laboratory daylight source modified by Kodak Wratten Filter No. 25 (red). Film names and times for Curves 2–9 are as follows:

2.	Kodak Panatomic-X Film (135)	13 min
3.	Kodak Plus-X Aerecon Film	10 min
4.	Kodak Special Order Product SO-1121	10 min
5.	Kodak Linagraph Shellburst Film	10 min
6.	Kodak Plus-X (135) Film	11 min
7.	Kodak Super-XX, Aerial Recon R.P.	10 min
8.	Kodak Tri-X (135)	14 min
9.	Eastman Panchromatic Separation Film, Type 5235 (35mm)	12 min

Development Time and Gamma

The films that were included in the investigation are listed and briefly described in Table I; also given are the gamma values determined from the sensitometric curves shown in Figs. 1, 2, and 3. Figure 1 shows the D-log E curves for D-19 development, Fig. 2 shows the curves for D-76 development, and Fig. 3 gives the curves for the color films.

Under the conditions of this investigation, reciprocity failure is not a major factor, although some slight shifts in the relative speed ratings of the films studied might occur at exposure times shorter than 0.001 sec. All sensitometric testing was done at 0.01 sec in this study.

Of the three color films, Kodachrome Film, Daylight Type (135), was processed by the Eastman Kodak Company at Rochester, N.Y. The Kodak Ektachrome Film, Daylight Type (135), and the Anscochrome 35mm Film, Daylight Type, however, were processed by commercial photofinishing firms. Extreme variations in color balance were obtained that are indicative of wide variations in processing in some commercial processing laboratories.

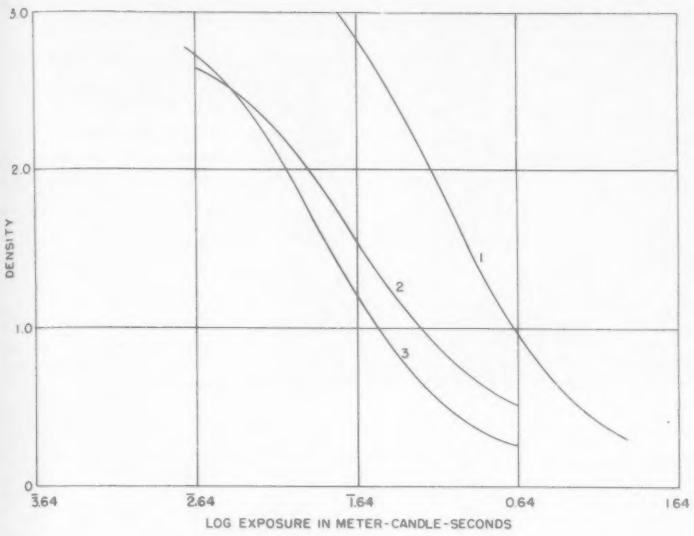

Fig. 3. Characteristic curves for reversal color films processed by commercial laboratories. Curve 1 — Kodachrome Film, Daylight Type (135); Curve 2 — Anscochrome 35mm Film, Daylight Type; Curve 3 — Kodak Ektachrome Film, Daylight Type (135).

Emulsion Speed

Ordinary methods of rating film speeds are not suitable for the special case where the quality of the photographic image is judged solely by the clarity with which an isolated object — in this case a missile — stands out against a blue sky background. In this problem two factors are important: (1) selection of the right criteria by which to measure the speed, and (2) consideration of the emulsion spectral sensitivity and the spectral distribution of the light reflected from the object and its background. In considering the first factor it is reasonable to assume that the method of measuring speed should be based on an exposure for the missile image that will produce optimum image quality on the film.

It has been established that the maximum resolving power obtainable with most photographic materials occurs at a background density of between 0.6 and 1.5.[2] However, when the background density is much above 1.0, the projected image of such a negative is generally difficult to evaluate because of low image brightness. A background density of about 0.6 is sufficient with most films to assure recording of the brighter, main object in the region of maximum emulsion contrast.

In view of these considerations it appeared that the speed measurement should be based on the exposure required to produce a given density above the base plus fog density. The value of 0.7 above fog was selected in accordance with Kardas.[3] The speed values given in Table II were derived by this method. The values are relative, with Kodak Linagraph Shellburst Film (gray base) assigned a value of 100, since at the time of this study it was the film most widely used in missile photography. The yellow and red filter factors for the laboratory daylight source are shown in the third and fourth columns of Table II. These factors indicate the increase in exposure necessary to maintain the 0.7 density level when the filters are used in laboratory daylight illumination, but obviously they do not indicate the exposure increase required when an object is photographed against a blue sky. Therefore, a set of filter factors was determined for actual skylight. Such data determined in Boston and in Florida, and their average values, are given in Columns 5–10 of Table II. These factors were obtained by photographing an area of clear blue sky at a 90° angle from the sun without filter and with yellow and red filters, measuring the densities of the sky images, and deriving from the characteristic curve of the same film processed similarly the log E increase required to obtain a density of 0.7 instead of the actual and lower image densities. This log E difference is the log of the filter factor.

These data may be used to calculate the exposure required for a new film, with or without filters, or to calculate the exposure increase required when shifting from a yellow to a red filter. For example, Linagraph Shellburst with a red filter has a relative speed of 100/10.5, or 9.5, while Plus-X Aerecon has a relative speed of 274/7.1, or 39. Thus it should require about 39/9.5 or 4.1 times less exposure than Linagraph Shellburst. Tri-X (135) under similar conditions would have a speed of 600/14, or 43. This indicates that Tri-X (135), although normally the fastest film of the group, is not appreciably faster than Plus-X Aerecon when used for missile photography.

Image Quality

The quality of an image cannot be measured easily. One relatively new approach is to measure the image contrast as a function of test pattern spacing; this is

termed the sine-wave response, or more generally, the transfer function. Such measurements, however, are difficult to make. A simpler and still the most widely used technique is to measure the resolving power of the emulsion. This was done in this investigation and a conventional target was used that consisted of 3-bar test objects. In a study of the film itself, such a test object must be used either in direct contact with the emulsion or photographed with an optical system that introduces negligible degradation.

The Resolving Power Test Camera

The resolving power test camera that was used (Fig. 4) images the target by means of a 17.5mm $f/2.3$ Baltar Lens onto 35mm roll film. The lens is used at $f/4.0$ because at this aperture image sharpness is at a maximum. The roll film magazine is a modified Kodak 35 camera with a special pressure platen that firmly presses a $^1/_4$-in. circular area of the film against a slightly smaller aperture during the exposure. The

TABLE I

Sensitometric Data for Films Investigated

Film	Brief Description	Gamma		Development Time (at 68 F, min)	
		D-19	D-76	D-19	D-76
Kodak Micro-File (35mm)	High contrast, slow, fine-grained recording film	4.00	1.25	5*	4†
Kodak Panatomic-X (135)	Fine-grained, low contrast amateur roll film	1.32	1.04	6	13
Kodak Plus-X Aerecon	High contrast aerial film with high red sensitivity	1.90	1.27	6	10
Kodak Special Order Product, SO-1121	Experimental high contrast aerial film with relatively low red sensitivity	1.84	1.10	6	10
Kodak Linagraph Shellburst (gray base)	High contrast long scale film designed for ballistic and shellburst photography against blue sky	1.68	0.98	6	10
Kodak Plus-X (135)	Medium speed, moderately fine-grained amateur roll film	1.23	0.98	5.5	11
Kodak Super-XX Aerial Recon. R.P.	Standard aerial photo material used by Armed Forces	1.48	1.02	6	10
Kodak Tri-X (135)	Fast, low contrast, moderately fine-grained amateur film	1.08	1.04	8	14
Eastman Panchromatic Separation Film, Type 5235 (35mm)	Fine-grained, slow pan film used for separation negatives	1.62	1.25	6	12
Kodak Infrared Aerographic (Hyper.)	Standard infrared film now used by Armed Forces	1.65	0.98	5	16
Ansco Anscochrome, Daylight Type (35mm)	35mm color reversal film of medium speed	Commercial Processing			
Kodachrome, Daylight Type (135)	35mm color reversal film of slow speed	Commercial Processing			
Kodak Ektachrome, Daylight Type (135)	35mm color reversal film of medium speed	Commercial Processing			

* Developed in Kodak Developer D-11.
† Diluted: 2 parts water to 1 part Kodak Developer D-76.

TABLE II

Relative Speeds and Filter Factors

Film	Daylight Speed (0.7 density above fog)		Filter Factors for Laboratory Daylight (5500 K)		Filter Factors for Blue Sky Background					
					Boston (Nov. 19, 1956)		Florida (Dec. 3, 1956)		Average Blue Sky Values	
	D-19	D-76	Yellow[a]	Red[b]	Yellow	Red	Yellow	Red	Yellow	Red
Kodak Micro-File (35mm)	6.6	1.8	2.5	c	3.4	c	c	c	3.4	c
Eastman Panchromatic Separation Film, Type 5235, Positive (35mm)	6.8	7.2	c	12.0	c	c	c	c	c	c
Kodak Panatomic-X (135)	76	66	c	9.0	3.2	13	3.8	14	3.4	14
Kodak Plus-X Aerecon	274	233	c	3.4	3.1	7.1	—	—	3.1	7.1
Kodak Linagraph Shellburst (gray base)	100	74	c	4.5	5.4	13	3.7	8	6.2	10.5
Kodak Special Order Product, SO-1121	230	140	c	7.0	2.8	13	—	—	2.8	13
Kodak Plus-X (135)	230	195	c	8.5	3.0	13	—	—	3.0	13
Kodak Super-XX Aerial Recon. R.P.	270	166	c	4.0	2.6	6.8	2.7	8.7	2.6	7.8
Kodak Tri-X (135)	600	525	c	8.0	4.0	13	3.8	14	3.9	14
Kodak Infrared Aerographic (Hyper.)	280	340	c	1.1[d]	c	11	c	c	c	11

[a] Kodak Wratten No. 12 Filter.
[b] Kodak Wratten No. 25 Filter.
[c] No data taken.
[d] Estimated, since sensitometer not corrected in infrared (value shown is probably low).

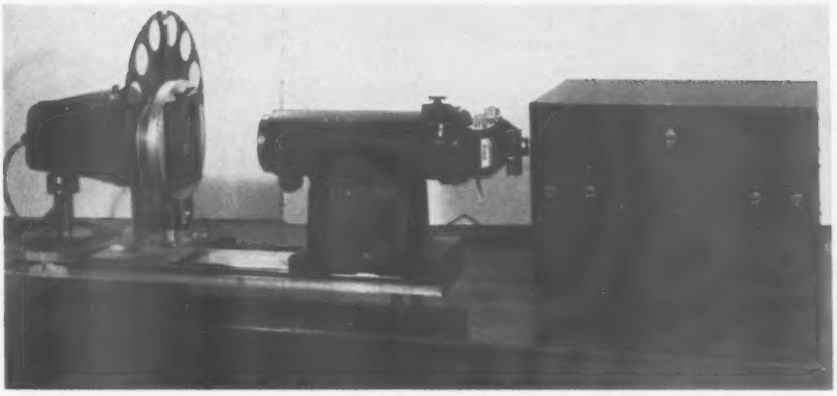

Fig. 4. The resolving power camera images the target at a 221:1 reduction.

target is transilluminated by light from a xenon discharge tube that is collected by aspheric condensers. Exposure times of 1/250, 1/500, and 1/2000 sec are available through appropriate adjustments in the flash tube power supply.

A circular filter wheel containing evaporated Inconel neutral density filters allows exposures to be made over a range in excess of 4.0 log units. Color filters can be added as desired.

Throughout the tests described here, a red filter was employed, except for Kodak Micro-File Film (35mm) which was exposed with a yellow filter.

Experimental Procedures

In addition to the quantitative resolving power data determined for high and low target contrast, photographs of simulated low and high contrast missile targets were made to obtain information about the image quality that could be expected from each film under real field conditions. The original plan was to examine the capability of the films with a high quality optical image, in which case the resolving power of the emulsion would be the only limiting factor, and then to repeat the test with a degraded image which would closely simulate the level of image quality actually obtained in the field. In this second analysis the optical image quality was to be low enough, relative to the image quality the film is capable of producing, so that it was expected the emulsion would have relatively little influence on the final image quality.

The targets, in addition to the resolving power chart, consisted of profiles of geometric shapes resembling missiles, uniformly transilluminated and lighter than their background, reproduced in a range of sizes

TABLE III

Image Sizes and Simulated Distances for a 60-ft Object and 60-in. Focal Length Camera

Missile Image Number	Simulated Distance in miles	Image Size in mm	
		Length	Width
1	10.9	1.57	0.224
2	13.7	1.24	0.178
3	17.25	0.985	0.141
4	21.8	0.783	0.112
5	27.4	0.621	0.0888
6	34.6	0.492	0.0704
7	43.8	0.391	0.0559
8	54.8	0.311	0.0444
9	69.2	0.247	0.0352
10	87.2	0.196	0.0282
11	110.0	0.155	0.0222
12	138.0	0.123	0.0176
13	174.0	0.0979	0.0140

Note: In the unsharp image study, described later, the three largest missile images were not used because of space limitations. The largest missile image in these photographs is No. 4 above.

Fig. 5. Reproduction of the simulated missile target. Size decreases in a $\sqrt[4]{2}$ ratio.

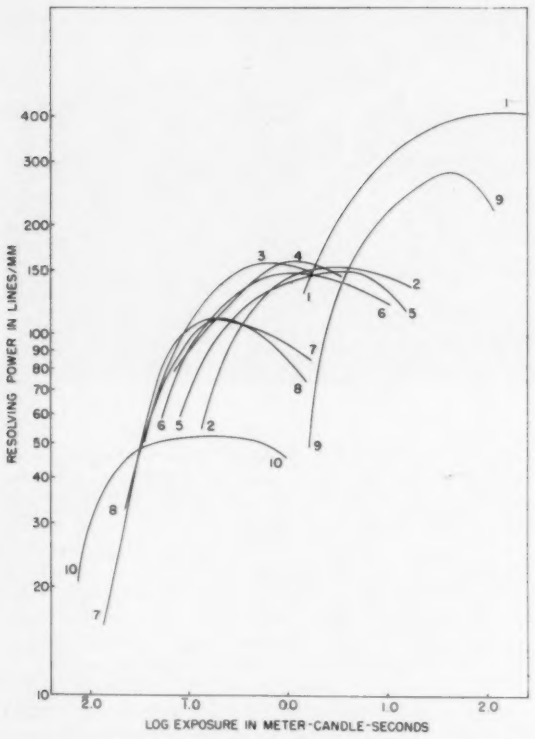

Fig. 6. Resolving power curves* for target contrast of 1.5 (log luminance ratio), processed in Kodak Developer D-19.†

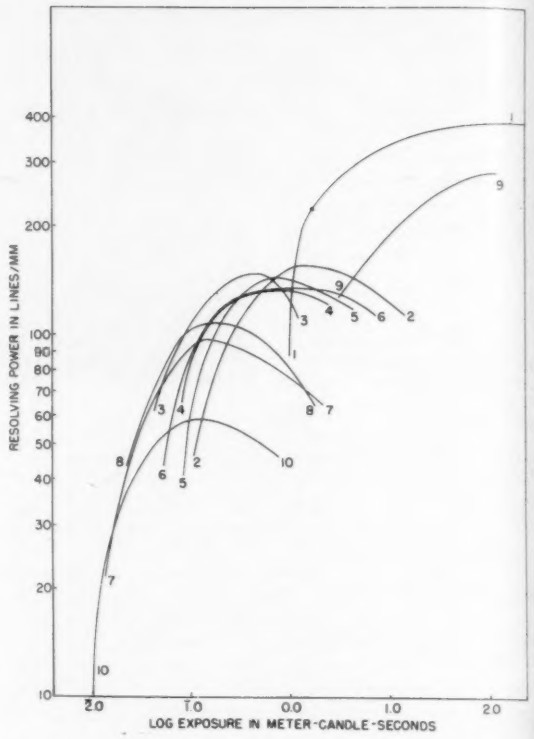

Fig. 7. Resolving power curves* for target contrast of 1.5 (log luminance ratio), processed in Kodak Developer D-76.†

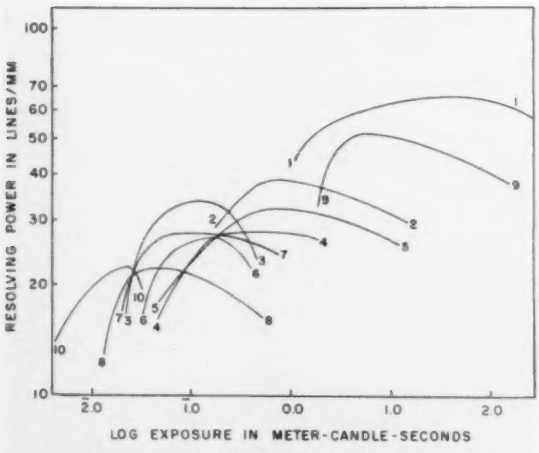

Fig. 8. Resolving power curves* for target contrast of 0.14 (log luminance ratio), processed in Kodak Developer D-19.†

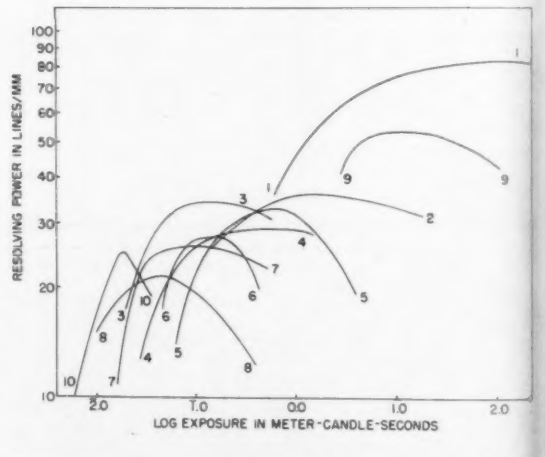

Fig. 9. Resolving power curves* for target contrast of 0.14 (log luminance ratio), processed in Kodak Developer D-76.†

* Log exposure in meter-candle-seconds — figures given are for before modification by filter.

† Except for Curve 1 — Kodak Micro-File (35mm) Film, processed in Kodak Developer D-11. Source for Micro-File modified by Kodak Wratten Filter No. 12 (yellow). Source for other nine films modified by Kodak Wratten Filter No. 25 (red). Film names for Curves 2–10 are as follows:

2. Kodak Panatomic-X Film (135)
3. Kodak Plus-X Aerecon Film
4. Kodak Special Order Product, SO-1121
5. Kodak Linagraph Shellburst Film
6. Kodak Plus-X Film (135)
7. Kodak Super-XX, Aerial Recon. R.P. Film
8. Kodak Tri-X Film (135)
9. Eastman Panchromatic Separation Film, Type 5235 (35mm)
10. Kodak Infrared Aerographic Film (Hyper.)

and at three levels of contrast. The contrast values in terms of log luminance ratios were 1.5, 0.14, and 0.08. The two latter values represent the region in which resolving power changes very rapidly with image contrast. This region is of particular interest because it encompasses conditions that are encountered when missiles are photographed at extreme distances and under poor atmospheric conditions. The 0.14 contrast target is reproduced in Fig. 5. The resolving power camera images this target at a reduction ratio of 22:1. In Table III are listed the simulated object distances assuming a 60-ft object and a 60-in. focal length lens. A red filter was used in all of this work since it was also used in practice.

All the resolving power and simulated missile photographs were processed in both D-19 and D-76 developers, as previously described.

The resolving power photographs were evaluated by a group of trained analysts, with binocular microscopes. The resolving power data obtained in this manner are plotted in relation to log E values in Figs. 6–10 for all the films and for contrast values of 0.14 and 1.5.

Reproductions of the sharp images of the simulated missiles are shown in Figs. 11 and 12. The emulsions are ranked generally in order of decreasing image quality. These enlarged reproductions were prepared from negatives with background densities closest to 0.7.

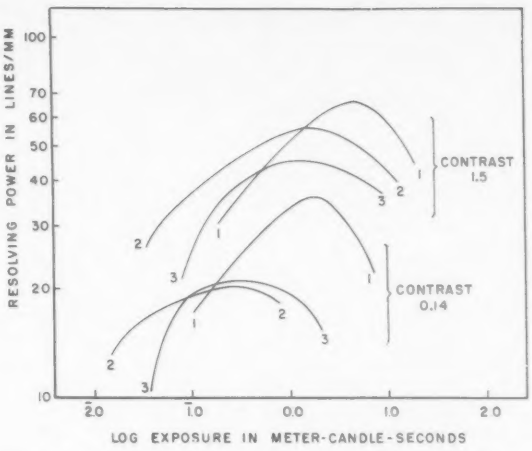

Fig. 10. Resolving power curves for three color films for target contrasts of 1.5 and 0.14 (log luminance ratio), processed by commercial laboratories. Curve 1 — Kodachrome Film, Daylight Type (135); Curve 2 — Anscochrome 35mm Film, Daylight Type; Curve 3 — Kodak Ektachrome Film, Daylight Type (135).

Unsharp Image Study

The three most promising films — Linagraph Shellburst, Plus-X Aerecon, and Tri-X (135) — were selected for comparison of their relative usefulness when exposed to a degraded image of the quality encountered in the field. A new combined resolving power target and simulated missile target was made. The unsharp images were produced by means of a diffraction limiting pinhole of 0.036-in. diameter placed directly in front of a 127mm Kodak Ektar

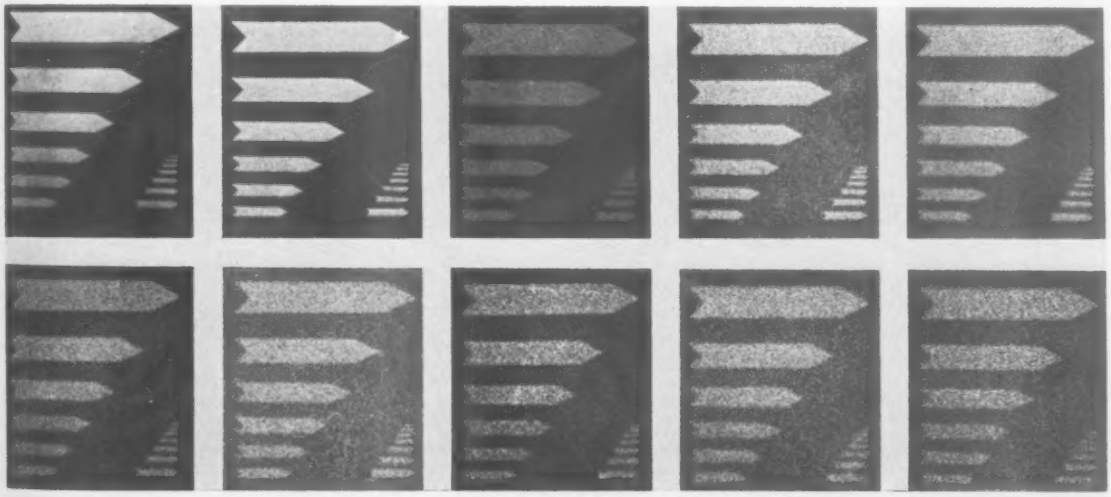

Fig. 11. Enlarged reproductions of the negatives having a background density close to 0.7 above fog; original target contrast, 0.14; length of largest missile on film, 1.57 mm. *Upper left-hand corner:* Kodak Micro-File (35mm) Film, exposed with Kodak Wratten Filter No. 12 (yellow), processed in Kodak Developer D-11. The other nine negatives, exposed with Kodak Wratten Filter No. 25 (red), processed in Kodak Developer D-19. *Upper row, starting with second from left:* Eastman Panchromatic Separation Film, Type 5235 (35mm); Kodak Panatomic-X Film (135); Kodak Plus-X Aerecon Film; Kodak Linagaph Shellburst Film. *Lower row, left to right:* Kodak Special Order Product, SO-1121; Kodak Plus-X Film (135); Kodak Super-XX, Aerial Recon. R.P. Film; Kodak Tri-X Film (135); Kodak Infrared Aerographic Film (Hyper.)

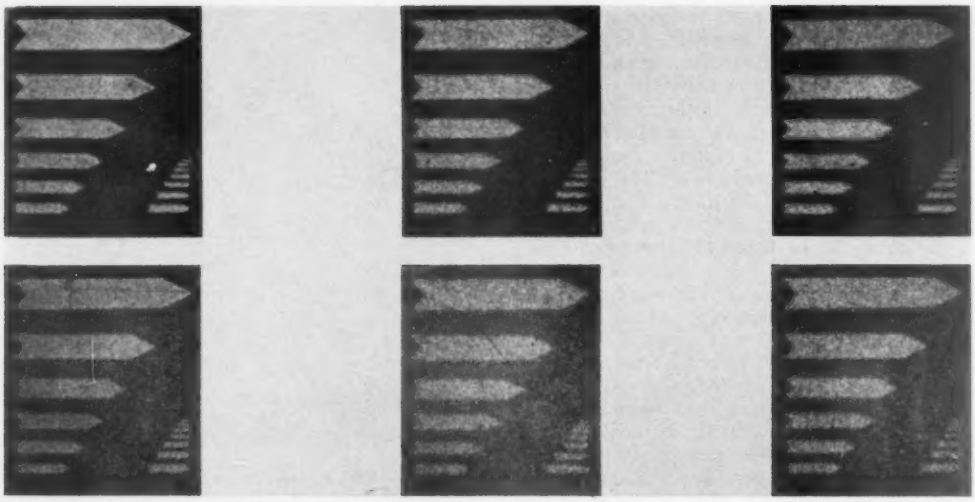

Fig. 12. Enlarged reproductions of the color film photographs having a background density close to 0.7 above fog for original target contrasts of 0.14 and 0.08. *Upper row, left to right:* Contrast 0.14 — Kodachrome Film, Daylight Type (135); Anscochrome 35mm Film, Daylight Type; Kodak Ektachrome Film, Daylight Type (135). *Lower row:* Contrast 0.08 — films arranged in same order.

Lens. The technique for this treatment of the image has been previously described.[4]

A series of exposures to this unsharp image for both the high (1.5) and the low (0.14) contrast targets was made on all three films. As in the sharp image study, the frames having a background density closest to 0.7 above base plus fog were selected for enlargement. It should be pointed out that for this degraded image, much greater latitude in exposure exists, that is, the image quality remains essentially the same over a much wider range of exposure. This has been borne out in examination of photographs of a B-36 aircraft made over Florida. In these images the resolution level is approximately the same as that for the diffraction limited images used in this study.

Enlargements of the unsharp images are shown in Figs. 13 and 14, and resolution values are given in Table IV. For both the high (1.5 density difference) and the low (0.14) contrast unsharp image, a slight but definite difference exists between the three films. At high contrast, all three films resolve at least the second unit (9.6 lines/mm), and all resolve about one unit less with the low contrast target. The percentage change in resolution with target contrast was much smaller, therefore, than with the sharp images in which the emulsion was the limiting factor. Tri-X (135) showed a lower contrast image than the other two films; this, rather than granularity, accounted for its lower resolution, even at the 10-line/mm level. The lower contrast would not be desirable in long range missile photography where, as the missile approaches the detection limit, the image contrast is even lower than the 0.14 value used here. Figure 15 shows a photograph of the specially painted B-36 aircraft at a distance of 15 miles and at an altitude of 40,000 ft, made on Plus-X Aerecon.

TABLE IV
Maximum Resolution Obtained With the Unsharp Image Using Kodak Developer D-19

Film	Resolution in lines/mm	
	Contrast 1.5	Contrast 0.14
Tri-X (135)	9.6	8.1
Linagraph Shellburst	10.8	9.1
Plux-X Aerecon	10.2	8.6

Conclusions

If one were to select an emulsion merely on the basis of the maximum resolving power, ignoring the question of sensitivity and contrast, Micro-File Film would be the first choice. Resolving power, however, is not the only factor, nor is it the most important one. The sensitivity of the emulsion to yellow or red light is of equal importance, since this directly influences the maximum shutter speed and, therefore, the image motion. The ability of the films to give good image contrast for an image that is of relatively poor contrast appears to be equally important. In surveying all the data that have been presented and studying actual photographs obtained in Florida with some of these emulsions, the following conclusions are drawn:

(1) Linagraph Shellburst offers a good compromise between red sensitivity and image quality and contrast.

(2) The new Plus-X Aerecon, however, provides equally good image quality and contrast, and requires

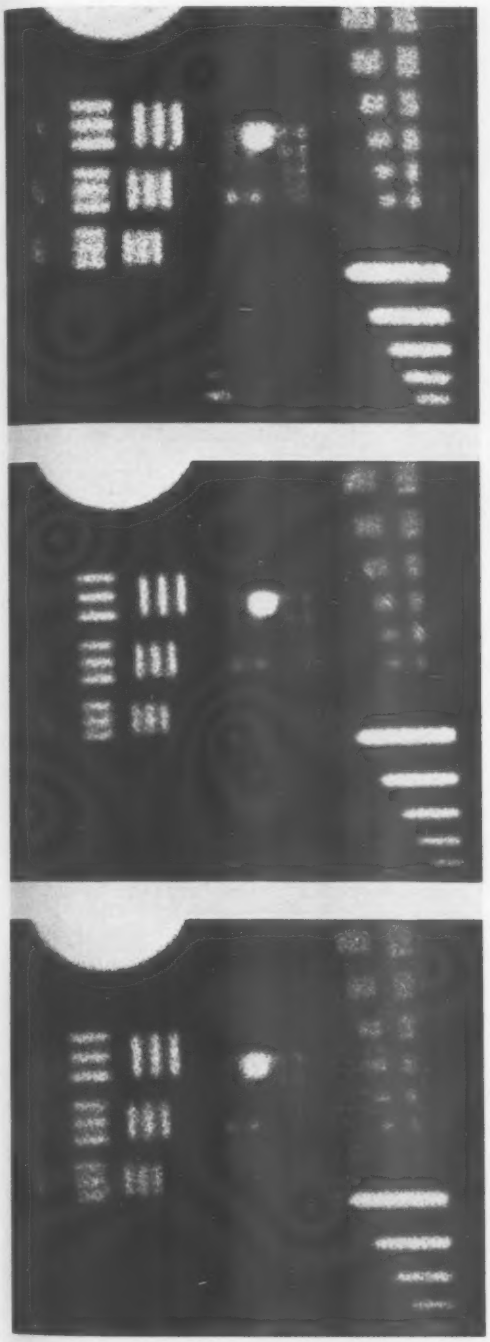

Fig. 13. Enlarged reproduction of 1.5 contrast target for lens resolution on the negative of 11 lines/mm, demonstrating lessened importance of emulsion for low image quality. *Top*, Kodak Tri-X (135) Film; *middle*, Kodak Linagraph Shellburst Film; *bottom*, Kodak Plus-X Aerecon Film.

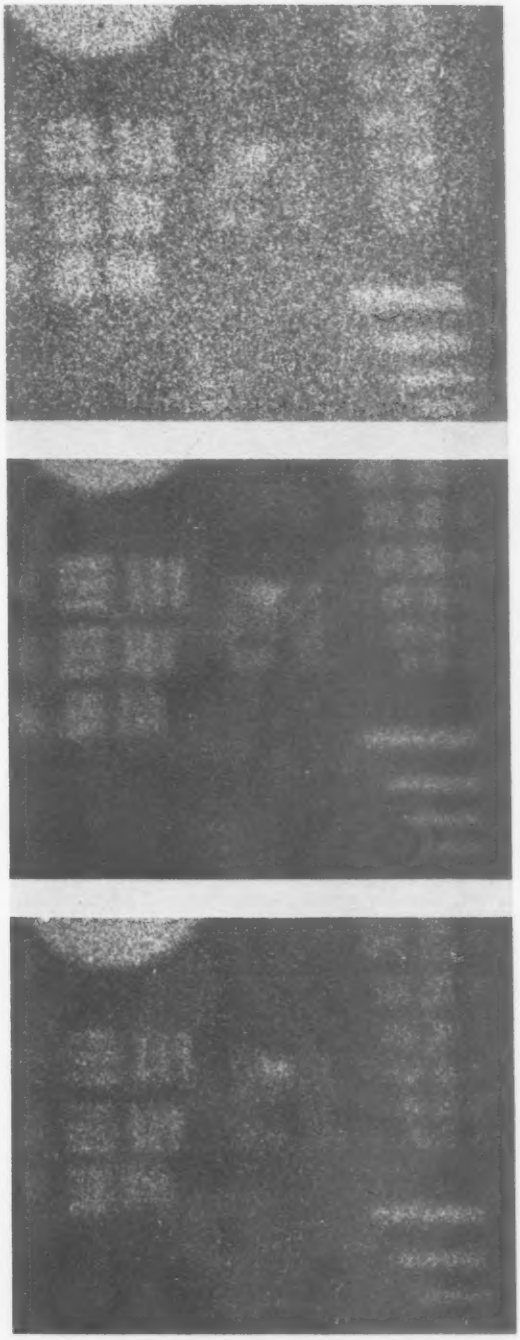

Fig. 14. Enlarged reproduction of 0.14 contrast target for lens resolution on the negative of 11 lines/mm, demonstrating a slight advantage imparted by the higher contrast Linagraph Shellburst and Plus-X Aerecon films. *Top*, Kodak Tri-X (135) Film; *middle*, Kodak Linagraph Shellburst Film; *bottom*, Kodak Plus-X Aerecon Film.

Fig. 15. Operational photograph of special B-36 aircraft on Kodak Plus-X Aerecon Film at range of 15 miles and altitude of 40,000 ft.

one-third to one-fifth the exposure that Linagraph Shellburst does for actual missile photography against a blue sky. It appears, therefore, that at the present time Plus-X Aerecon is an optimum black-and-white film for missile photography. Further study of this film under field conditions is certainly warranted.

(3) Tri-X (135) has about the same speed at Plus-X Aerecon when used against the blue sky with a red filter, but produces considerably lower contrast. At very long ranges, where image size and the image contrast approach the threshold of detection, Tri-X (135) is considerably poorer than either Linagraph Shellburst or Plus-X Aerecon. It should be pointed out, however, that for relatively near distances (perhaps up to 40 miles) Tri-X (135) may yield adequate contrast, particularly when the missile is well illuminated and painted white or orange.

(4) Of all the other black-and-white films tested, only Panatomic-X Film (135) might be worthy of consideration for use with relatively fast optical systems and in instances where the predicted image quality and contrast is high owing to unusually good atmospheric conditions. Panatomic-X (135) has low red sensitivity and inherently low contrast, as compared with Plus-X Aerecon and Linagraph Shellburst, but its resolving power was second only to Micro-File and Eastman Panchromatic Separation Film, Type 5235 (35mm). It would require about twice the exposure that Linagraph Shellburst requires. Micro-File, used with a yellow filter instead of a red filter, would require about five times the exposure of Linagraph Shellburst.

(5) There is little or no advantage to be gained from the use of D-76 developer instead of the currently used D-19 developer. With the D-76 developer, a loss in emulsion speed occurred in all cases and no significant improvements in resolving power were obtained, even in the sharp image study. The only advantage that D-76 offers over D-19 is that lower gamma values can be obtained even on prolonged development. Generally this is not desirable; however, when photographs are made at near distances and under good atmospheric conditions, that provide unusually good image contrast, development in D-19 developer sometimes leads to excessively high gamma values with Linagraph Shellburst and Plus-X Aerecon.

(6) Although no experimental work directly relating to the printing of missile images was done in this study, investigations in the field of aerial photography have proven that a much wider range of tones can be reproduced in positive transparency prints than in the usual opaque paper prints. For example, short range photographs made of B-36 aircraft have such a wide density range that it is quite difficult to retain all the detail in a paper print but excellent prints can be made on transparency film.

References

1. Watson, J. T., and Howell, H. K., *An Experimental Study of Factors Affecting Long Range Haze Penetration in Long Range Photography*, Boston University Technical Note 124 (SECRET), Dec. 1955.
2. Mees, C. E. K., *Theory of the Photographic Process*, rev. ed., The Macmillan Co., New York, 1954, pp. 1020, 1022.
3. Kardas, R., *Analysis of Film Factors Affecting the Quality of Images Obtained by Optical Instrumentation*, Study Report, Patrick Air Force Base, 5 July 1956.
4. Macdonald, X. Z., and Watson, J. T., "Detection and Recognition of Photographic Detail," Part I, *J. Opt. Soc. Am.*, *46*: 715 (1956).

PHOTOGRAPHIC SCIENCE AND ENGINEERING
Volume 2, Number 2, August 1958

• Technicalia Photographica

FRANK SMITH

• Cameras, Components, and Accessories

Long Range Infrared Reconnaissance Camera

A long range camera with which close-up pictures can be made of scenes 30 miles away has been announced by the Department of the Army. The camera was developed by the U.S. Army Signal Engineering Laboratories, Fort Monmouth, N.J., and the Kalart Co., Inc., Plainsville, Conn. It easily outperforms other standard Army cameras. A 100-in. infrared transmitting lens is used that makes possible photography through haze and under other conditions of poor visibility. The camera accepts standard or Polaroid 5 × 7-in. film.

Internal mirrors are used to fold the optical path into a "Z" shape. This eliminates the long extension tube needed in previous, experimental version of the camera. The total weight of the camera is about 150 lb, the weight of the lens 40 lb.

Pinhole Camera for Intense Radiation

A pinhold camera constructed of lead and uranium and weighing 29 lb has been developed by the Knolls Atomic Power Laboratory, operated by General Electric Co. for the Atomic Energy Commission. The camera is used to locate radioactive contamination too "hot" for effective use of other detection instruments.

The camera, which was designed by John Payne, carries two types of film, one making conventional negatives by ordinary light, and the other, an x-ray film, recording atomic radiation. After development, the x-ray film is superimposed on the conventional film to isolate the location of the "hot" radiation sources.

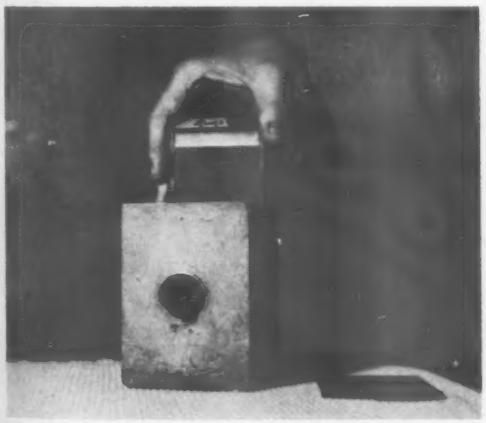

Photographic "Flying Saucer"

A photographic flying saucer, the "Fotodome," designed to aid missile research, has been developed by Traid Corp., Encino, Calif. It is mounted piggyback on the wing of an airplane or guided missile to record photographically the accuracy of the carrier or obtain other desired data.

One of several versions of the Fotodome consists of a circular aluminum base plate 24 in. in diameter, covered by a clear plastic dome which is optically ground and polished. Two 16mm motion picture cameras mounted inside the dome obtain an undistorted view in any direction. The camera exposures are set by means of automatic controls which adjust the lens diaphragms to compensate for changes in light conditions.

Rolleiflex 4 × 4-cm Miniature Reflex Camera

Burleigh Brooks, Inc., 10 West 46th Street, New York 36, N.Y., American agents for the Rolleiflex

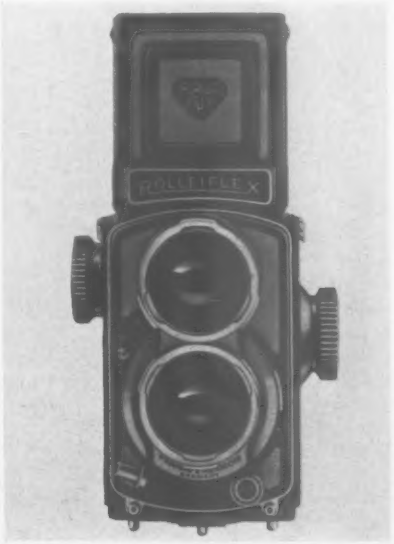

cameras, has announced that the new Rolleiflex 4 × 4-cm Miniature Reflex Camera is now available. Production on it was suspended in 1941.

The camera uses No. 127 roll film and yields twelve 4 × 4-cm ($1^5/_8 \times 1^5/_8$-in.) pictures per roll. The camera is normally equipped with a Schneider Xenar *f*/3.5 lens and, with the exception of the hood, accepts the same lens accessories (Size I) which fit the bayonets of the 6 × 6 Rolleis. The Synchro Compur Shutter has ten shutter speeds from 1/500 to 1 sec, and and X-M contacts for electronic flash and normal flash synchronization. The camera measures $4^3/_4 \times 2^1/_2 \times 3^1/_4$ in. and weighs 24 oz.

Argus C-44 Color-Slide Camera

Argus Cameras Division, Sylvania Electric Products, Inc., has introduced a new Argus C-44 color-slide camera which has a rapid film winding mechanism and a turret viewfinder.

Two strokes of the wind lever advance the film and cock the camera shutter. The turret viewfinder includes appropriate optical systems that match the C-44 interchangeable taking lenses, the 50mm standard, the 35mm wide-angle, and the 100mm telephoto.

The new C-44 also will accommodate a small, precision-coupled exposure meter that will be marketed later this year.

Super Graphic 45 Press Camera

Graflex, Inc., Rochester 3, N.Y., has announced the Super Graphic 45, a new all-metal 4 × 5 press camera. The lens board of the new camera can be tilted and swung, and shifted laterally and up and down. A forward tilt of 30° can be obtained by means of the tilting lens board and drop bed. The drop bed also accommodates wide-angle lenses. A revolving back is provided into which film holders may be inserted from top, bottom, right, or left.

A new-style double-cam-action slide lock holds any accessory such as the Graphic or Graflok back-sheet film magazine, roll film holder, film pack adapter, Polaroid back, or Graflarger. The camera body is made of extruded aluminum and weighs $4^3/_4$ lb.

• Illumination

A Mirror-Condenser Lamp for 8mm Projectors

P. M. van Alphen and M. Bierman, *Philips Tech. Rev.*, Vol. 19, No. 7–8, pp. 233–235 (1957–58—published 10 Feb. 1958).

Described is a small 50-w projection lamp designed for 8mm projectors. The lamp operates at 8 v and 6.25 amp. The silvered rear surface of this bulb is ellipsoidal, the front surface is spherical and partially covered with a silvered annulus. The ellipsoidal mirror functions as a condenser and forms an unsharp image of the filament approximately 12 mm beyond the front surface of the bulb. This makes for adequately even illumination in the image plane. The luminous flux on the screen is much higher with this new low-voltage lamp than with a conventional lamp and condenser system. This makes it possible to build 8mm projectors that are lighter and cheaper than models now in use. Illus., 5 ref.

The Xenon Lamp for Film Projection

E. J. G. Belson, W. A. Bocock, A. P. Castellain, and F. A. Tuck, *Brit. Kinematog.*, Vol. 32, No. 3, pp. 59–74 (Mar. 1958).

A report of the recent progress and development work by the British Thomson-Houston Co., especially with a d-c operated xenon lamp, with particular reference to its application to 35mm and 16mm film projection. The paper is divided into four main sections: (1) the Mazda xenon lamp itself; (2) the 35mm lantern and its power supply; (3) the results and economics of 35mm xenon operations; and (4) the 16mm application.

The authors feel that the xenon lantern forms one of the major single steps towards motion-picture automation and simplicity of operation, and that for this reason alone this light source has come to stay. Illus.

Variable Delay Spark Illumination for Single-Shot High-Speed Photography

G. Hodgson, *Electronic Eng.*, Vol. 29, pp. 608–610 (1957).

A method of taking a series of high quality photographs of a reproducible phenomenon by delaying the illuminating spark for a known, controllable time is described. The delay is variable from 100 msec to 1 sec after the object has interrupted a light beam. The photographs are taken with a conventional camera, each photograph having an exposure of 20 μsec. Illus., 5 refs.

Transistor-Powered Portable Electronic Power Units

Greater economy and lighter weight are features of the new Ascorlight transistor-powered Series 400 portable electronic power units.

The B-422 power unit is rated at 100 wsec, and the B-423 unit is rated at 200 wsec. They cover a range of power from 25 to 200 wsec and incorporate push-button switching from high to quarter power, two light connectors, a trigger tube circuit for sensitive slave operation and a-c or "D" cell photoflash and nickel-cadmium battery operation.

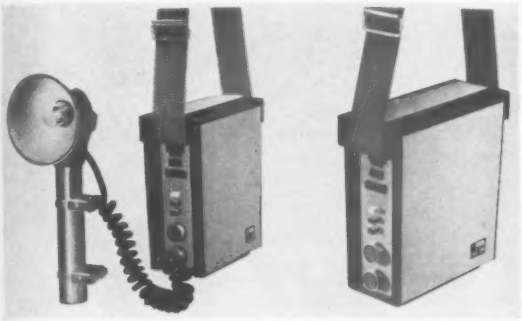

The B-422 power supply measures 9 × $3^5/_8$ × $7^1/_2$ in.; its weight, without batteries, is $4^1/_2$ lb. The B-423 measures 9 × $3^5/_8$ × 9 in. and is $5^1/_2$ lb without batteries. A full line of accessories is available. Additional information may be obtained from the manufacturer, American Speedlight Corp., 63-01 Metropolitan Ave., Middle Village 79, N.Y.

Improved Light Valve for the Photographic Recording of Vibrations

Gopala Menon Streek-Antath, *J. Acoustical Soc. Amer.*, Vol. 29, pp. 1034–1035 (1957).

In a "Letter to the Editor," the author gives a brief description of the improved light valve which consists of two coarse transmission plane optical gratings, *A* and *B*, having opaque and transparent elements of equal width. They are mounted, one close behind the other, with their vertical planes parallel and with the lines parallel to a vertical narrow slit. The slit is illuminated by an intense source of white light. The transmitted light is collimated and directed perpendicularly onto the gratings *A* and *B*. The light transmitted by the gratings falls onto a second achromatic converging lens which generates diffraction spectra of various orders at its focal plane. The central or zero order is isolated from the rest with the help of a slit of suitable width and a sharp image of the slit is formed on a photographic film held in the focal plane of the lens. A variable density record is produced and mechanical vibrations can be photographically recorded in this fashion.

Heiland Futuramic Strobonar

Minneapolis-Honeywell Regulator Co., Heiland Division, 5200 East Evans Ave., Denver 22, Colo., has released some details covering their new electronic flash unit, the Futuramic Strobonar.

The completely self-contained electronic flash unit operates from three photoflash batteries or from ac. The power source is built into the lamp head. A new, small reflector, special flash tube, and lens give good light distribution over a field of 70°.

The new Eveready E95D batteries that are used give over 500 flashes in the Transistor model, 250 flashes in the Standard model. Ordinary photoflash batteries give 200 and 100 flashes respectively. Heiland Permaclad Batteries (permanent, rechargeable nickel-cadmium D-cells) may be used for greater economy and faster cycling in either model. Recharging time is 8–12 sec. The weight of the unit, without batteries, is 35 oz.

Tiny Zirconium-Filled Flash Lamps

A new, thimble-sized photoflash lamp that yields nearly the same illumination as former lamps four times its size has been announced by Sylvania Electric Products, Inc. The new M-25 lamp, which contains shredded zirconium foil, reaches its peak light output of 16,000 lm-sec in 17 msec. The present Press 25 lamp reaches a peak light output of 20,000 lm-sec in 20 msec. The new lamp has a superior performance because zirconium burns more efficiently, creates less pressure at the peak of the flash, and burns cleaner.

Commercial production of the clear M-25 and a blue M-25B bulb for use with color film was scheduled to begin in the first quarter of 1958.

Sylvania has also announced two new small-base lamps, M-5 and M-5B, that are only one-fourth the size of the Press 25 flash lamp but have equivalent light output. The peak intensity is reached in 20 msec, and therefore full synchronization at M-shutter setting is obtained.

The M-25, M-25B, M-5, and M-5B lamps complete the Sylvania line of small-based flash lamps that includes also the aluminum-filled M-2 and M-2B lamps.

Generator-Powered Flash Holder

A compact, generator-powered flash holder has been introduced by the Eastman Kodak Company, Rochester, N.Y. It is named the Kodak Generator Flasholder. A half turn of a small nylon handwheel stores enough electricity in a capacitor to fire one M-2, No. 5, M-5, or M-25 flash lamp.

The unit is available in two types. Type 1 fits directly onto Kodak Brownie, Star, Pony, and Signet-type cameras. Type 2 has shoe fittings and a cord for mounting in the accessory clip of cameras such as the Kodak Retina series. The cord has interchangeable tips for ASA or continental flashpost connectors. The folded flash holder measures approximately $3^1/_4 \times 3 \times 1^3/_4$ in.

Eveready "Energizer" Flash Batteries

The National Carbon Co., Division of Union Carbide Corp., 30 East 42nd Street, New York 17, N.Y., manufacturer of Eveready batteries, has announced the new "Energizer" E-95 D-size battery for photoflash work. The "Energizer" is claimed to give as much as ten times the service previously obtained from standard carbon-zinc dry batteries of the same sizes.

The battery is of the alkaline type and uses a potassium hydroxide electrolyte, a zinc negative pole, and a manganese dioxide depolarizer. It is hermetically sealed in a steel can and is leakproof. The operating voltage is 1.5-1.6 v at 10 amp-hr. A maximum short circuit current of 20-25 amp is obtainable. The new battery functions satisfactorily in temperatures from −40 F to 200 F.

The battery can also be used in portable radios, phonographs, and tape recorders, and in portable electronic flash units and portable still and motion-picture cameras. The main advantage in low-drain work such as conventional photoflash is a much longer life. In high-drain work such as electronic flash, the operating efficiency is considerably higher.

The battery is also made in a "half-cell" size, the E-94, which is half the length of the E-95 and delivers a little less than half the ampere-hours at the same voltage.

Millimicrosecond Duration Light Source

J. H. Malmber, *Rev. Sci. Instr.*, Vol. 28, pp. 1027–1029 (1957).

A simple circuit utilizing a hydrogen flash tube is described. The duration of the pulses of light is equal to or less than one millimicrosecond. Illus., 3 refs.

Mecablitz 100 Transistorized Electronic Flash Unit

A new electronic flash unit imported from Germany incorporates in the generator circuit a power transistor which replaces the conventional vibrator and is used for converting direct current from dry cell batteries to the needed alternating current.

The power transistor is one-third the size of a vibrator and its associated transformer is much smaller and lighter than that required for the vibrator. The transistor circuit supplies frequencies between 5,000 and 10,000 cycles (compared with 100 to 200 cycles with vibrators), and this accounts in large part for increased efficiency. The Mecablitz 100 is fitted with a new, high-output, bar-shaped lamp and a specially designed parabolic reflector. It weighs approximately 4 lb with batteries (flashlight "D" cells). The unit is available at Burleigh Brooks, Inc., 10 West 46th St., New York, N. Y.

GE "Stick" Light for Enlargers and Printers

The General Electric Co., Photo Lamp Dept., Nela Park, Cleveland 12, Ohio, has announced a new $6^1/_2$-in. pencil-shaped light bulb developed especially for photographic equipment such as projectors and printers. A multiple array of the tubular lamps is used to yield a flat plane of light of uniform brightness. Most existing enlarger lamps have the familiar pear shape, are burned base up, and range in length from 3 to 10 in. The new lamps are placed side by side and have a diameter of only $^3/_8$ in. The high brightness of the new light array will permit increased printing speeds.

The new lamps are at present available only in 100-w size, but other sizes are planned. They are made of clear glass, operate on 110 v, and have a cap base. The expected life is 10 hr.

GE Power Mite M5 Zirconium-Filled Flash Lamp

The Power Mite M5, a new, zirconium-filled flash lamp, has been announced by General Electric Company, Photo Lamp Dept., Cleveland, Ohio. It is the same size and shape as present M2 miniature lamps.

The M5 is a miniature No. 5 flash lamp, but it has the same effective light output and color quality as the No. 5 lamp. It synchronizes at all shutter speeds.

The high light output of the Power Mite M5, 16,000 lm-sec, versus 20,000 lm-sec for the No. 5, is rooted in the use of shredded zirconium foil and increased oxygen content. Although the total light output of the M5 is lower than that of the No. 5 lamp, its smaller size makes for greater efficiency when it is used in a 3-in. reflector. For this reason, the guide numbers are the same for both lamps with this size reflector.

Self-Powered Flash Lamp

A technical note in the *Battelle Technical Review* for April 1958, p. 16, describes an experimental-type photographic flash lamp in which the power source is contained within the lamp itself.

A relatively simple cell composed of alternating thin layers of magnesium foil, absorbent paper, and silver-plated copper is incorporated within the metal base of the lamp. The cell surface measures 1 sq in.

Power is generated in the cell when the base of the lamp is moistened with water. The cell continues to produce sufficient power to flash the lamp for about 20 min after moistening.

Dr. John McCallum, leader of the Battelle research team that developed the lamp, reports that there are no plans at present for commercial manufacture of the new light source.

• Instrumentation

Diode Counter Calibrates Missile Testing Camera

Samuel E. Dorsey, *Electronics* (*Eng. Ed.*), Vol. 31, No. 7, pp. 93–95 (Feb. 14, 1958).

The speed of continuously moving film in a shutterless 35mm camera used for smear photography is calibrated in feet per second by means of a frequency tachometer. The heart of the meter is a loaded-diode counter whose amplified output drives a pen oscillograph. Although the counter was developed for a specific camera, it may be used with any camera having similar focusing provisions. Illus.

Kerr Cell with Improved Circuit for 0.01-μsec Exposure

An exposure time of 0.01 μsec has been achieved with a Kerr cell electro-optical shutter and an improved pulse generator circuit devised by Avco Mfg. Corp., Research and Advanced Development Div., Lawrence, Mass.

The complete shutter, redesigned into a compact 12 × 12 × 5-in. package, is now being marketed by Avco. The package includes the pulse generator and a specially designed spark gap to provide the required driving signal. The unit operates from an external

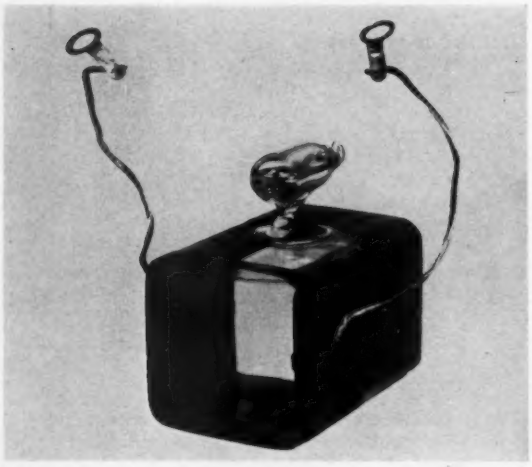

0-50 kv power supply and a low-voltage trigger source.

The 2-in.-square shutter has been used in aerodynamic simulation studies of long-range missile reentry problems. Exposure times in the range of 10^{-8} to 10^{-7} sec are required to prevent image blur in this work in which scaled-down projectiles are fired at very high velocities.

The key to the new technique is a pulse generator which consists of an RG8/U coaxial cable and the spark gap. The Kerr cell is connected directly across a load resistor on the transmission line and does not require an impedance matching network or pulse transformer.

Original work on the pulse generator was performed at the Los Alamos Scientific Laboratory under the auspices of the Atomic Energy Commission.

Shock Wave Photography of Large Subjects in Daylight

Harold E. Edgerton, *Rev. Sci. Instr.*, Vol. 29, No. 2, pp. 171–172 (Feb. 1958).

This is a note describing a method of photographing shock waves outdoors in daylight in large-scale experiments. The system consists of an efficient small-volume, short-exposure electronic flash source near the lens of the camera and a "black" Scotchlite screen for a background. The subject is placed about three-quarters of the distance from the camera to the screen so that refraction at the subject of light from the lamp shows a shadow pattern on the screen. Illus., 1 ref.

Automatic Data Recording Device for Aerial Photographs

The Digital Data Recording Device developed by the Federal Telecommunications Laboratories, Research Division of the International Telephone and Telegraph Corp., records in code the location, speed, altitude, and other pertinent data directly on photographic film as the camera aircraft flies over its target.

The instrument was developed for the Wright Air Development Center, Air Research and Development Command, USAF. Information about the position of the aircraft is relayed from various instruments to the Digital Data Recorder and displayed in code form on a 1-in. cathode-ray tube that is positioned in the field of view of the camera lens. As the camera turns, the digital data are recorded automatically on a very small area of the film. During development of the film, the ground-based portion of the recording device automatically decodes and prints the information in numerical form directly below the photographic image.

Due to Air Force restrictions, this photograph of lower Manhattan has no relation to the coded information shown on the picture.

Photographic Instrumentation for Collision Injury Research

Derwyn N. Severy, *J. SMPTE*, Vol. 67, No. 2, pp. 69–77 (Feb. 1958).

A study was made of the two impacts that are part of every automobile collision, the contact between the two automobiles, and the contact between the occupants and the interiors of the automobiles. Special photographic methods permitted collection of precise quantitative data as well as important qualitative information. Superposition of before and after photographs of the underbody of each vehicle facilitated analysis of the deformation of each car's structure. Camera coverage from every important angle was used to supplement extensive electronic measurement of the forces involved in each collision.

High-speed motion-picture cameras provided the primary data. Close-ups of the rapid injury-producing events yielded new insight into the mechanism of these events. Illus.

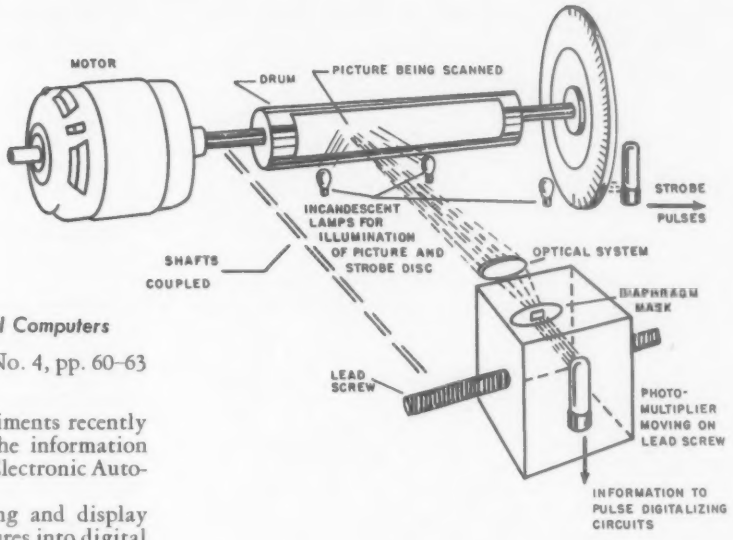

Processing Pictorial Information on Digital Computers

Anon., *NBS Tech. News Bull.*, Vol. 42, No. 4, pp. 60–63 (Apr. 1958).

Described are the exploratory experiments recently carried out on the manipulation of the information content of pictures on SEAC, the NBS Electronic Automatic Computer.

With the aid of appropriate scanning and display equipment, the computer converts pictures into digital form suitable for computer input, processes the information according to some prearranged routine, and displays the results as a visual output. Additional technical information is contained in "Experiments in Processing Pictorial Information with a Digital Computer," by R. A. Kirsch, L. Cahn, L. C. Ray, and G. H. Urban, in *Proceedings of the Eastern Joint Computer Conference* (IRE-AIEE-ACM), 1957. Illus., 1 ref.

Project Stratoscope — Solar Photographs From 80,000 Feet

John B. Rogerson, *Sky and Telescope*, Vol. 17, No. 3, pp. 112–115 (Jan. 1958).

A brief review and discussion of balloon ascents which were made on Sept. 25 and Oct. 17, 1957.

A 12-in. reflecting telescope was carried above 80,000 ft by an unmanned Skyhook balloon and solar photographs of unprecedented definition were obtained. Some 8,000 35mm photographs were taken on the first flight at an altitude 82,500 ft at intervals of one second. The telescope with accessory equipment weighed 1,400 lb. It incorporated an $f/8$ paraboloidal mirror and an enlarging lens system which produced an effective focal length of 200 ft. Illus.

A Cine-Theodolite Control System Used on Guided Missile Ranges

Electronic Engineering, Vol. 30, No. 361, pp. 128–134. (March 1958).

Cine-theodolites are used to determine the trajectory and velocity of experimental guided missiles, a number of them being dispersed on the range and operated by a central controller. The controller operates the cine-theodolite shutters and triggers flash lamps which expose the theodolite bearing and elevation readings on the film. The lamps are flashed synchronously, the interval between flashes being 200 msec $\pm$ 100 μsec. Shutter operations are synchronized to within $\pm$1 msec. These limits correspond to $\pm$1 ft in determining the missile trajectory and $\pm$0.1% of the velocity. Illus., 1 ref.

Infrared Recording Today

C. E. Engel, *Brit. J. Phot.*, Vol. 105, No. 5099, pp. 68, 69–71, and 73 (Feb. 7, 1958).

This brief survey covers the principal infrared recording systems in current use. Included are the Czerny Evaporograph, the Baird-Atomic Evaporograph, phosphorography, image converters, and direct infrared photography using infrared sensitive films. Also mentioned is the Vertoscope, an instrument manufactured by Meteor Apparateban, Siegen, Germany, which utilizes infrared radiations and a phosphor screen to make it possible to view a negative as a positive. Included in the survey is a large list of current infrared films, with their characteristics. Illus., 15 ref.

• New Materials

Kodacolor Film for 35mm Camera Use

Kodacolor film is now available in 20-exposure cartridges for 35mm cameras, according to the Eastman Kodak Company, Rochester, N.Y. The film was available previously only in roll film sizes. It is a color negative material balanced for picture taking under daylight or clear flash illumination. Differences in color balance produced by these types of illuminants are compensated in the printing operation.

Kodacolor film has an exposure index of 32 for daylight, and sufficiently fine grain to permit good quality projection prints.

Ansco Super Hypan Film in No. 120 and 620 Roll and 35mm Sizes

Super Hypan, a new high-speed black-and-white film, is now available in No. 120 and 620 roll and 20-exposure 35mm sizes, according to Ansco, Binghamton, N.Y.

The ASA Exposure Index of Super Hypan Film is 200 for daylight and 160 for tungsten light, but the manufacturer recommends Exposure Index values of 500 and 400, respectively. The film is said to have very high speed as well as fine grain, excellent definition, and low fog, even on forced development.

Super Hypan Film is also available in professional sheet film and 70mm sizes.

Ansco Fast Indoor Color Film for the Industrial Motion Picture Field

Super Anscochrome Tungsten film is now available in 16mm, 35mm (long length), and 70mm sizes, according to Ansco, Binghamton, N.Y. This new film, which is ten times faster than other reversal color films, has a tungsten film speed index of 100 with normal processing.

The high film speed makes it possible to obtain satisfactory color photographs under dim indoor illumination. The film is well suited to many engineering and scientific studies that require high-speed motion analysis, data recording, stress analysis, etc.

Kodak Super Aerographic Positive Plate

A new photographic plate of improved flatness has been announced by the Eastman Kodak Company, Government Sales Division, Rochester 4, N.Y. The surface flatness tolerance of the new plate is 35 times smaller than that of former aerographic plates. The new plates are intended for the preparation of positive glass plate transparencies from aerial negatives.

The illustration shows a Kodak engineer calibrating inspection standards for the new plate by measuring the "wedge of air" between the flat and the plate sample under monochromatic, helium-source light.

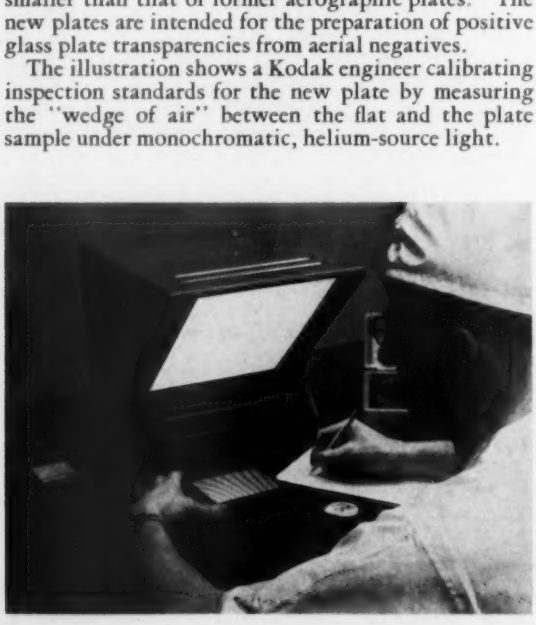

Beseler Slide-O-Film

The Charles Beseler Co., East Orange, N.J., has announced the development of a new photographic product named "Slide-O-Film." This material yields black-and-white negatives from color slides in 1 min, as well as projection positives from these black-and-white negatives, or black-and-white positive projection transparencies from any black-and-white negative.

The film can be handled under ordinary room light since it is sensitive only to ultraviolet radiation. The base of the film is Mylar. The latent image produced through exposure to ultraviolet radiation is developed through brief application of heat. The image is virtually grainless and exhibits excellent sharpness and very high resolution. The image is produced through controlled light scattering, rather than by light absorption, as in conventional silver halide materials.

Slide-O-Film is available in 35mm 36-exposure rolls and $2^1/_4 \times 2^1/_4$-in. 24-sheet packs.

Kodak Photo-Recording Paper for Instantaneous Visible Image

A new photo-recording paper, capable of providing an instantaneous visible record of instrumentation test data, is now available from Eastman Kodak Co., Graphic Reproduction Sales Division, Rochester 4, N.Y. Designated as Kodak Linagraph Direct Print Paper, the new photo-recording material may be used in conjunction with several new mirror galvanometer oscillographs and in control, production, and computing operations. While records on the new Direct Print Paper are said to maintain their sharpness and legibility adequately, a high degree of permanence may be obtained by chemically fixing the paper by conventional photographic means.

• Non-Silver Processes

Powdered Liquids Start Revolutions

Charlotte Mooers, *Chemistry*, Vol. 31, No. 7, pp. 1–4 (Mar. 1958).

A short review of the development of "No Carbon Required" (NCR) business forms made by the National Cash Register Co., Dayton, Ohio. Liquids are formed into droplets of microscopic size and the droplets coated with a thin layer of gelatin. The resulting capsule is about a millionth of an inch in diameter and consists of 70% liquid and 30% gelatin. The capsules form a dry powder which is coated on one side of the paper. The opposite side of the paper is coated with clay. Pressure, as from typewriter keys, applied to the top sheet of a stack, crushes the capsules and releases a special oil which reacts with the clay to form a blue dye.

Oils containing dyes sensitive to light have been developed. The dyes, called metachromic, may form the basis for a new dry photographic process. If paper coated with capsule powder is given a photographic

image by suitable light exposure, the image can be made permanent by pressure. This crushes the capsules on the sheet, the oil evaporates and the remaining dye is deposited on the sheet. Illus.

• Optics

Zoomar Supersonic Lens

A new lens which is built to withstand heat, friction, shock, and vibration at speeds of Mach 4 and higher, will be distributed for Zoomar, Inc., Glen Cove, N.Y., by Traid Corp., Encino, Calif. The new lens is designed for use in high-speed fighters, bombers, drones, guided or ballistic missiles, and upper-air research aircraft. Ordinary optical glass becomes red hot between Mach 1 and Mach 2, and cannot be used for photographic purposes at such speeds. The new lens unit is a combination of a periscope and an anamorphic lens, and projects only slightly into the airstream. It serves as a periscope for a 16mm camera, and has a 30° field of view. The focal length is 22 mm and the maximum aperture is $f/3.5$. The lens may be used at distances of 3 to 9 in. from the camera.

The lens is small and may be mounted in wings that have thin leading edges. It is made of fused quartz and silicon and resists temperatures up to 800 F. Higher temperature resistance is available in special models. The iris diaphragm operates under loads up to 25 G. Waterhouse stops are available for high acceleration loads.

Glass: Its Transparency and Structure

H. H. Holscher, *The Glass Industry*, Vol. 39, No. 2, Part I, pp. 81–89, 110, 112 and 114 (Feb. 1958); Part II, No. 3, pp. 143–150 (Mar. 1958); Part III, No. 3, pp. 212–220, 228, and 230 (Apr. 1958).

This is a discussion of some of the "hows" and "whys" of the transparency of glass. Part I covers electromagnetic theory, atomic structure, bonding, and transparency. Part II deals with transparent colors, surface and optical effects, presence of particles, and transparency. Part III covers transparency and structure of liquids and glasses. The author concludes that glass is a rigid liquid or a mixture of miscible liquids within each other, and should be considered a polymer in which the structural units are approaching several times the size of the small SiO_4 tetrahedron. Profusely illus., 56 ref.

Fiber Optics

N. S. Kapany, *The Frontier* (Armour Research Foundation), Spring 1958, pp. 18–22.

Colored glass fibers for photographing color television, or a flexible gastroscope for seeing around the corners of the stomach are possible with fiber objectives. An application that seems to hold promise in cryptography is an optical device for coding and decoding photographs, maps, and written matter. Illus.

Method for Fabricating Paraboloidal Mirrors

George Hass and James R. Jenness, Jr., *J. Opt. Soc. Am.*, Vol. 48, No. 2, pp. 86–87 (Feb. 1958).

Paraboloidal mirrors have been made, using a convex plastic paraboloid formed by centrifugal casting on a mercury surface as the master for fabricating plastic replica mirrors. Mirrors with disk of confusion diameters less than 1 mm have been obtained by the process. Illus., 6 ref.

The Optics of the Lenticular Color-Film Process

Rudolf Kingslake, *J. SMPTE*, Vol. 67, No. 1, pp. 8–13 (Jan. 1958).

Although lenticular film is not new, it has become a subject of current interest as a possible new tool for color television. This paper provides a basic description of the film and its associated equipment, and reviews the capabilities and limitations of this method of recording color information on black-and-white emulsion. Differences in technique and new equipment requirements peculiar to lenticular film are covered from an over-all system viewpoint. Filter requirements and lens design are outlined, as are possible designs for cameras, projectors, printers, and viewers. Illus., 8 ref.

• Photomechanical Processes

LogEtronic Continuous Strip Printer, Model SP 10/70

LogEtronics, Inc., Alexandria, Va., has announced a new Continuous Strip Printer, Model SP 10/70. In the new printer, transport speed is continuously variable up to 40 ft per min. At a typical printing speed of 25 ft per min for 9-in. aerial film, a production rate of approximately thirty 10 × 10-in. prints per minute is achieved.

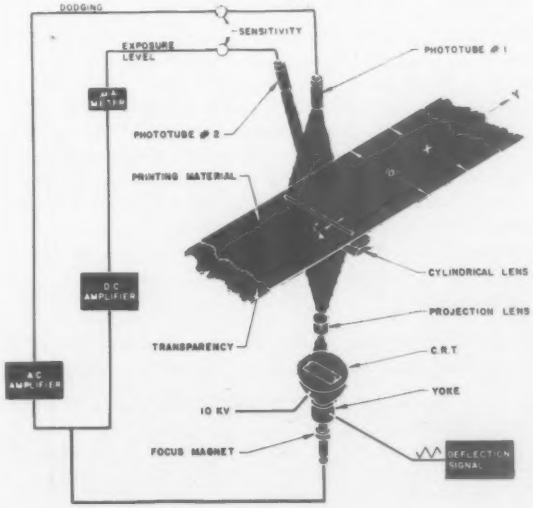

The printer utilizes the basic LogEtronic principle of inverse feedback which involves modulation of the intensity of a scanning spot of light on the face of a cathode-ray tube (CRT) in accordance with the varying densities of the image. In the continuous strip printer, the light source is a single line scan on the face of the CRT, and the other axis of scan is provided by the motion of the transparency and the printing material that are driven across a narrow slit aperture. The dodging phototube drives an ac-coupled inverse feedback loop to control and modulate the intensity of light within the scanning slit. A second phototube feeds back a d-c signal to the CRT to maintain an over-all constant light level required for proper exposure of the film or paper at the particular transport speed selected.

• Processing Equipment and Techniques

An Instantaneous Electronic Color-Film Analyzer

Bernard D. Loughlin, Charles E. Page, William F. Bailey, Charles J. Hirsch, Arthur J. Miller, and Leonard Giarraputo, *J. SMPTE*, Vol. 67, No. 1, pp. 17–26 (Jan. 1958).

The analyzer for negative or positive color film instantaneously displays a positive color picture on a color TV tube when a color original is inserted in the device. Color balance and density are adjusted by calibrated controls whose settings are used by a printer to produce a positive closely approximating the displayed picture. The device uses TV techniques to simulate additively the subtractive properties of positive film in spectral taking sensitivities, contrast, and unwanted dye absorptions. Illus.

A Means of Preventing the Formation of Newton's Rings During Contact Printing of Motion Picture Film

Charles E. Osborne, *J. SMPTE*, Vol. 67, No. 3, pp. 169–171 (March 1958).

Certain film structure and processing conditions may result in smooth-surfaced processed negatives and intermediate films which cause Newton's rings when contact printed to smooth-surfaced print films. An application of a fine, evenly distributed spray of a commercially available printers' nonoffset solution to such a film, before printing, effectively prevents these printing defects. The equipment and method of application are described. Illus., 1 ref.

Ultrasonic Agitation of Photographic or Radiographic Developer

A. L. Dighton and W. D. Stump, *Nondestructive Testing*, Vol. 16, No. 1, pp. 40–41 (Jan.-Feb. 1958).

The application of ultrasonic agitation to film processing solutions is described. The resulting effects on radiographic film are pointed out and shown by means of photographs and graphs, which, however, do not reveal all the detail of the original film. Illus.

Rapid Processing Photographic Projector

Anon., *Instrument Practice*, Vol. 12, No. 4, pp. 388–389 (Apr. 1958).

With this equipment, a 35mm film can be processed and projected with the minimum of delay onto a screen of suitable size according to the intensity of the illumination required. A positive or negative image is available to suit personal preference. The unit is completely self-contained and fully automatic. It accepts 1,000-ft reels of film, which, at a normal film speed of 4 exposures per minute, gives a continuous operating period of approximately 24 hr. The film is rapidly processed and dried by means of a jet spray system. During processing, each frame is subjected to a spray of processing chemical from three venturi jets. Each chemical is applied individually to prevent intermixing of the developer, fix, and bleach.

The apparatus is a product of Kelvin and Hughes, Ltd. Illus.

The Simultaneous Developing and Fixing of Photographic Emulsions

Harry S. Keelan, *J. Phot. Sci.*, Vol. 5, No. 6, pp. 144–145 (Nov.–Dec. 1957).

An improved developing-fixing bath incorporating phenidone is described. Variables which must be controlled for best results from any one emulsion are discussed. Illus., 3 ref.

On the Effect of Granularity on Dynamic Range and Information Content of Photographic Recordings

Leo Levi, *J. Opt. Soc. Am.*, Vol. 48, No. 1, pp. 9–12 (Jan. 1958).

The presence of granularity in a photographic emulsion provides a threshold below which a signal will not be detectable and thus acts as a limiting factor on dynamic range. Granularity data of photographic emulsions are used to determine the minimum usable spot size when the dynamic range or the discernible grey steps of the recording is specified, or the resulting dynamic range, if the resolution element size is specified. A brief analysis is made of the information content as affected by the element size, i.e., scanning spot size. Illus., 6 ref.

• Projection

Transistorized Magnetic and Photoelectric Input Circuits for Motion Picture Projectors

Stephen F. Bushman, *J. Audio Eng. Soc.*, Vol. 6, No. 1, pp. 4–9 (Jan. 1958).

A transistor input stage designed to work from a magnetic stripe on motion picture film through a reproducing head is described. Direct expressions for amplification of induced voltage are given, both with and without series feedback. Similar expressions are given for input impedance, and the effect of input im-

pedance on frequency response is discussed. Photo detectors for use with optical sound tracks and with transistor amplifiers are compared, and a universal input stage using a phototransistor is shown schematically. Illus.

A New Technique for Projecting Color Photographs

William Glenn, (from a paper presented at a meeting of the Optical Society of America, Washington, D.C., March 27, 1958).

A new technique is described for recording "color" information in tiny ripples on a clean gelatin film. The ripples in the film serve as a diffraction-grating system, and a special projector is used to "translate" the diffraction patterns into brilliant primary colors that are projected onto a screen.

The author states that by placing a special mask in front of the film in an ordinary camera, color photographs can be taken directly on black-and-white negative materials. For his clear and transparent "color slides," the author prints the diffraction-grating ripples on chromated gelatin. His black-and-white "color slides" utilize fine-grain photographic film. Illus.

• Radiography

LogEtronic Simplification in Simulated Color Radiography

Louis J. Bonann, and Andrew H. Dowdy, *Radiology*, Vol. 70, No. 4, pp. 585–587 (April 1958).

The LogEtronic procedure has simplified the preparation of simulated color roentgenograms. Development of the required negatives of the selected roentgenograms is automatic, and standardized facsimile duplication is attained. The process is shortened and numerous factors of variability are eliminated. The revised and modified procedure is outlined and supplemented by tabular instructions. Illus., 4 ref.

Television Techniques for Contrast Enhancement and Color Translations of Roentgenograms

J. F. Fisher and J. Gershon-Cohen, *Amer. J. Roentgenol., Radium Therapy and Nuclear Med.*, Vol. 79, No. 2, pp. 342–347 (Feb. 1958).

Described are a new apparatus and television techniques for contrast enhancement and color translation of roentgenograms. The limitations of the human eye in perceiving contrast are reviewed and illustrations are given of the television techniques which partially overcome these ocular limitations. Improved contrast on a television monochrome, supplemented by color translation on a color monitor, results in a gain of diagnostic information from the ordinary roentgenogram which can be varied over a wide range. With this additional information, the limits of roentgenographic diagnosis are extended. Illus.

A Simple Apparatus for Contact Microradiography Between 1.5 and 5 Kv

B. Combee and A. Recourt, *Philips Tech. Rev.*, Vol. 19, No. 7–8, pp. 221–232 (1957–58—published 10 Feb. 1958).

Described is an apparatus for contact microradiography (CMR 5) equipped with a sealed-off x-ray tube having a beryllium window only 50 μ thick and a focal spot of 0.3 × 0.3 mm. The apparatus contains a small high-voltage generator for the x-ray tube and controls for varying the anode voltage (max, 5 kv) and the tube current (max, 5 ma). The maximum permissible power is 10 w. The filament current is stabilized. The resolution, which is determined by the film, is 0.5 to 1 μ. Some of the many applications in the fields of biological and medical research are discussed. Finally, some experiments with anode voltages lower than 1 kv are described. Although the microradiographs can be examined with an optical microscope, the resolution of the film was found to be 0.2 μ, which is better than that of an optical microscope; therefore the microradiographs were magnified in an electron microscope. Illus., 18 ref.

An X-ray Image Intensifier of the Closed Circuit Television Type

Arthur F. Wegener, *Nondestructive Testing*, Vol. 16. No. 1, pp. 6, 18, 20–23 (Jan.-Feb. 1958).

Each one of the four basic intensifier systems known today has characteristic limitations but they all have one fundamental limitation—statistical fluctuation. These fluctuations in the various transducing processes set the ultimate limit of any intelligence-gathering system, including the human eye.

As far as the dynamic range of light pick-up is concerned, or the mere detection of the presence of light, no device known to date can even approach the human eye. Under practical medical and industrial fluoroscopic conditions, however, we are more concerned with improving perception of signals in the range from 10^{-4} to 1 mlm. At high light levels we can distinguish objects which are only 0.005 in. apart. As the brightness decreases, however, there is a reciprocal relationship between image size and contrast. Some fluoroscopy is carried out at approximately "starlight" level and consequently under poor visual conditions. With the light intensifier under discussion, originally developed by R. H. Morgan, and R. E. Sturm at Johns Hopkins Hospital, a number of valuable results have been obtained in the x-ray field as well as in other low light level applications. Penetrameter sensitivities close to radiographic levels have been obtained in some ranges.

The four basic types of image intensifiers which have been developed to date are: 1. The closed-circuit television type; 2. The solid-state type (electroluminescent); 3. The Coltman image tube and

variations thereof; and, 4. The "flying spot" system (Moon). Each of these four systems is briefly reviewed. Illus., 15 ref.

Direct Color Roentgenography; The Theory and Facts of Color Roentgenography

Louis J. Banann, *Amer. J. Roentgenol., Radium Therapy and Nuclear Med.*, Vol. 79, No. 2, pp. 333–341 (Feb. 1958).

The theory and facts of direct color roentgenography are reviewed. A short historic survey of the literature has been made to substantiate the theoretical presentation of color effects of roentgen radiation on various chemicals and chemical substances. Experimental details are not presented, but merely indicated because of the nonstandardization of experimental procedures at this time. The importance of color contrast is again stressed as an aid and amplification of the visual acuity of the radiologist. Illus., 28 ref.

A New Thermal Image-Converter

W. R. Harding, C. Hilsum, and D. C. Northrop, *Nature* (London), Vol. 181, No. 4610, pp. 691–692 (March 8, 1958).

A simple thermal image-converter is described which is based on the dependence upon temperature of the absorption threshold in a semiconductor. When a sample of a suitable material is viewed by transmitted monochromatic light at a wavelength near the threshold, any variations in temperature appear as differences in the transmitted intensity. If a scene in which there are objects of various temperatures and emissivities is focused on the semiconductor, a visible picture will result. Illus., 4 ref.

Application of Gamma Radiography to Concrete

J. A. Forrester, *The Engineer* (London), Vol. 205, No. 5327, pp. 314–315 (Feb. 28, 1958).

The use of gamma radiography as a nondestructive and relatively inexpensive method of testing certain properties of cement products is discussed. Radiographs showing the location and condition of steel reinforcement and the condition of concrete are shown, and a technique for studying the effect of vibration on the movement of aggregates is described. Illus., 4 ref.

Apparatus for Precision Flash Radiography of Shock and Detonation Waves in Gases

Herbert T. Knight and Douglas Venable, *Rev. Sci. Instr.*, Vol. 29, No. 2, pp. 92–98 (Feb. 1958).

An apparatus is described which is based on the technique introduced by Kistiakowsky in which the absorption of soft x-rays is used to measure the densities of gaseous shock and detonation waves. Illus., 12 ref.

• Sensitometry

Devices for Making Sensitometric Exposures on Embossed Kinescope Recording Film

Edward M. Crane and C. H. Evans, *J. SMPTE*, Vol. 67, No. 1, pp. 13–16 (Jan. 1958).

Two different sensitometers are used in the Kodak Research Laboratories for making test exposures on Eastman Embossed Kinescope Recording Film, Type 5209. One of these instruments, designed to simulate practical color-kinescope recording conditions quite closely, uses an RCA Type 5ZP16 kinescope as the light source. The other, designed for convenience and repeatability of performance, employs filtered light from an electronic flash unit. Special features of the sensitometers are discussed, and some test procedures are suggested. Illus., 2 ref.

• Techniques and Applications

Photography Applied to the Study of Rock Blasting

E. M. Patterson, *J. Phot. Sci.*, Vol. 5, No. 6, pp. 137–143 (Nov.-Dec. 1958).

The application of high-speed photographic techniques to the study of certain aspects of the displacement and breakage of rock by high explosives is described. Short-duration, argon-filled, explosive-flash units yield a single photograph at a predetermined interval after the explosion. Photographs at 1000 frames per sec with a camera of the rotating prism type give a continuous record of the blast. Supplementary illumination of rock faces is generally necessary. Serial ignition of flash bulbs is convenient and is capable of being used as the sole illuminant on sites where daylight is absent. Illus., 10 ref.

Timer Shutters CRT for Single Frame Photos

Andrew A. Tarnowski and Kenneth G. Lisk, *Electronics* (*Eng. Ed.*), Vol. 31, No. 15, pp. 83–85 (Apr. 11, 1958).

An electronic timer that incorporates four thyratrons is used to switch on a cathode-ray tube picture for the $^1/_{30}$-sec interval required to complete exactly two interlaced television fields. Vertical drive pulses from the TV sync generator provide time-reference triggering. Clean, single-frame photographs of the presentation are made with an open-shuttered still camera. Utilization of a stabilized high-voltage supply minimizes the usual problems with defocusing. Illus., 1 ref.

Print Timer Controls Density and Contrast

James D. Weir, *Electronics* (*Eng. Ed.*), Vol. 31, No. 7, pp. 108–109 (Feb. 14, 1958).

An electronic timer is described with which the proper combination of exposure time and color filter can be determined in color printing. Illus.

The Scope of High-Speed Photography

W. Deryck Chesterman, *J. Phot. Sci.*, Vol. 5, pp. 102–105 (1957).

Picture exposure time and frame repetition rate are the two fundamental parameters which define most high-speed systems. The various light sources, continuous and short-duration, are reviewed. Air sparks and xenon-filled gas tubes have the advantage of short durations of a few microseconds and can be used as either single flashes or in multiple form. 9 refs.

High-Speed and Ultra-High-Speed Photography in Electrical Engineering

A. F. B. Young and J. G. C. Steele, *J. Phot. Sci.*, Vol. 5, pp. 112–120 (1957).

This paper describes photographic techniques and high-speed motion-picture cameras which are being used in research and development work on the large high-voltage electrical circuit-breakers employed at power stations. When these circuit-breakers interrupt current an electrical arc is formed between the opening contacts. Motion-picture photography is used to study the growth and extinction of the arc and the movement of the products of arcing. A description is given of the special measures adopted to make it possible to photograph events within the circuit-breakers. Illus.

Time-Lapse Drive Unit

The Electro-Mechanical Development Co., 2337 Bissonet Street, Houston, Texas, has developed a general purpose Time-Lapse Drive Unit, Model 1325, for use with Cine-Kodak Special I or II cameras.

The self-contained unit is attached to an aluminum plate and so positioned that a flexible coupling can be connected with the one-frame-per-turn shaft of a Cine-Kodak Special camera mounted on the same plate.

The unit operates on 120 v 60 cycle ac. It measures $11\frac{1}{2} \times 8\frac{1}{2} \times 5$ in. and weighs 8 lb net.

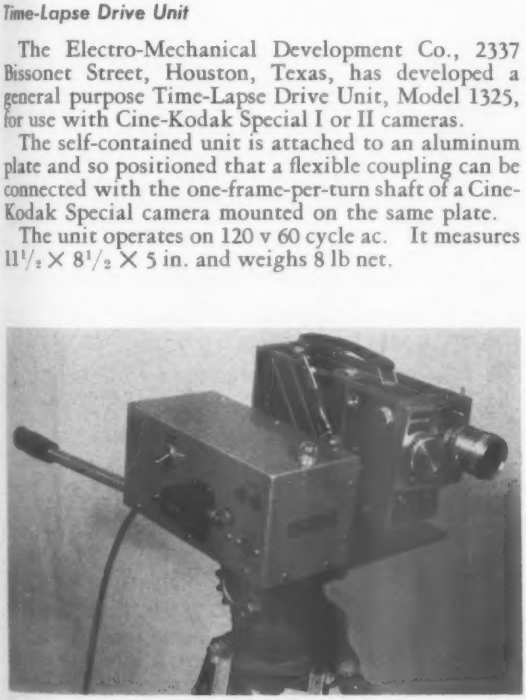

Time-Magnification Study of a Rattlesnake Strike

Sam C. Dunton and Henry M. Lester, *J. SMPTE*, Vol. 67, No. 2, pp. 65–68 (Feb. 1958).

An ultra-slow motion-picture sequence of a rattlesnake's strike was required to disclose detail in certain mechanical action, as part of an educational film on the behavior of reptiles. The authors, assisted by the staff of the Bronx Zoo, succeeded in recording this event in color at 2400 pictures per second. The approach to the problem and the method of synchronization are described. Illus.

Photographic Determination of Reaction Rates

Anon., *NBS Tech. News Bull.*, Vol. 42, No. 2, pp. 27–28 (Feb. 1958).

A brief description of a technique for measuring the rate at which a solid surface is attacked by a corrosive gas. Time-lapse photographs are made of the reacting solid to secure a permanent record of the reaction progress at specified time intervals. Illus., 1 ref.

Sources of Entoptic Stray Light

Donald W. DeMott and Robert M. Boynton, *J. Opt. Soc. Am.*, Vol. 48, No. 2, pp. 120–125 (Feb. 1958).

A technique is described for photographing the light scattered from the various ocular media. The results indicate that about 70% of scattered light stems from the cornea, the remainder from the lens. Illus., 2 ref.

Application of High-Speed Photography to Textile Problems

G. A. J. Archard, *J. Phot. Sci.*, Vol. 5, pp. 126–131 (1957).

A brief review is given of the difficulties which are encountered when high-speed photography is applied to problems of the textile industry. Examples from various sections of the industry are cited. Illus.

Cinematography of Combustion in Diesel Engines

J. G. G. Hempson and R. Watts, *J. Phot. Sci.*, Vol. 5, pp. 121–125 (1957).

Methods used to film injection and combustion chambers are described. Rates up to 15,000 frames per sec were used with suitable lighting to show the distribution of injected fuel prior to self-ignition. Illus., 5 refs.

A Studio-Type and a Portable-Type System for Synchronizing ¼-Inch Magnetic Tape with Perforated Motion-Picture Film

Edward P. Kennedy, *J. SMPTE*, Vol. 67, No. 2, pp. 95–97 (Feb. 1958).

The utilization of synchronously-driven toothed sprockets engaging complementary film sprocket holes

for sound-film production is an old technique. The introduction in 1947 of sound magnetic tape having a thin and easily torn base of cellulose acetate made sprocket holes highly impractical.

The two systems discussed in this paper employ magnetic equivalents of sprocket holes recorded along the tape simultaneously with the recorded sound and at the exact time of frame exposure in the camera. The "latent magnetic sprocket holes" are later reproduced to serve as a master speed-control device to govern the speed of the picture film through playback equipment. (U.S. Patent No. 2,822,722, issued 11 Feb. 1958). Illus.

Color TV Recording on Black-and-White Lenticular Film

J. M. Brumbaugh, E. D. Goodale, and R. D. Kell, *IRE Trans. on Broadcast and Television Receivers*, Vol. BTR-3, No. 2, pp. 71–75 (1957).

For about eight years, monochrome TV shows have been recorded on film for later rebroadcast and record purposes. Several systems have been under study for similar storage of color programs. The first to achieve commercial usage is based on a refinement of the early Kodacolor process. Red, green, and blue "separation images" are focused, in register, on the emulsion through the cylindrical lenses embossed in the film base. Color information is recovered through essentially inverse optics. The electronic and optical systems are described in the paper. Illus.

Printing Motion-Picture Films Immersed in a Liquid

John G. Stott, George E. Cummins, and Henri E. Breton, *J. SMPTE*, Vol. 66, pp. 607–612 (1957); *Part I, Contact Printing.*

A printing method is described that gives high quality motion-picture prints from badly scratched negatives. Both the negative and the print film are completely immersed at the printing aperture in a liquid having an index of refraction close to that of the gelatin and acetate support. The process almost completely eliminates the printing effect of scratches and other surface irregularities of the negative, and improves the definition of positive prints by providing a continuous optical medium through which the exposing light passes from the negative to the print film. A step-contact and a continuous-contact liquid-immersion printer are described. Illus., 3 refs.

Ibid., pp. 612–615; *Part II, Optical Printing.*

A method is described for optical printing of motion-picture film by the use of a projection gate that immerses the film in a liquid of matching refractive index. This permits highly specular printing illumination since, under these conditions, scratches and surface irregularities on the film have relatively little optical effect. Experimental trials of this method have been carried out using Eastman color films at a speed of 90 ft per min. Illus., 1 ref.

An Application of Television for the Discovery of Variable Stars

J. Borgman, *Philips Tech. Rev.*, Vol. 19, pp. 140–142 (1957–1958).

Apparatus which consists essentially of a flying-spot scanner with MC 13-16 cathode-ray tube is arranged to scan simultaneously two photographs of the same region of the sky. The signals from two photomultipliers are subtracted, the difference signal serving as the picture signal for a television display tube. When the two plates are identical, the picture signal is zero, but when the photographic images differ, owing to the movement of a variable star, the point appears lighter or darker than its surroundings on the screen. The instrument allows more rapid investigation than is possible by microscopic methods and offers a much better chance of detecting variable stars. Mention is made of other possible uses of the instrument, including the detection of heavenly bodies whose positions relative to the "fixed" stars change, of differences between aerial photographs made at different times, and of forgeries. Illus., 3 refs.

• Miscellaneous

Simulating Sharpness in Color Television

M. W. Baldwin, Jr., *Bell Labs Record*, Vol. 35, pp. 481–484 (1957).

A brief description and discussion of a "defocusing" projector which has been developed to make color pictures that are measurably blurred. The blurring obtained with out-of-focus projection can simulate the blurring that results when a color TV picture is transmitted over a circuit of limited bandwidth. Four projectors are used with independent focusing adjustments and directed at a common projection screen. Additive color synthesis is utilized, i.e. red, green, and blue light superimposition. The fourth projector is available for showing a comparison picture. Illus.

Electroluminescence—Light of the Future

A. V. J. Martin, *Radio and TV News*, Vol. 59, No. 1, pp. 35–38 (Jan. 1958).

A brief review of the subject, covering principles and applications, including image forming qualities and others. Illus.

An Improved High-Gain Panel Light Amplifier

B. Kazan, *Proc. IRE*, Vol. 45, pp. 1358–1364 (1957).

A grooved photoconductor light-amplifying picture panel is described, with a gain more than ten times that of previous amplifiers and with reduced threshold for input light. These improvements have been obtained with a new electrode structure which allows more efficient operation and by the use of a more sensitive photoconductive powder. Meas-

ured input-output characteristics are shown, comparing the new and the earlier types of operation and also indicating the effects of different supply frequencies. The time-integrated energy gain for one-second excitation is of the order of 100 with input light of the same spectral distribution as the output. The asymtotic energy gain after a longer excitation interval is about 800 with optimum spectral matching of the photoconductor. Although the decay is of the order of seconds, as with early amplifiers, the shape of the decay curves and the rate of decay are changed by the new method of operation. Illus., 2 refs.

Theoretical Resolving Power and Practical Resolving Power in Photography

Vasco Ronchi, *Camera* (Lucerne), No. 1, pp. 29–31 (Jan. 1958); No. 2, pp. 73–76 (Feb. 1958); and No. 3, pp. 122–23 (March 1958).

In a three-part comprehensive review of the subject, the author compares the classical or mathematical theory of resolving power with results of experimental evaluations. He concludes that mathematical analysis is valuable, but that experimental studies must be made also and given due consideration. Illus.

Electroluminescence

H. K. Henisch, *Science News 47* (Penguin Books Ltd., Great Britain), pp. 13–30 (Feb. 1958).

This is a comprehensive technical treatment of the subject, written in easily understandable language. After a brief introduction, the author covers electroluminescence of powder aggregates, electroluminescent lamps and indicators, light amplifiers and optrons, picture display panels and image converters, experiments on single crystals, and theory of electroluminescence in single ZnS crystals. Illus., 11 ref.

Ultra-Cold Weather Photography

Richard R. Conger, *J. SMPTE*, Vol. 67, No. 1, pp. 35–37 (Jan. 1958).

The U.S. Navy expeditions to Antarctica, as well as its Arctic operations over the past several decades, have yielded new information about camera performance in subzero weather, techniques, and "winterization" of equipment. The use of still and motion-picture cameras in cold weather is discussed in detail and their application during Operation Deepfreeze is described. Illus.

Recent Developments in Shaped Beam Display and Recording Techniques

R. M. Peterson and R. C. Ritchart, Stromberg-Carlson Co., 1895 Hancock St., P. O. Box 2449, San Diego 12, Calif.

Considerable improvements have been made recently in shaped beam tube characteristics such as character selection and deflection, phosphor and matrix resolution, tube length, and dynamic control of character size. Equipment has also been developed for combining these tubes with photographic and xerographic recorders.

• Notes from the Editor

A New Editor for P S & E

Dr. T. Howard James will become the editor of this journal starting with the next issue, Volume 2, Number 3. He does not require a special introduction to readers of this or any other scientific photographic publication because his work and his papers on the theoretical and practical aspects of photographic development have been pre-eminent in their field. However, Dr. James's interests and his knowledge of the photographic process are not confined to one phase of our wide and far-ranging discipline. On the contrary, his interests are with all of photography, as indeed they must be for an editor of P S & E. Of course, he will have the indispensable help of the members of the Editorial Review Board, of the Managing Editor, and of the Associate Editors, all of whom guide and shape the material that is printed in these pages.

Positions Available/Positions Wanted Dept.

The Board of Directors of this Society decided at its last meeting that notices about positions that are available or wanted will be published henceforth in the National News Letter rather than in P S & E. This will ensure wider circulation of these notices since the News Letter reaches many more readers than the journal; it will also make available badly needed space in the larger issues of P S & E that will be published in the future. — *Peter Krause*

• Patent Postscripts

ROBERT H. ZAPPERT

Polyamines as Short Stop Agents for Azine Color Developers

U.S. 2,827,375, Andreyev to General Aniline and Film Corp.

The derivatives of 4,6-metanilic acid which are used as color developing agents in the azine process are substantive to gelatin and, therefore, difficult to remove from the emulsion after development. The residual developing agent causes stain and color development fog. These defects can be avoided by the use of a short stop bath which contains an acid, a polyamine such as hexamethylenetetramine or glycosine, and glyoxal bisulfite as a clarifying agent.

Copolymers and Photographic Emulsions Containing Same

U.S. 2,829,053, Weaver to E. I. du Pont de Nemours & Company, Inc.

Photographic emulsions are prepared using in place of gelatin a colloid obtained by amination or quaternarization of a hydrolyzed polyvinyl ester/allyl glycidyl ether copolymer. A typical material is prepared by heating a copolymer of 95 parts of vinyl acetate and 5 parts of allyl glycidyl ether with dimethylamine to accomplish quaternarization, and subsequently hydrolyzing the reaction mixture with sodium methylate in a methanol solution.

Process of Washing and Protecting Photographic Silver Images

U.S. 2,830,900, Land, Blout, and Haas to Polaroid Corp.

The silver images obtained in cameras by the diffusion transfer process are rather thin and their stability is further endangered by retained traces of processing agents, particularly oxidized developing agents and residual hypo. These pictures are stabilized by swabbing them with a solution of a vinyl pyridine polymer in a mixture containing water, an organic solvent such as ethanol or acetone, and a small amount of acetic acid.

Light-Sensitive Polymers for Photography

U.S. 2,835,656, Unruh and Smith to Eastman Kodak Co.

A light-sensitive polymer is obtained by heating a copolymer of styrene and maleic anhydride with the monoester of ethylene glycol and cinnamic acid. The polymer is dissolved in ethyl methyl ketone, coated on paper and exposed through a negative. The exposed paper is developed with ethyl methyl ketone, dampened, and treated with a greasy ink to yield a positive picture.

Photographic Diffusion Transfer Process for Producing Multiple Direct Positive Copies

U.S. 2,834,676, Stanley, Dughi, and Hey to Sperry Rand Corp.

In the conventional diffusion transfer process, the silver halide emulsion layer is developed to a negative with a developer containing a silver halide solvent. The undeveloped silver halide in the unexposed areas diffuses to the light-insensitive reception layer where it is reduced to metallic silver in the presence of development nuclei, such as silver sulfide, to form a positive image. This procedure does not permit the preparation of multiple positives because the negative emulsion which is impregnated with the developer fogs rather quickly after the first transfer, thus converting the silver halide into metallic silver which can no longer be transferred.

Multiple copies can be prepared by the use of a modified developer which contains, in addition to the developing agent and the silver halide, the following ingredients:

1. An alkali or ammonium chloride as a fixation accelerator;
2. Cupric, mercuric, zinc or manganese chloride as a latent image desensitizer, and an alkali or ammonium nitrate as a gelatin softener.

The total contact time for a fourth copy is 25 sec as compared with 17 sec for the first copy.

Photographic Short Stop Concentrates

U.S. 2,836,493, Kimura and Stich to Morton Chemical Co.

Short stop concentrates are described which contain mixtures of ammonium bisulfate and sodium bisulfate and in which the amount of ammonium bisulfate ranges from $2^1/_3$ to $5^2/_3$ mols/mol of sodium bisulfate. The equivalent sulfuric acid content is at least 100 grams, but preferably 500 grams/liter. The use of these mixtures permits the shipment of stock solution at below freezing temperatures.

The Society of Photographic Scientists and Engineers

Box 1609 • Main Post Office • Washington, D.C.

OFFICERS

President	GEORGE T. EATON, Bldg. 59, Kodak Park, Rochester 4, New York
Executive Vice President	STEVEN LEVINOS, 308 Academy Drive, Vestal, New York
Engineering Vice President	JOHN A. MAURER, 116–118 West 29th Street, New York 1, New York
Editorial Vice President	PETER KRAUSE, 29–11 Bell Boulevard, Bayside, New York
Financial Vice President	HERBERT MEYER, 325 Sequoia Drive, Pasadena 2, California
Secretary-Treasurer	NORTON GOODWIN, 826 Connecticut Avenue NW, Washington 6, D.C.
Managing Secretary	EDWARD S. COBB, Box 1609, Main Post Office, Washington, D.C.

CHAPTERS *and* CHAPTER OFFICERS

Binghamton, New York	*President*	IRA B. CURRENT, 26 Woodland Avenue, Binghamton, N. Y.
	Secretary	E. SCUDDER MACKEY, Stone Road, RD No. 2, Binghamton, N. Y.
Boston, Massachusetts	*President*	NICHOLAS CEDRONE, 73 Pond Street, Waltham, Mass.
	Secretary	ARTHUR J. ROSENBAUM, 44 Gleason Street, Framingham, Mass.
Cleveland, Ohio	*President*	R. E. BIRR, c/o General Electric Lamp Division, Nela Park No. 281, Cleveland 12, Ohio
	Secretary	CLINTON K. HAMLINK, 2230 South Overlook Road, Cleveland 6, Ohio
Ithaca, New York	*President*	COLONEL WILLIAM ALLEN, 216 Forest Home Drive, Ithaca, New York
	Secretary	DAVID O. FLETCHER, 1314 East State Street, Ithaca, New York
Monmouth, New Jersey	*President*	JOSEPH MANGIARACINA, 30 Brook Avenue, Little Silver, New Jersey
	Secretary	MISS MARILYN LEVY, 100 McLaren Street, Red Bank, New Jersey
New York, New York	*President*	FRANK G. BACK, 55 Sea Cliff Avenue, Glen Cove, New York
	Secretary	LT. HAYDEN B. PEAKE, Army Pictorial Center, 35-11 35th Avenue, Long Island City 1, New York
Rochester, New York	*President*	DONALD B. GRIM, Building 29, Eastman Kodak Company, Rochester 4, New York
	Secretary	ROBERT W. MAHER, Eastman Kodak Company, 343 State Street, Rochester 4, New York
Southern California	*President*	HERBERT MEYER, 325 Sequoia Drive, Pasadena 2, California
	Secretary	GEORGE W. BOEMLER, 22632 Collins Street, Woodland Hills, California
Southern Lake Michigan	*President*	HENRY COOPMAN, 9118 Greenwood Avenue, Ballard Acres, Des Plaines, Illinois
	Secretary	ROBERT J. MAZOR, 1438 West 123rd Street, Chicago 43, Illinois
Washington, D.C.	*President*	DWIN R. CRAIG, 815 Fisher Street, Falls Church, Virginia
	Secretary	LEE M. RECORDS, 1335 Tewksbury Place NW, Washington, D.C.

Sustaining Members / Society of Photographic Scientists and Engineers

Abrams Instrument Corporation

Aero Service Corporation

Ansco

Argus Camera

Bar-Ray Products, Incorporated

Bausch & Lomb Optical Company

Bell & Howell Company

Charles Beseler Company

Cameraflex, Incorporated

Chemco Photoproducts Company, Incorporated

Chicago Aerial Industries, Incorporated

Consolidated Film Industries

De Jur Amsco Corporation

E. I. du Pont de Nemours & Company

Eastman Kodak Company

Ednalite Optical Company, Incorporated

Elgeet Optical Company, Incorporated

Enteco Industries, Incorporated

Fairchild Camera & Instrument Corporation

Farrand Optical Company, Incorporated

Federal Manufacturing & Engineering Corporation

Oscar Fisher Company, Incorporated

The F-R Corporation

General Electric Company

General Film Laboratories Corporation

Graflex, Incorporated

Grant Photo Products

W. & L. E. Gurley Company

Haloid Xerox Incorporated

Hardale Associates

Houston-Fearless Corporation

Charles A. Hulcher Company

Philip A. Hunt Company

Hycon Manufacturing Company

Kalart, Incorporated

Kollmorgen Optical Corporation

LogEtronics, Incorporated

J. A. Maurer, Incorporated

The Morse Instrument Company

National Research and Chemical Company

North American Aviation, Incorporated

Pako Corporation

Photogrammetry, Incorporated

Polaroid Corporation

Simmon Brothers, Incorporated

Sperry Rand Corporation,
Remington Rand Division

Technicolor New York Corporation

Wollensak Optical Company

Zoomar, Incorporated